



## 15 **Abstract**

16 Trait-based approaches are of increasing concern in predicting vegetation changes and  
17 linking ecosystem structures to functions at large scales. However, a critical challenge for such  
18 approaches is acquiring spatially continuous plant functional trait maps. Here, six key plant  
19 functional traits were selected as they can reflect plant resource acquisition strategies and  
20 ecosystem functions, including specific leaf area (SLA), leaf dry matter content (LDMC), leaf N  
21 concentration (LNC), leaf P concentration (LPC), leaf area (LA) and wood density (WD). A total  
22 of 34589 in-situ trait measurements of 3447 seed plant species were collected from 1430 sampling  
23 sites in China and were used to generate spatial plant functional trait maps (~1 km), together with  
24 environmental variables and vegetation indices based on two machine learning models (random  
25 forest and boosted regression trees). To obtain the optimal estimates, a weighted average algorithm  
26 was further applied to merge the predictions of the two models to derive the final spatial plant  
27 functional trait maps. The models showed a good accuracy in estimating WD, LPC and SLA, with  
28 average  $R^2$  values ranging from 0.48 to 0.68. In contrast, both the models had weak performance  
29 in estimating LDMC, with average  $R^2$  values less than 0.30. Meanwhile, LA showed considerable  
30 differences between the two models in some regions. Climatic effects were more important than  
31 those of edaphic factors in predicting the spatial distributions of plant functional traits. Estimates  
32 of plant functional traits in the northeast China and the Qinghai-Tibet Plateau had relatively high  
33 uncertainties due to sparse samplings, implying a need of more observations in these regions in the  
34 future. Our spatial trait maps could provide critical supports for trait-based vegetation models and  
35 allow exploration into the relationships between vegetation characteristics and ecosystem  
36 functions at large scales. The six plant functional traits maps for China with 1 km spatial  
37 resolution are now available at <https://figshare.com/s/c527c12d310cb8156ed2> (An et al., 2023).

## 38 **1 Introduction**

39 Climate change has been affecting vegetation distributions and biogeochemical cycling globally  
40 and altering their feedbacks to the climate system (Kirilenko et al., 2000; Finzi et al., 2011;  
41 Jónsdóttir et al., 2022). Dynamic global vegetation models (DGVMs) are powerful tools for  
42 predicting changes in vegetation and ecosystem-atmosphere exchanges (e.g., water, carbon and  
43 nutrient cycling) in a changing climate (Foley et al., 1996; Peng, 2000). However, conventional  
44 DGVMs are still insufficient realistic, largely due to their dependence on the plant functional types  
45 (PFTs) assumption (Sitch et al., 2008; Yurova and Volodin, 2011; Scheiter et al., 2013). PFTs in  
46 conventional DGVMs commonly have fixed attributes (mostly trait values) (~~Van-van~~ Bodegom et  
47 al., 2012; Wullschleger et al., 2014) that do not reflect plant adaptation to environments, limiting  
48 the quantification of carbon-water-nutrient feedbacks between terrestrial ecosystems and the  
49 atmosphere (Zaehle and Friend, 2010; Liu and Yin, 2013). Trait-based approaches can provide a  
50 robust theoretical basis for developing the next generation of DGVMs (~~Van-van~~ Bodegom et al.,  
51 2012; Sakschewski et al., 2015; Matheny et al., 2017). Plant functional traits, which are closely  
52 associated with ecosystem functions (Diaz et al., 2004; Yan et al., 2023), can effectively reflect  
53 response and adaptation of plants to environmental conditions (Myers-Smith et al., 2019; Qiao et  
54 al., 2023).

55 Attempts to predict spatially continuous trait maps have been conducted at regional to global  
56 scales (e.g., Madani et al., 2018; Moreno-Martínez et al., 2018; Boonman et al., 2020; Loozen et  
57 al., 2020; Dong et al., 2023). Webb et al. (2010) proposed that the environment creates a filtered  
58 trait distribution along an environmental gradient, and such trait-environment relationships offer  
59 fundamental supports to predict the spatial distributions of plant functional traits through  
60 extrapolating local trait measurements. Boonman et al. (2020) mapped the global patterns of  
61 specific leaf area (SLA), leaf N concentration (LNC) and wood density (WD) based on a set of  
62 climate and soil variables. As the number of available regional and global trait databases increases  
63 (Wang et al., 2018; Kattge et al., 2020), trait-environment relationships are becoming increasingly  
64 quantitative and accurate (Bruehlheide et al., 2018; Myers-Smith et al., 2019). Alternatively, remote  
65 sensing approaches, such as empirical methods and physical radiative transfer models (e.g., partial  
66 least squares regression and PROSPECT model), have been developed to estimate plant  
67 physiological, morphological and chemical traits (e.g., leaf chlorophyll content, SLA, LNC and  
68 leaf dry matter content (LDMC)) (Darvishzadeh et al., 2008; Romero et al., 2012; Ali et al., 2016).  
69 Vegetation indices, such as normalized difference vegetation index (~~NDVI~~) and enhanced  
70 vegetation index (EVI), have been successful in estimating plant functional traits of croplands,  
71 grasslands and forests (Clevers and Gitelson, 2013; Li et al., 2018; Loozen et al., 2018). Loozen et  
72 al. (2020) demonstrated that EVI was the most important predictor for mapping the spatial pattern  
73 of canopy nitrogen in European forests. Admittedly, a recent study has suggested that combining  
74 environmental variables and vegetation indices can improve the predictive accuracy of canopy

75 nitrogen compared to those based on vegetation indices alone (Loozen et al., 2020).

76 Although there have been reports on plant functional trait distributions in China in some  
77 global or regional researches (e.g., Yang et al., 2016; Butler et al., 2017; Madani et al., 2018;  
78 Moreno-Martínez et al., 2018; Boonman et al., 2020), ~~they~~-there are still large uncertainties in  
79 characterizing the spatial distributions of plant functional traits in China. First, global studies  
80 generally have relatively few-~~and~~ unevenly distributed sampling sites across China (Butler et al.,  
81 2017; Madani et al., 2018; Boonman et al., 2020), impeding our understanding of the true spatial  
82 characteristics of trait variability. Second, the spatial patterns of traits among these studies are  
83 usually inconsistent. For example, Moreno-Martínez et al. (2018) and Madani et al. (2018)  
84 demonstrated that SLA values were low in the southeast areas but high in the southwest areas of  
85 China, whereas Boonman et al. (2020) found the opposite. Third, most studies focused on leaf  
86 traits (Yang et al., 2016; Loozen et al., 2018; Moreno-Martínez et al., 2018), whereas traits  
87 associated with the whole-plant strategies, such as WD, were ignored. Therefore, mapping and  
88 verifying the spatial patterns of key functional traits that reflect the whole plant economics  
89 spectrum in China is a top priority.

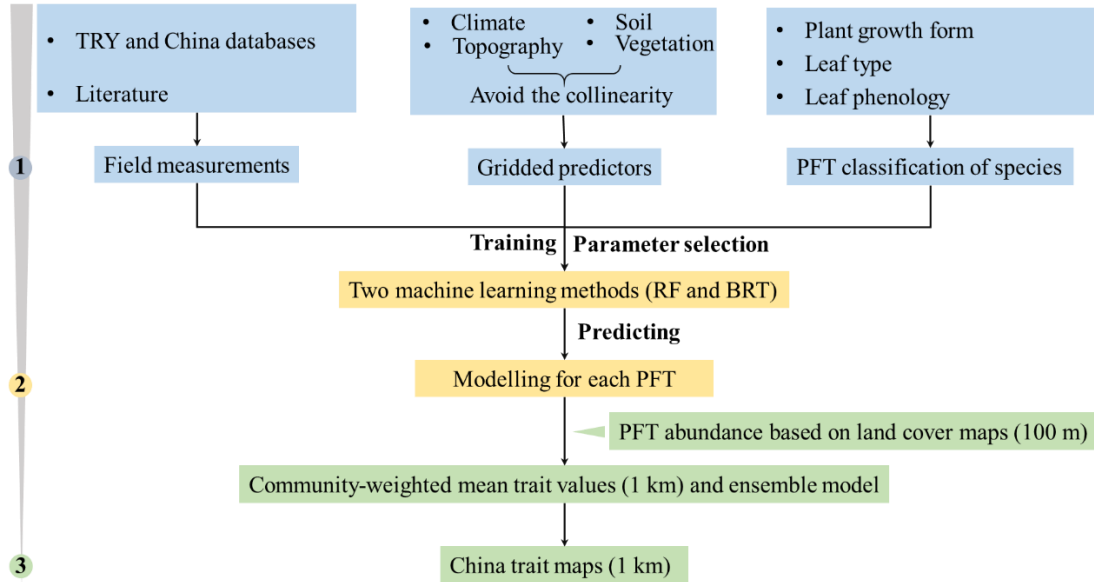
90 In this study, our main objective was to generate spatial maps for several key plant functional  
91 traits, through combining field measurements, environmental variables and vegetation indices. We  
92 selected six plant functional traits including SLA, LDMC, LNC, LPC, LA and WD. As key leaf  
93 economics traits, SLA, LDMC, LNC and LPC were selected because they are closely linked to  
94 plant growth rate, resource acquisition and ecosystem functions (Wright et al., 2004; Diaz et al.,  
95 2016). LA is indicative of the trade-off between carbon assimilation and water-use efficiency  
96 (Wright et al., 2017), and WD reflects the trade-off between plant growth rate and support cost,  
97 with a higher WD linked to a lower growth rate, a higher survival rate and a higher biomass  
98 support cost (King et al., 2006). For each plant functional trait, we predicted spatial patterns at a 1  
99 km resolution using an ensemble modelling algorithm based on two machine learning methods  
100 (i.e., random forest and boosted regression trees).

## 101 **2 Materials and Methods**

### 102 **2.1 Overview**

103 The spatial maps of plant functional traits in China were generated based on machine learning  
104 methods trained by a large dataset of in-situ field measurements, environmental variables and  
105 vegetation indices in three steps (Fig. 1). First, in-situ field measurements of six plant functional  
106 traits were collected from TRY and China databases as well as published literature, and the PFTs  
107 of plant species were classified based on plant growth form, leaf type and leaf phenology. Multiple  
108 gridded predictors of climate, soil, topography and vegetation indices were used after avoiding the  
109 collinearity among them. Second, random forest and boosted regression trees were used to train  
110 the relationships between plant functional traits and predictors for each PFT individually. Third,

111 the spatial abundance of each PFT within 1 km grid cell was calculated using land cover map (100  
 112 m). Community-weighted trait values within 1 km grid cell ~~were~~ calculated based on these  
 113 abundances of each PFT and their predicted trait values in Step 2. To reduce the variability of  
 114 different single-models, we derived the final spatial maps of plant functional traits using an  
 115 ensemble model algorithm to merge the predictions of random forest and boosted regression trees  
 116 according to their cross-validated  $R^2$  values.



117  
 118 **Figure 1.** Methodological workflow for spatial mapping of plant functional traits. Trait  
 119 mapping is performed in three steps. Step 1: in-situ field measurements of plant functional traits,  
 120 PFT classification of plant species and gridded predictors were collected. Step 2: two machine  
 121 learning methods were used to predict trait values by training ~~the~~ field measurements and  
 122 predictors for each PFT. Step 3: spatialization of trait maps by calculating the abundance of each  
 123 PFT using 100 m land cover map and predicted trait values within 1 km grid cells. PFT, plant  
 124 functional type; RF, random forest; BRT, boosted regression trees.

## 125 2.2 Plant functional trait collection and data processing

126 The information on the six plant functional traits and their ecological meanings are described in  
 127 Table 1. Plant trait data was obtained and collected via two main sources. The first source was  
 128 public trait databases, including the TRY database (Kattge et al., 2020) and the China Plant Trait  
 129 Database (Wang et al., 2018). The second source was from literature (listed in Appendix A). To  
 130 ensure data quality and comparability, we only included trait observations that met the following  
 131 five criteria: 1) Measurements must be obtained from natural terrestrial fields in order to minimize  
 132 the influences of management disturbance, and observations from croplands, aquatic habitats,  
 133 control experiments and gardens were excluded; 2) According to the mass ratio hypothesis, the  
 134 effect of plant species on ecosystem functioning is determined to an overwhelming extent by the  
 135 traits and functional diversity of the dominant species and is relatively insensitive to the richness

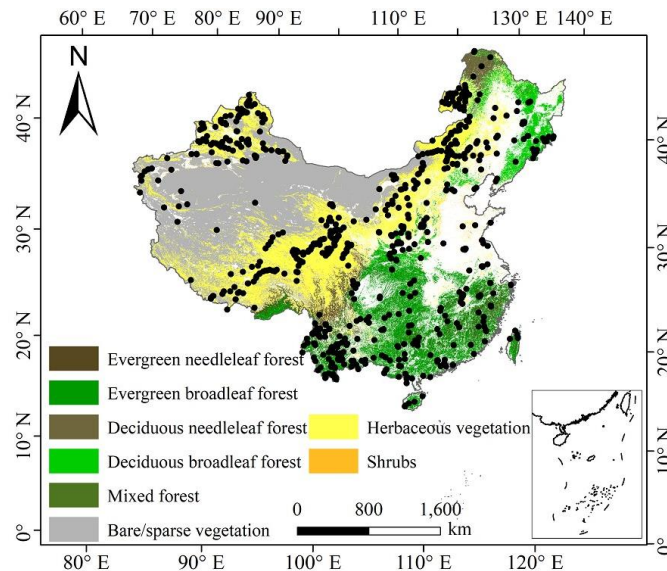
136 of subordinate species (Grime, 1998). Thus, we only included studies that measured plant trait  
 137 observations from all species or dominant species within a community; 3) In order to consider the  
 138 intraspecific trait variation, when the same species occurred ~~in~~at the same sampling site from  
 139 different studies, we included all original observed data from different studies rather than  
 140 averaging the values at the species level (Jung et al., 2010; Siefert et al., 2015); 4) Plant trait  
 141 observations must be made on mature and healthy plant individuals, so some specific growth  
 142 stages (e.g., seedling) and size classes (e.g., sapling) were excluded to reduce the confounding  
 143 effect of ontogeny ~~and seasonality~~ (Thomas, 2010); 5) We only included studies with clear  
 144 geographical coordinates to match predictor variables. The sampling location and sampling time  
 145 ~~information~~ were also included in the dataset. The sampling time mostly focused on the growing  
 146 season of a year (i.e., May-October), which can ensures the relative consistency of sampling time  
 147 to minimize the effects of seasonality. Plant functional traits must be sampled and measured  
 148 according to standardized measurement procedures (Perez-Harguindeguy et al., 2013) to reduce  
 149 the variation and uncertainty among different data sources. In this study, we included SLA  
 150 measurements on sun-leaves, and WD measurements on main stem of woody species.

151 **Table 1** Description of plant functional traits selected in this study and their relevant  
 152 ecosystem functions.

Trait	Abbreviation	Description	Relevant ecosystem functions
Specific leaf area	SLA	As a core leaf economics trait (Wright et al., 2004), it is related to trade-off between leaf lifespan and <del>C</del> <u>carbon</u> acquisition as well as light competition (Reich et al., 1991)	Productivity, litter decomposition, competitive ability (Bakker et al., 2011; Smart et al., 2017)
Leaf dry matter content	LDMC	Strongly related to resource availability and potential growth rate (Hodgson et al., 2011)	Productivity, litter decomposition, herbivore resistance, and drought tolerance (Bakker et al., 2011; Smart et al., 2017; Blumenthal et al., 2020)
Leaf N concentration	LNC	As a core leaf economics trait, it is strongly related to photosynthetic capacity (Wright et al., 2004)	Productivity, nutrient cycling, litter decomposition (LeBauer and Treseder, 2008; Bakker et al., 2011)
Leaf P concentration	LPC	As a core leaf economics trait, it is strongly related to photosynthetic capacity (Wright et al., 2004)	Productivity, nutrient cycling, litter decomposition (LeBauer and Treseder, 2008; Bakker et al., 2011)
Leaf area	LA	Trade-off between <del>C</del> <u>carbon</u> assimilation and water use efficiency, it is related to energy balance (Wright et al., 2017)	Productivity (Li et al., 2020)
Wood density	WD	A measure of carbon investment, representing the trade-off between growth and mechanical support (Martínez-Vilalta et al., 2010)	Drought tolerance, productivity (Hoeber et al., 2014; Liang et al., 2021)

153 The plant trait data was checked for possible errors and corrected in three steps as follows.  
 154 First, species name and taxonomic nomenclature were corrected and standardized according to the  
 155 Plant List (<http://www.theplantlist.org/>) using the “plantlist” package. Second, illogical values,

156 repeated values and outliers were removed, which were defined by observations exceeding 1.5  
 157 standard deviations ~~of~~ from the mean trait value for a given species (Kattge et al., 2011). Third, we  
 158 appended information on plant growth form, leaf type and leaf phenology from the TRY  
 159 categorical traits database (<https://www.try-db.org/TryWeb/Data.php#3>) and *Flora Reipublicae*  
 160 *Popularis Sinicae* (<http://www.iplant.cn/frps>), which were used to match species names to PFTs.  
 161 We associated each species with a corresponding PFT based on plant growth form (tree, shrub and  
 162 grass), leaf type (broadleaf and needleleaf) and leaf phenology (evergreen and deciduous). For  
 163 example, the information on *Salix matsudana* is: tree, deciduous and broadleaf, thus, we were able  
 164 to associate the PFT of deciduous broadleaf forest (DBF) to this species. The species that did not  
 165 correspond to any PFT were discarded. After these treatments, we collected a total of 34589 trait  
 166 measurements from 1430 sampling sites for our database, representing 3447 species from 195  
 167 families and 1066 genera (Fig. 2). Information on the statistics for the six plant functional traits  
 168 collected in this study is shown in Table B1 in Appendix B.  
 169



170 **Figure 2.** ~~Location~~ The spatial distribution of sample sites and land cover map across  
 171 different ecosystems in China. The white areas represent artificial land cover types.  
 172

## 173 2.3 Preparing predictor variables

### 174 2.3.1 Climate data

175 Twenty-one climate variables were used in this study, including 19 bioclimate variables, solar  
 176 radiation (RAD) and aridity index (AI) (Table B2 in Appendix B). The 19 bioclimate variables and  
 177 RAD were obtained from ~~the~~ WorldClim version 2.1 for the period from 1970 to 2000  
 178 (<https://www.worldclim.org/data/worldclim21.html>). The AI data was extracted from the CGIAR  
 179 Consortium of Spatial Information (CGIAR-CSI) ~~website~~  
 180 (<http://www.csi.cgiar.org>) (Trabucco and Zomer, 2018). The spatial resolution of climate data is 1  
 181 km.

### 182 2.3.2 Soil data

183 Twelve soil variables were included in this study, representing ~~the~~ different aspects of soil  
184 properties, i.e., soil texture, bulk density (BD), pH and soil nutrients (Table B2 in Appendix B).  
185 All soil variables were extracted from the Soil Database of China for Land Surface Modeling  
186 (<http://globalchange.bnu.edu.cn/research/soil2>) (Shangguan et al., 2013). Given the importance of  
187 topsoil properties on community composition (Bohner, 2005), we averaged the first four layers to  
188 represent the topsoil properties (~ 30 cm) in our study. The spatial resolution is 1 km.

### 189 2.3.3 Topography

190 The topographic variable was elevation. Elevation data was extracted from the STRM 90m dataset  
191 in China, based on the SRTM V4.1 database (<https://www.resdc.cn/data.aspx?DATAID=123>). The  
192 spatial resolution is 1 km.

193 Given the collinearity among climate and soil variables, we reduced the dimensionality of  
194 these predictors based on Pearson's correlation coefficient ( $r$ ) (Figs. B1 and B2 in Appendix B).  
195 Among a set of highly correlated variables ( $r > 0.75$ ), only one variable was retained in subsequent  
196 analysis to ensure a combination of different environmental variables. The final selection of  
197 environment predictors included ~~nineteen~~ twenty variables: mean annual temperature (MAT),  
198 mean diurnal range (MDR), min temperature of the coldest quarter (Tmin), max temperature of  
199 the warmest quarter (Tmax), temperature seasonality (TS), mean annual precipitation (MAP),  
200 precipitation seasonality (PS), precipitation of the wettest quarter (PEQ), precipitation of the driest  
201 quarter (PDQ), AI, RAD, elevation, soil sand content (SAND), pH, BD, soil total N (STN), soil  
202 total P (STP), soil available P (SAP), soil alkali-hydrolysable N (SAN) and cation exchange  
203 capacity (CEC).

### 204 2.3.4 Vegetation indices

205 Three categories of vegetation indices were included in this study (Table B2 in Appendix B). First,  
206 EVI was extracted from the MOD13A3 V006 product  
207 (<https://lpdaac.usgs.gov/products/mod13a3v006/>). This product is available as a monthly average  
208 with the spatial resolution of 1 km, ranging from January 2000 to December 2018. Second,  
209 MODIS reflectance data was also extracted from the MOD13A3 V006 product, including MIR  
210 reflectance, NIR reflectance, red reflectance and blue reflectance. Third, the MERIS terrestrial  
211 chlorophyll index (MTCI) was extracted from the Natural Environment Research Council Earth  
212 Observation Data Centre (NERC-NEODC, 2005) (<https://data.ceda.ac.uk/>). MTCI data is  
213 available globally as a monthly average at 4.63 km spatial resolution, and ranges from June 2002  
214 to December 2011. It is noted that valid MTCI values should be greater than 1, so our study  
215 deleted any values less than 1.

216 To avoid collinearity, we also reduced the dimensionality of vegetation indices based on  
217 ~~Pearson's correlation coefficient ( $r$  values)~~ (Fig. B3 in Appendix B). Most selected variables were  
218 related to growing seasons due that plant functional traits were measured during the growing  
219 season. Furthermore, based on the results of Pearson's correlation ~~coefficient ( $r$ )~~ analysis, MTCI,  
220 MIR, NIR, red and blue in January showed low correlations with those in growing season, thus



221 they were included in subsequent analysis. The final selection included 36 variables: annual EVI,  
222 monthly EVI (May, June, July, August and September), monthly MTCI, MIR, NIR, red and blue  
223 (all for January, June, July, August and September).

224 Both environmental variables and vegetation indices ~~variables~~ were resampled to a consistent  
225 spatial resolution of 1 km using the nearest neighborhood method.

226 PFT is also an important factor in influencing the variation of plant functional traits  
227 (Verheijen et al., 2016; Loozen et al., 2020), thus the trait predictions were performed for each  
228 PFT individually. We used the 2015 land cover map at a 100 m spatial resolution to calculate the  
229 relative abundance of each PFT within 1 km grid cells, which was extracted from the Copernicus  
230 Global Land Service (CGLS-LC100, Version 3) (<https://land.copernicus.eu/global/products/lc>)  
231 (Buchhorn et al., 2020). We focused on natural terrestrial vegetation, so all artificial land cover  
232 types or (e.g., croplands) areas were thus eliminated in our dataset. Seven categories were  
233 included: evergreen needleleaf forest (ENF), evergreen broadleaf forest (EBF), deciduous  
234 needleleaf forest (DNF), deciduous broadleaf forest (DBF), shrubland (SHL), grassland (GRL)  
235 and bare/sparse vegetation.

## 236 **2.4 Model fitting and validation**

237 To predict spatial patterns of plant functional traits, we used two machine learning models, i.e.,  
238 random forest and boosted regression trees.

239 Random forest is an ensemble machine learning method based on classification and  
240 regression trees using collections of regression trees to classify observations according to a set of  
241 predictive variables (Breiman, 2001). This method repeatedly constructs a set of trees from  
242 random samples of training data, and the final prediction is produced by integrating the results of  
243 all individual trees, which makes it a robust method. The model is controlled by two main  
244 parameters: the number of sampled variables (mtry) and the number of trees (ntree). The mtry was  
245 set to range from 1 to 57 (at an interval of 1), and the ntree was set as 500, 1000, 2000, 5000 and  
246 10000 in subsequent runs. This analysis was performed using the ‘randomForest’ function in the  
247 ‘randomForest’ package (Liaw and Wiener, 2002).

248 Boosted regression trees are machine learning methods based on generalized boosted  
249 regression models and using a boosting algorithm to combine many sample tree models to  
250 optimize predictive performance (Elith et al., 2006). There is no need for prior data transformation  
251 or the elimination of outliers, and this method can fit complex non-linear relationships while  
252 automatically handling interaction effects between predictors (Elith et al., 2008). The four  
253 parameters to optimize in these models are the number of trees, interaction depth, learning rate  
254 and bag fractions. We varied the parameter settings to find the optimal parameter combination that  
255 achieves minimum predictive error. The number of trees was set to 3000, the interaction depth  
256 varied from 1 to 7 (at an interval of 1), the learning rate was set to 0.001, 0.01, 0.05 and 0.1, and  
257 the bag fraction was set to 0.5, 0.6, 0.7 and 0.75. PFT was used as a dummy variable in the

258 boosted regression trees models. This analysis was conducted using the ‘gbm’ function in the  
 259 ‘gbm’ package (Ridgeway, 2006).

260 We built separate predictive model for each plant functional trait. To select the optimal  
 261 parameter combination and to evaluate the final model performance for each trait, we calibrated  
 262 the models 10 times using randomly selected 80% of the data for training ~~the~~ models and  
 263 validating against the remaining 20% based on cross-validation (Table B3 in Appendix B). The  
 264 predictive performance was evaluated by regressing the predicted and observed trait values from  
 265 all repetitions of the cross-validation. The fitting performances of the random forest and boosted  
 266 regression trees ~~were~~ was evaluated using determinate coefficient ( $R^2$ ), normalized root-mean-  
 267 square error (NRMSE) and mean absolute error (MAE). These scores are calculated following Eq.  
 268 (1), Eq. (2) and Eq. (3):

$$269 \quad R^2 = 1 - \frac{\sum_{i=1}^n (p_i - o_i)^2}{\sum_{i=1}^n (p_i - \hat{o}_i)^2} \quad (1)$$

$$270 \quad \text{NRMSE} = \frac{\sqrt{\frac{1}{n} \sum_{i=1}^n (p_i - o_i)^2}}{p_{\max} - p_{\min}} \quad (2)$$

$$271 \quad \text{MAE} = \frac{1}{n} \sum_{i=1}^n |o_i - p_i| \quad (3)$$

272 where  $p_i$  and  $o_i$  are the predictive values and observed values, respectively;  $\hat{o}_i$  is the mean of the  
 273 observed values.

274 To quantify the relative importance of each predictor across the two models consistently, we  
 275 used the method proposed by Thuiller et al. (2009). This method applies correlation between the  
 276 standard predictions fitted with the original data and predictions where the variable under  
 277 investigation has been randomly permuted. If the correlation is high, which indicates little  
 278 difference between the two predictions, the variable permuted is considered not important for the  
 279 model. This step was repeated multiple times for each predictor, and the mean correlation  
 280 coefficient over runs was recorded. Then the relative importance of each predictor was quantified  
 281 as one minus the Spearman rank correlation coefficient (see Boonman et al., 2020). In addition,  
 282 we used generalized additive models to fit the relationships between plant functional traits and the  
 283 most important variables using the ‘gam’ function in the ‘mgcv’ package.

## 284 **2.5 Generation of plant functional trait maps and model performance**

285 The generation of spatial maps of plant functional traits was performed in three steps. First, we  
 286 predicted trait values for each natural PFT (e.g.i.e., EBF, ENF, DBF, DNF, SHL and GRL) within 1  
 287 km grid cell separately. Second, the abundance of individual natural PFT within 1 km grid cell  
 288 was estimated using a land cover map with a spatial resolution of 100 m. Third, refer to the Eq. (4)  
 289 that has been widely applied in a community (Garnier et al., 2004), the final trait value in a given  
 290 1 km grid cell was calculated as the sum of the predicted trait values multiplying by corresponding  
 291 abundance of each natural PFT.

$$292 \quad \text{CWM} = \sum_{i=1}^n W_i X_i \quad (4)$$

293 where  $n$  is the total number of PFT in a given grid;  $W_i$  is the relative abundance of the  $i$ th natural  
294 PFT; and  $X_i$  is the predicted trait value of the  $i$ th natural PFT.

295 To reduce the variability of different single-models and to construct a more stable and  
296 accurate model, the ensemble model was further applied to merge the predictions of random forest  
297 and boosted regression trees according to their cross-validated  $R^2$  values. The ~~predictive-predicted~~  
298 value of ensemble model was calculated in a given grid cell as described by Eq. (5) (Marmion et  
299 al., 2009). The model accuracy was calculated by regressing the ~~predictive-predicted~~ values of  
300 ensemble model against the observed trait values.

$$301 \text{Pred\_EM}_t = \frac{\sum_{m=1}^2 (\text{pred}_{m,t} \times r_{m,t}^2)}{\sum_{m=1}^2 r_{m,t}^2} \quad (5)$$

302 where  $\text{Pred\_EM}_t$  is the ~~predictive-predicted~~ values of  $t$  trait in ~~the~~-ensemble model;  $\text{pred}_{m,t}$  is the  
303 ~~predictive-predicted~~ values of  $t$  trait in  $m$  model;  $r_{m,t}^2$  is the cross-validated  $R^2$  of  $t$  trait in  $m$  model.

304 To evaluate the model performance (i.e., the variability in the prediction across models), the  
305 coefficient of variation (CV) was calculated as the difference between the predictions of random  
306 forest and boosted regression trees methods and ~~the~~-ensemble ~~prediction~~model. CV is calculated  
307 as following Eq. (6):

$$308 \text{CV}_t = \frac{\sqrt{\sum_{m=1}^2 (\text{pred}_{m,t} - \text{obs}_t)^2 + r_{m,t}^2}}{\sum_{m=1}^2 r_{m,t}^2} \quad (6)$$

309 where  $\text{pred}_{m,t}$  is the ~~predictive-predicted~~ values of  $t$  trait in  $m$  model;  $\text{obs}_t$  is the values of  $t$  trait  
310 in ~~the~~-ensemble model;  $r_{m,t}^2$  is the cross-validated  $R^2$  of  $t$  trait in  $m$  model.

## 311 2.6 Uncertainty assessments

312 Multivariate environmental similarity surface analysis (MESS) was used to identify the range of  
313 the extrapolated predictor values across ~~the~~-locations in the plant trait dataset (Elith et al., 2010).  
314 This method is often used to evaluate the extent of extrapolation and the applicability domain. If  
315 the values ~~are-is~~ negative, this indicates that at a given grid cell, at least one predictor variable is  
316 outside the extent of ~~the~~ referenced predictor layer. This analysis was conducted using the ‘mess’  
317 function in the ‘dismo’ package.

318 All analyses were performed in R 4.0.2 (R Core Team, 2020).

## 319 3 Results

### 320 3.1 Performances of prediction models

321 Cross-validation showed that the performance of the predictive models differed greatly among the  
322 plant functional traits (Table 2, Tables C1 and C2 in Appendix C). WD had the best performance  
323 in all three models, with  $R^2$  values of 0.64, 0.68 and 0.67 for random forest, boosted regression  
324 trees and ensemble model, respectively. SLA and LPC had  $R^2$  values greater than 0.45, while  
325 LDMC performed the worst, with  $R^2$  values below 0.30.

326 **Table 2** Results of plant functional traits for cross-validated R<sup>2</sup>, NRMSE and MAE for  
 327 random forest, boosted regression trees and ensemble model.

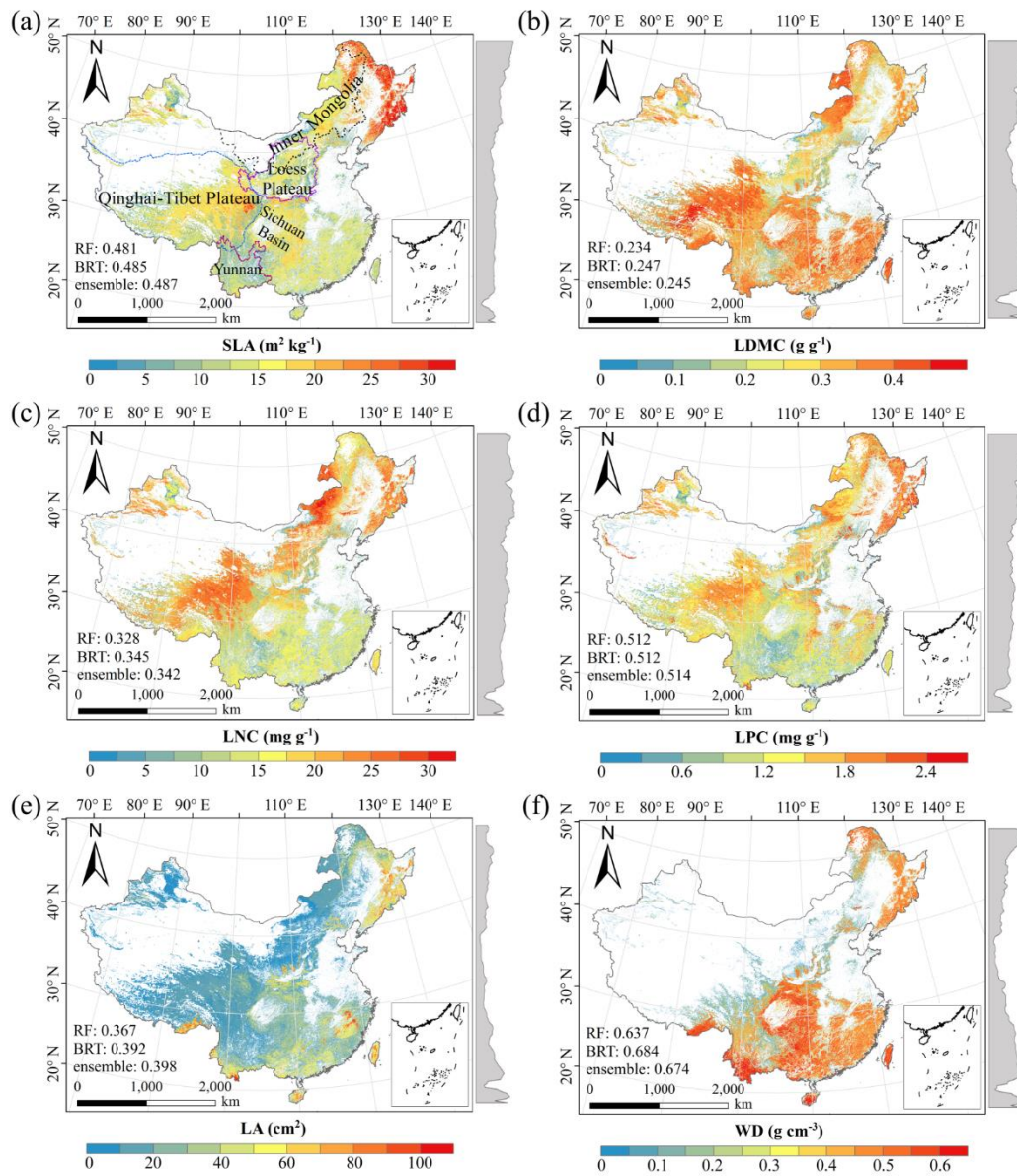
Traits	Random forest			Boosted regression trees			Ensemble model		
	R <sup>2</sup>	NRMSE	MAE	R <sup>2</sup>	NRMSE	MAE	R <sup>2</sup>	NRMSE	MAE
SLA	0.48	0.22	5.10	0.48	0.20	5.08	0.49	0.21	5.07
LDMC	0.23	0.21	0.07	0.28	0.18	0.07	0.24	0.20	0.07
LNC	0.33	0.19	4.92	0.34	0.18	4.85	0.34	0.19	4.85
LPC	0.51	0.24	0.53	0.51	0.22	0.53	0.51	0.27	0.53
LA	0.37	0.45	26.76	0.39	0.51	27.47	0.40	0.58	26.59
WD	0.64	0.20	0.10	0.68	0.13	0.10	0.67	0.17	0.10

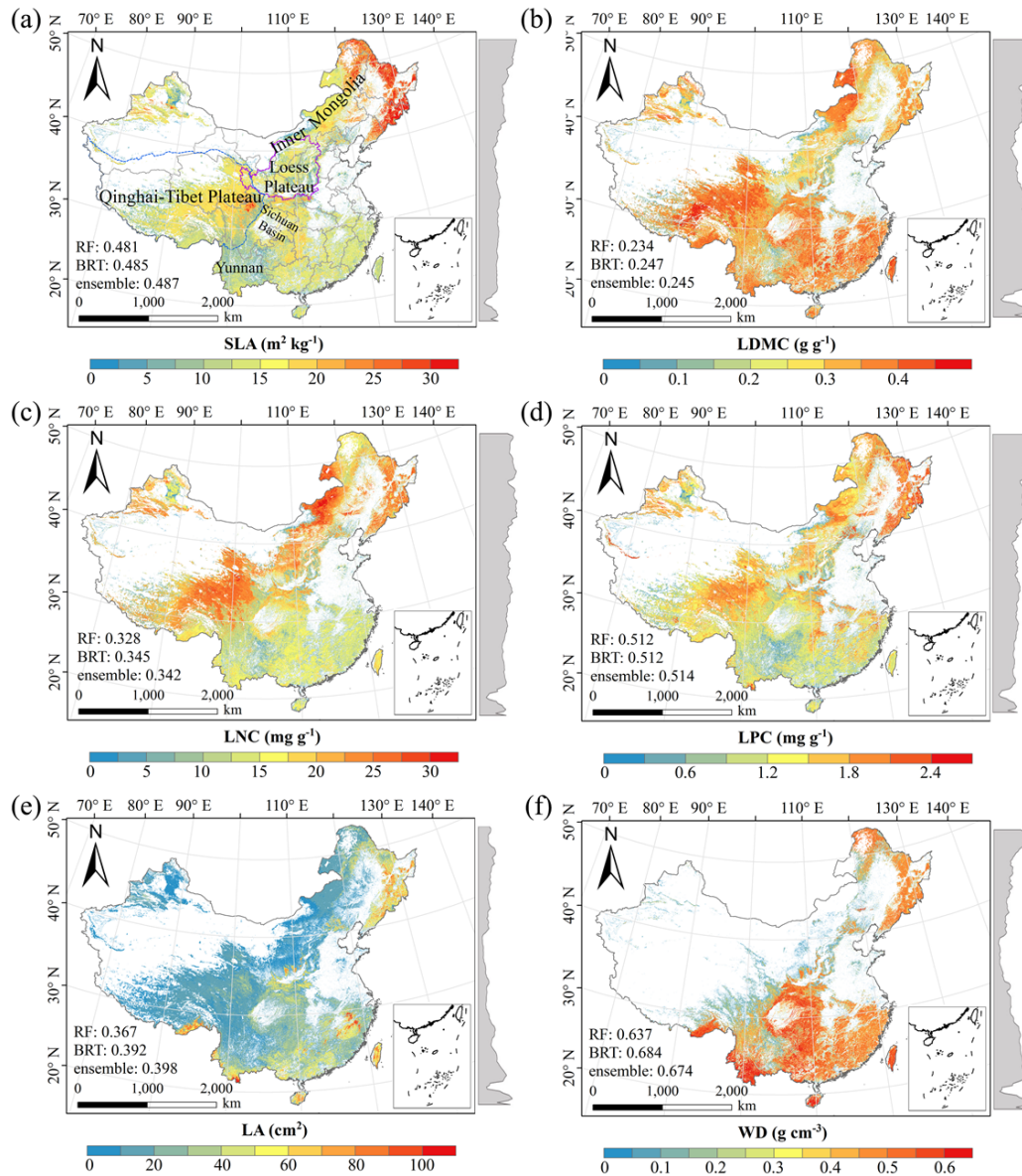
328 SLA, specific leaf area (m<sup>2</sup> kg<sup>-1</sup>); LDMC, leaf dry matter content (g g<sup>-1</sup>); LNC, leaf N concentration  
 329 (mg g<sup>-1</sup>); LPC, leaf P concentration (mg g<sup>-1</sup>); LA, leaf area (cm<sup>2</sup>); WD, wood density (g cm<sup>-3</sup>); R<sup>2</sup>,  
 330 determinate coefficient; NRMSE, normalized root-mean-square error; MAE, mean absolute error.

### 331 3.2 Spatial patterns of predicted plant functional traits

332 There were relatively consistent spatial patterns for SLA, LNC and LPC, with high values in the  
 333 northeastern and northwestern ~~regions-China~~ and the southeastern Qinghai-Tibet Plateau, and low  
 334 values in ~~the~~ southwestern China (Figs. 3a, 3c and 3d, Figs. D1, D2, D3, D5 and D6 in Appendix  
 335 D). SLA and LPC increased with latitude, while LNC did not vary significantly along ~~the~~  
 336 latitudinal gradient. For SLA, LNC and LPC, the variability was low among random forest,  
 337 boosted regression trees and ensemble model, with an overall CV less than 0.30 (Figs. 4a, 4c and  
 338 4d). LDMC values were relatively high in most regions of China, and the low values were mainly  
 339 located in ~~the~~ eastern Yunnan ~~Province~~ and the Loess Plateau (Fig. 3b, Figs. D1, D2 and D4 in  
 340 Appendix D). LA showed high values in the northeastern and southern regions (except for the  
 341 Sichuan Basin), and the southeastern Qinghai-Tibet Plateau (Fig. 3e, Figs. D1, D2 and D7 in  
 342 Appendix D). The strong latitudinal gradient was observed in LA, where the values decreased  
 343 with latitude.

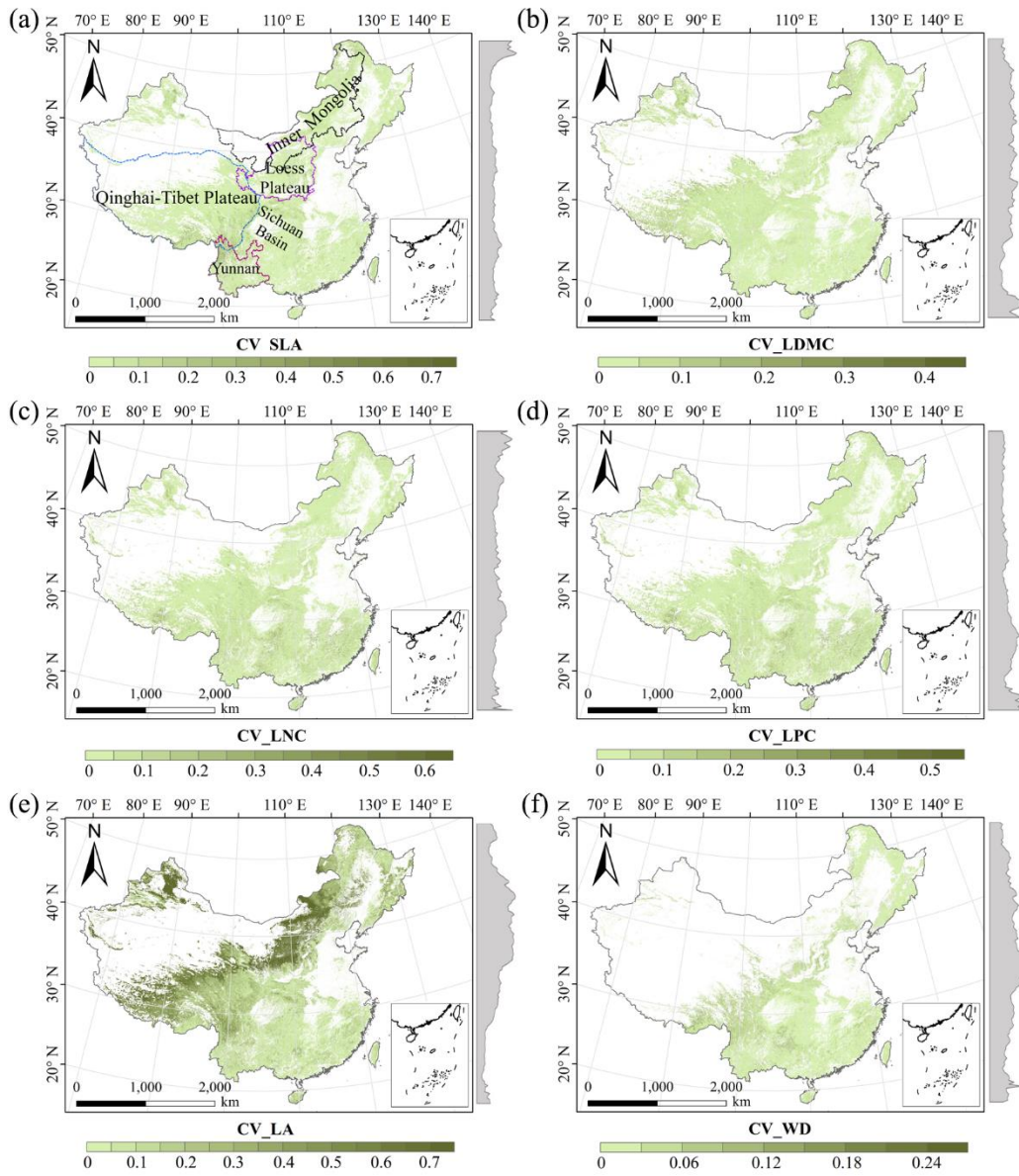
344 The CV values of LPC decreased with latitude, but other traits did not show latitudinal  
 345 patterns (Fig. 4). The CV values of LA were relatively high, especially in the northwestern ~~region~~  
 346 ~~China~~ and the Inner Mongolia-Loess Plateau region (Fig. 4e). WD had high values in the  
 347 northeastern and southern regions (Fig. 2f, Figs. D1, D2 and D8 in Appendix D), while CV values  
 348 for WD ~~in-China~~ were low throughout China (Fig. 4f).

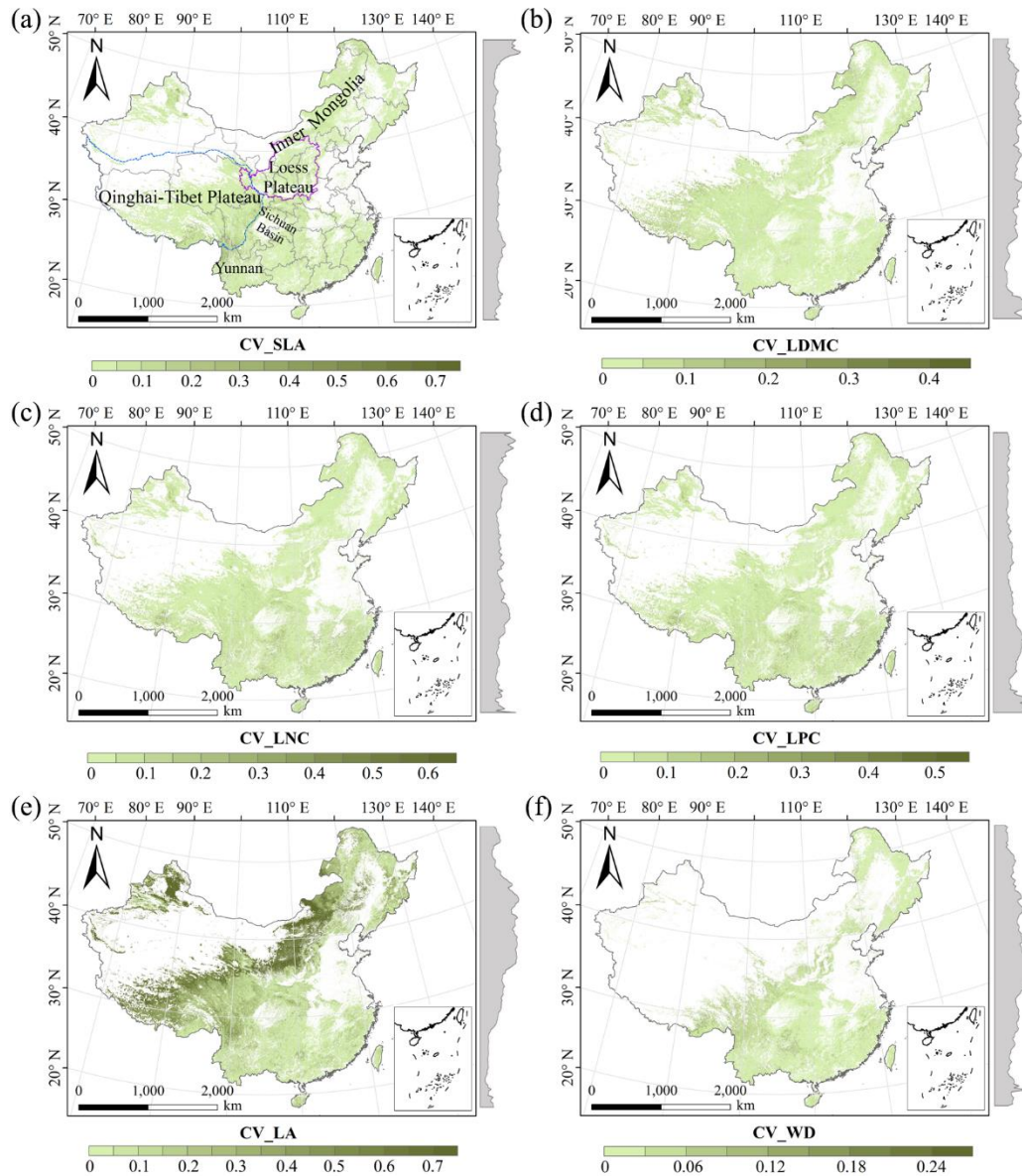




350

351 **Figure 3.** Spatial patterns of predicted plant functional traits in China based on the ensemble  
 352 model. The grey curves to the right of the maps display trait distribution along with latitude. The  
 353 white areas represent artificial land cover types and bare vegetation. The lines in grey, blue and  
 354 purple represent the boundaries of province, the Qinghai-Tibet Plateau and the Loess Plateau,  
 355 respectively. RF, random forest; BRT, boosted regression trees; ensemble, ensemble model; SLA,  
 356 specific leaf area; LDMC, leaf dry matter content; LNC, leaf N concentration; LPC, leaf P  
 357 concentration; LA, leaf area; WD, wood density.





359

360 **Figure 4.** The variability in plant functional trait predictions among random forest, boosted  
 361 regression trees and ensemble model. The grey curves to the right of the maps display coefficient  
 362 of variation along with latitude. The white areas represent artificial land cover types and bare  
 363 vegetation. The lines in grey, blue and purple represent the boundaries of province, the Qinghai-  
 364 Tibet Plateau and the Loess Plateau, respectively. SLA, specific leaf area; LDMC, leaf dry matter  
 365 content; LNC, leaf N concentration; LPC, leaf P concentration; LA, leaf area; WD, wood density.

### 366 3.3 Relative importance of predictive variables

367 The dominant factors explaining spatial variation differed greatly among plant functional traits  
 368 (Table 3). Overall, climate variables were more important for predicting plant functional traits  
 369 than were soil variables. Temperature variables (i.e., MAT, MDR and TS) showed close  
 370 relationships with SLA, LDMC, LPC and WD, while precipitation variables (i.e., PS, PEQ, MAP



371 and PDQ) were more important for predicting the spatial patterns of LNC, LPC and LA. RAD was  
 372 the fourth most dominant factor in predicting the spatial patterns of SLA and WD. Elevation also  
 373 played an important role in ~~the~~-LDMC and LPC predictions. Within soil variables, soil nutrients  
 374 (i.e., pH and SAP) showed close associations with SLA and LNC. In addition to the environmental  
 375 variables, MTCI emerged as an important predictor for explaining SLA, LDMC and LA. Finally,  
 376 EVI was the most important predictor for LA, and MIR in January and May were the primary  
 377 predictors of WD. The relationships between plant functional traits and the most important  
 378 variables were shown in Figs. E1 and E2 in Appendix E.

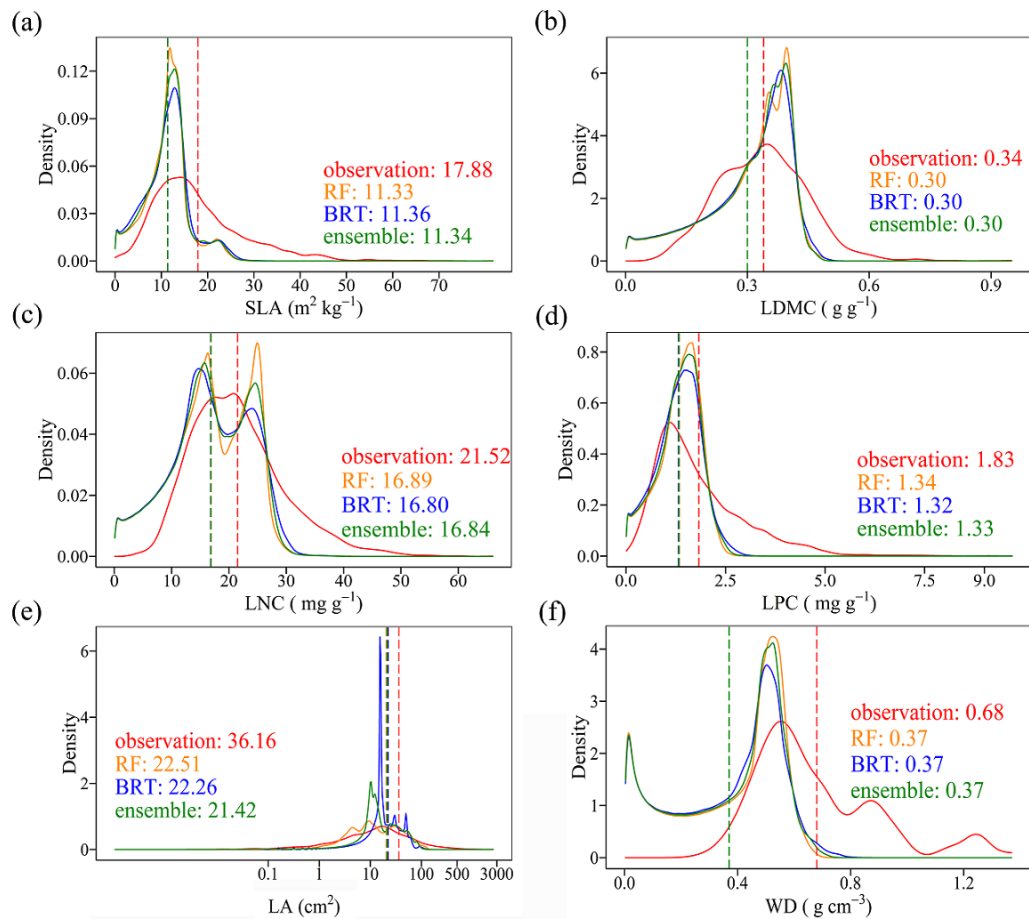
379 **Table 3** List of the eight most important variables for plant functional trait predictions.

Rank	SLA	LDMC	LNC	LPC	LA	WD
1	SAP	MAT	PS	MDR	EVI5	MIR1
2	TS	Elevation	SAP	PDQ	PEQ	TS
3	blue9	MTCI5	pH	Elevation	MTCI9	MIR5
4	RAD	blue8	MDR	MIR8	NIR9	RAD
5	MTCI4	MTCI4	MAP	Tmax	AI	MIR6
6	MTCI6	MTCI6	PEQ	MTCI6	MTCI6	pH
7	Elevation	NIR1	MIR1	MIR7	MAP	red5
8	MTCI7	CEC	Tmax	MIR9	red5	PS

380 SLA, specific leaf area ( $\text{m}^2 \text{kg}^{-1}$ ); LDMC, leaf dry matter content ( $\text{g g}^{-1}$ ); LNC, leaf N concentration  
 381 ( $\text{mg g}^{-1}$ ); LPC, leaf P concentration ( $\text{mg g}^{-1}$ ); LA, leaf area ( $\text{cm}^2$ ); WD, wood density ( $\text{g cm}^{-3}$ ); SAP, soil  
 382 available P; TS, temperature seasonality; blue, blue reflectance; RAD, solar radiation; MTCI, MERIS  
 383 terrestrial chlorophyll index; MAT, mean annual temperature; NIR, near-infrared reflectance; CEC,  
 384 cation exchange capacity; PS, precipitation seasonality; MDR, mean diurnal range; MAP, mean annual  
 385 precipitation; PEQ, precipitation of ~~the~~ wettest quarter of a year; MIR, middle infrared reflectance;  
 386 Tmax, max temperature of ~~the~~ warmest month of a year; PDQ, precipitation of ~~the~~ driest quarter of a  
 387 year; EVI, enhanced vegetation index; AI, aridity index; red, red reflectance.

### 388 3.4 Model performance

389 The distributions of the ~~predictive-predicted~~ ~~trait~~-values based on random forest, boosted  
 390 regression trees, and ensemble model were consistent with the original ~~trait~~-observations,  
 391 especially the peak values (Fig. 5). The mean values of trait observations were relatively higher  
 392 than those of the ~~predictive-predicted~~ values.

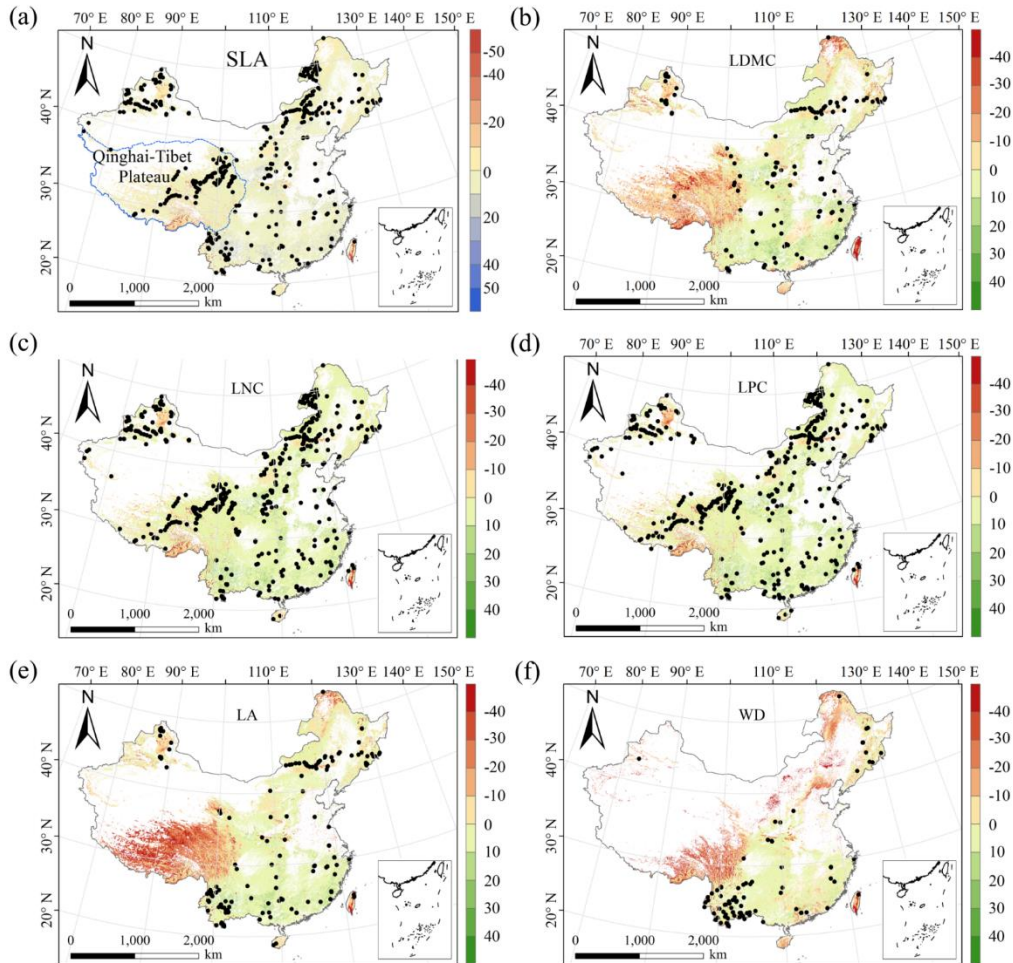


393

394 **Figure 5.** Comparison of trait distribution between observations and predictions predictive  
 395 values in each of the different three models. Each panel depicts the distribution of observations in  
 396 solid red, of the random forest (RF) ~~model~~ in yellow, of the boosted regression trees (BRT) ~~model~~  
 397 in blue, and of the ensemble model in green. The dashed vertical lines indicate mean values. SLA,  
 398 specific leaf area; LDMC, leaf dry matter content; LNC, leaf N concentration; LPC, leaf P  
 399 concentration; LA, leaf area; WD, wood density.

### 400 3.5 Uncertainty assessments

401 The MESS values of all plant functional traits were positive in most regions, indicating a wide  
 402 applicability domain of our models (Fig. 6). Nevertheless, trait predictions should be interpreted  
 403 carefully for the northeastern China and the Qinghai-Tibet Plateau due to ~~the~~ sparse samplings in  
 404 these regions.



405

406

407

408

409

410

411

412

**Figure 6.** Multivariate environmental similarity surface (MESS) assessments for the six plant functional traits. The blue line represents the boundary of the Qinghai-Tibet Plateau. The black dots represented the locations of trait observations. More intense shades indicate greater similarity (blue) or difference (red) in environmental conditions of the location compared to the predictive factors covered by the training dataset. The white areas represent artificial land cover types and bare vegetation. SLA, specific leaf area; LDMC, leaf dry matter content; LNC, leaf N concentration; LPC, leaf P concentration; LA, leaf area; WD, wood density.

413

## 4 Discussion

414

### 4.1 Comparison with previous work

415

416

417

418

419

420

Our study predicted the spatial patterns of six key plant functional traits across China using machine learning methods and identified the applicability domain of the models. WD had the highest precision with an average of  $R^2$  of 0.66, which was higher than the global WD prediction (Boonman et al., 2020). This improvement in precision may be attributed to the large number and dense occurrence of sample sites as well as the inclusion of vegetation indices in our study. In addition, SLA and LPC also showed good accuracy with  $R^2$  values of 0.50, which was higher than

421 that of Boonman et al. (2020) and consistent with that of Moreno-Martínez et al. (2018). However,  
422 LNC and LA showed relatively poor performance, which may be related to the reason that these  
423 two traits were more influenced by phylogeny than environmental variables (Yang et al., 2017; An  
424 et al., 2021). In addition, we found that mean values of trait predictions were lower than those of  
425 observations, which may be attributable to the reason that the mean values of trait observations  
426 were from the individual level, while the mean values of predicted values were based on the  
427 relative abundance of PFTs and corresponding predicted values within 1 km grid cell.

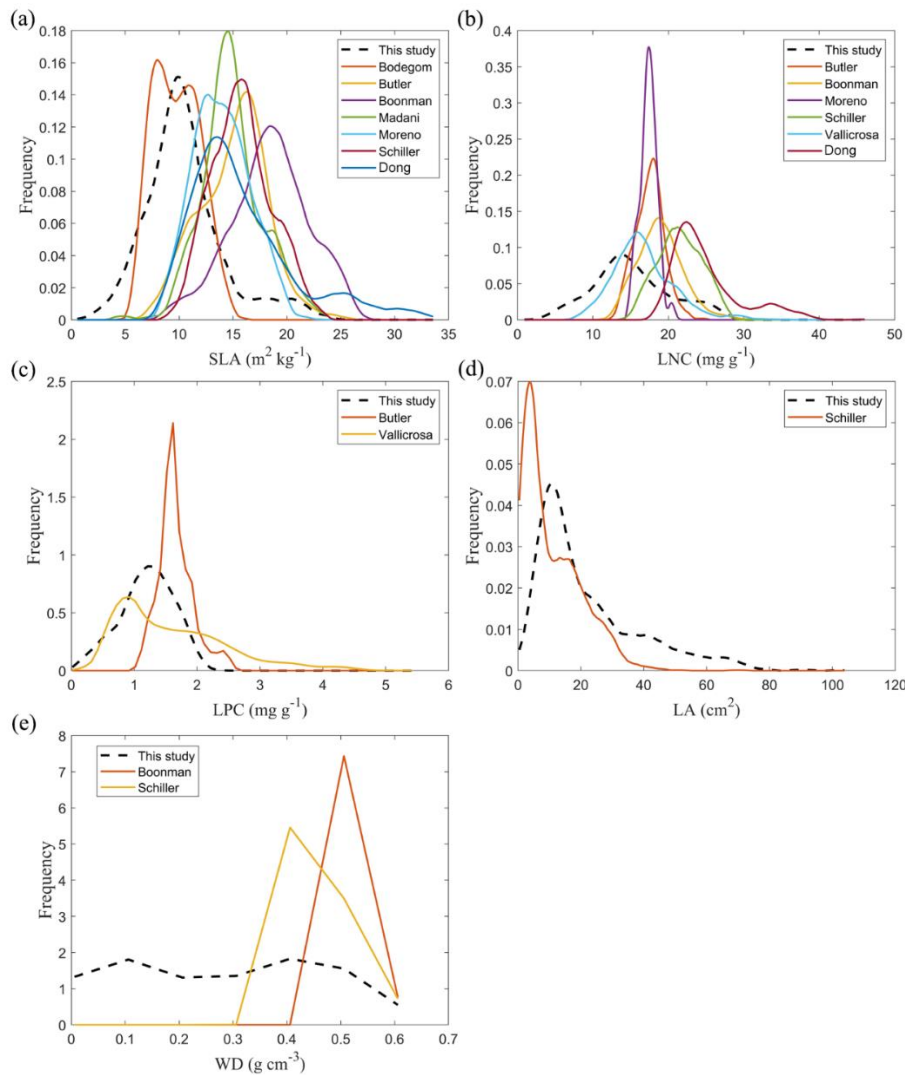
428 The frequency distributions of plant functional traits in China differed between our study and  
429 previous studies (Fig. 7, Fig. F1, Table F1 in Appendix F). Given that the spatial resolution of trait  
430 maps in most previous studies ~~is~~ was  $0.5^\circ$  (except for Moreno-Martínez et al. (2018) and  
431 Vallicrosa et al. (2022)), we resampled the data products of previous studies and our study to  $0.5^\circ$   
432 spatial resolution. The distributions in our study contained more predictions at lower values of  
433 SLA, LNC and LPC and ~~was~~ were broader than those for SLA and LNC in previous global studies.  
434 However, the distribution of LNC in our study was consistent with that in the study of Vallicrosa  
435 et al. (2022) ~~at with a 1 km spatial resolution the 1 km spatial resolution~~ (Fig. F1 in Appendix F).  
436 LA in our study contained more predictions at higher values and was also broader than those in  
437 previous global studies. WD did not show ~~the~~ lower and higher ~~predictive~~ predicted values in this  
438 study, however, the WD values in the studies of Boonman et al. (2020) and Schiller et al. (2021)  
439 had more predictions at higher values and no lower values ( $< 0.30 \text{ g cm}^{-3}$ ). Our predicted values of  
440 SLA showed the highest spatial correlation with those of Dong et al. (2023), and LNC showed the  
441 strongest spatial correlation with those of Butler et al. (2017) (Table 54). LA and WD showed the  
442 best spatial correlation with those of Schiller et al. (2021), but LPC showed relatively weak spatial  
443 correlation with those of published studies.

444 In addition, we compared our results ~~to~~ with the other studies focused on China. Yang et al.  
445 (2016) predicted the spatial distributions of leaf mass per area (i.e.,  $1/\text{SLA}$ ) and LNC based on  
446 trait-environment relationships in China and had ~~an~~ R<sup>2</sup> values of 0.13-0.16. The lower predictive  
447 precision may be because Yang et al. (2016) only used MAT, MAP and RAD as predictors in  
448 estimating the spatial patterns of leaf mass per area and LNC, which likely led to poor  
449 performance and low heterogeneity. These results also demonstrated the advantage of our methods  
450 in mapping the spatial patterns of plant functional traits at a regional scale.

451 **Table 5-4** Spatial correlations for SLA, LNC, LPC, LA and WD between this study and other  
 452 previous trait maps, labelled by the first author of the corresponding publication (see Table F1 in  
 453 Appendix F for citations)

Spatial correlation	Dong	Vallicrosa	Schiller	Boonman	Moreno	Madani	Butler	Bodegom
SLA	<u>0.398</u> <u>0.40</u>		-0.082	<u>0.32733</u>	0.242	<u>0.13614</u>	-0.042	<u>0.31932</u>
LNC	0.156	<u>0.35936</u>	<u>0.22923</u>	0.252			0.394	
LPC		<u>0.13614</u>					<u>0.05706</u>	
LA			0.514					
WD			<u>0.64765</u>	<u>0.10711</u>				

454 The spatial correlation of leaf dry matter content (LDMC) between our study and previous studies was  
 455 not included, as the LDMC maps were not available. SLA, specific leaf area ( $\text{m}^2 \text{kg}^{-1}$ ); LNC, leaf N  
 456 concentration ( $\text{mg g}^{-1}$ ); LPC, leaf P concentration ( $\text{mg g}^{-1}$ ); LA, leaf area ( $\text{cm}^2$ ); WD, wood density ( $\text{g cm}^{-3}$ ).  
 457



458  
 459 **Figure 7.** Frequency distributions of plant functional traits in our study (“This study”, dashed  
 460 black lines) and other trait maps, identified by the first author of the corresponding publication

461 (see Table F1 for citations). SLA, specific leaf area ( $\text{m}^2 \text{kg}^{-1}$ ); LNC, leaf N concentration ( $\text{mg g}^{-1}$ );  
462 LPC, leaf P concentration ( $\text{mg g}^{-1}$ ); LA, leaf area ( $\text{cm}^2$ ); WD, wood density ( $\text{g cm}^{-3}$ ).

## 463 **4.2 Spatial patterns of plant functional traits in China**

464 Our study revealed the spatial patterns of different plant functional traits across China, and the  
465 variability among the two machine learning methods was relatively low. We compared the spatial  
466 differences of trait maps between our study and previous studies at the global scale (Figs. F2-F6 in  
467 Appendix F). For example, our study showed high SLA values in the southeastern Qinghai-Tibet  
468 Plateau, which concurred with the global study of Boonman et al. (2020). The spatial difference of  
469 SLA between our study and [van Bodegom et al. \(2014\)](#) was relatively low, and the ~~predictive~~  
470 ~~predicted~~ values in most regions were slightly lower in our study than those in [van Bodegom et al.](#)  
471 (2014). The spatial pattern of difference in SLA between our study and [Moreno et al. \(2018\)](#),  
472 [Bulter et al. \(2017\)](#) and [van Bodegom et al. \(2020/2014\)](#) was consistent, and the values were higher  
473 in [the](#) northeastern China and [the](#) southwestern Qinghai-Tibet Plateau in our study than those  
474 studies. Our study showed higher LNC values in the northern Inner Mongolia-the Loess Plateau-  
475 the eastern Qinghai-Tibet Plateau and [the](#) northwestern China than those ~~global studies-at the~~  
476 ~~global studies-~~ ([Butler et al., 2017](#); [Moreno-Mart ínez et al., 2018](#); [Boonman et al., 2020](#); [Vallicrosa](#)  
477 [et al., 2022](#); [Dong et al., 2023](#)), reflecting the consistent spatial pattern among these studies.  
478 However, [Yang et al. \(2016\)](#) predicted high LNC values in [the](#) northeastern and [the](#) northwestern  
479 China, [the](#) northern Inner Mongolia and the entire Qinghai-Tibet Plateau, and SLA and LNC had  
480 low heterogeneity overall. The discrepancy with [Yang et al. \(2016\)](#) may be attributed to spatial  
481 extrapolation based on trait-climate relationships with a low predictive precision. There was no  
482 consistent spatial pattern in LPC between our study and previous studies. Consistent with the  
483 global pattern ([Wright et al., 2017](#)), LA was larger in [the](#) southern regions than in [the](#) northern  
484 regions and showed a decreasing trend with latitude. In addition, LA and WD values in our study  
485 were lower in most regions than those ones at the global scale. These discrepancies between our  
486 study and previous studies at the global scale may be related to three reasons. First, there is bias in  
487 the available in-situ field measurement data from China in ~~these~~-global studies, with [a large gaps](#)  
488 in [the](#) western China for SLA and no data in China for WD ([Boonman et al., 2020](#)). Second, some  
489 trait-environment relationships may be scale-dependent ([Bruehlheide et al., 2018](#)), and these studies  
490 we compared are from the global scale because the trait maps in China are not available. Third, the  
491 methods used for trait mapping were different among studies, including eco-evolutionary  
492 optimality models ([Dong et al., 2023](#)), Convolutional Neural Networks based on RGB  
493 photographs ([Schiller et al., 2021](#)), machine learning algorithms ([Vallicrosa et al., 2022](#); [Boonman](#)  
494 [et al., 2020](#)) and multiple regression analysis ([van Bodegom et al., 2014](#)).

495 Moreover, our study also identified the applicability domain of our models for predicting the  
496 spatial patterns of plant functional traits across China. Five leaf traits and WD appeared to have  
497 poor applicability in [the](#) northeastern China and the Qinghai-Tibet Plateau, primarily due to sparse

498 samplings. Future studies predicting plant functional traits across a large scale through remote  
499 sensing observations or other supplementary data will be needed to re-evaluate our results.

### 500 **4.3 The role of predictive variables**

501 Our study ~~indicates~~indicated that environmental variables ~~are~~were important for predicting the  
502 spatial patterns of plant functional traits, especially climate variables. Temperature variables were  
503 primary predictors for SLA, LDMC, LPC and WD. The relationships between leaf traits and  
504 temperature have been widely discussed in global and regional studies (Reich and Oleksyn, 2004;  
505 Bruelheide et al., 2018). The positive linkage between WD and temperature may be driven by  
506 changes in water viscosity. Plants can adapt to ~~the~~ low water viscosity at high temperatures by  
507 reducing the diameter and density of their vessels and ~~by~~ thickening cell walls (Roderick and  
508 Berry, 2002; Thomas et al., 2004). Precipitation variables were important predictors for leaf  
509 nutrient traits and LA. For example, precipitation of ~~the~~ wettest quarter of a year was the factor  
510 that most influenced LA variation, which has been confirmed by a previous study (An et al., 2021).  
511 A smaller LA could be an adaptive strategy to decrease water loss via reducing the surface area for  
512 transpiration under dry environmental conditions (Du et al., 2019). Although the effects of soil on  
513 trait predictions were relatively weak, we found that SAP and pH played key roles in SLA and  
514 LNC predictions. These results were similar with the previous studies ~~that reported~~reporting that  
515 soil pH was an important driver of trait variation at the global scale and in tundra regions (Maire et  
516 al., 2015; Kemppinen et al., 2021). Additionally, from the perspective of cost-efficient theory, the  
517 strong effects of SAP reflected that high SLA may be an adaptation for facilitating soil exploration  
518 more efficiently in fertile soils (Freschet et al., 2010).

519 Vegetation indices have recently been proposed as important predictors of spatial patterns of  
520 plant functional traits (Loozen et al., 2018). Our results corroborated these findings and further  
521 suggested that EVI, MTCI and MIR reflectance ~~are~~were important predictors in models. Here, the  
522 underlying mechanisms between vegetation indices and plant functional traits ~~are~~were not further  
523 discussed due to their complexity~~and uncertainty~~. However, our results indicated that vegetation  
524 indices and NIR reflectance ~~are~~were not key predictors of LNC estimation, which ~~contrasts~~  
525 contrasted the findings from global and regional studies (Wang et al., 2016; Loozen et al., 2018;  
526 Moreno-Martínez et al., 2018). This may be related to the multitude of factors that influence the  
527 relationships between LNC and vegetation indices and NIR reflectance, such as forest type and  
528 canopy structure (Dahlin et al., 2013).

### 529 **4.4 Uncertainties**

530 Although our study mapped the spatial patterns of key functional traits ~~in terrestrial ecosystems~~  
531 ~~seed plants in~~across China through large-scale field investigations and compared the predictions  
532 with previous studies ~~performed~~ at global and regional scales, there ~~persists~~persisted some  
533 uncertainties in the interpretation of these results. First, the predictive ability of models was

534 relatively worse for certain traits, especially LDMC. Beyond the environmental effects, the  
535 variation in plant functional traits is also regulated by phylogenetic structure among plant species  
536 (e.g., family, order and phylogenetic clade) (Li et al., 2017). Consequently, incorporating ~~the~~  
537 phylogenetic information will be a promising avenue for further improving the accuracy of spatial  
538 predictions of plant functional traits (Butler et al., 2017). A second potential issue is sampling bias;  
539 there ~~were-are~~ major spatial gaps in field investigations in ~~both~~ the northeastern China and the  
540 Qinghai-Tibet Plateau. Due to the few measurements for shrubs and ~~the lack of~~ herbs, WD data is  
541 mainly confined to eastern forests, and the overall quantity of WD data ~~was-is~~ much lower than  
542 that of leaf traits, even in the TRY database. The environmental information of sampling sites was  
543 not always obtained from original literature, thus using the public environmental products is a  
544 common resolution in large-scale plant trait studies (Boonman et al., 2020; Vallicrosa et al., 2022).  
545 Such mismatch between in-situ trait measurements and predictors should be resolved in further  
546 work. Finally, ~~an~~ additional key challenges in data availability must be resolved to scale up from  
547 the species to the community levels, in particular with data surrounding species co-occurrence and  
548 their relative cover or abundance in ecological communities (He et al., 2023). For example, Global  
549 biodiversity data (e.g., sPlot and Global Biodiversity Information Agency databases) that contains  
550 information on species occurrence or the proportion of species in a community has the potential  
551 for enabling the calculation of community-weighted trait values and the re-evaluation of our  
552 results in future work (Telenius, 2011; Bruelheide et al., 2019). The lack of consistent time period  
553 and spatial resolution of predictors due to limitation of data availability is ~~another-a~~ key challenge  
554 in the spatial mapping of plant functional traits. In addition, although WorldClim version 2.1  
555 product has high spatial resolution and includes various aspects of climatic parameters, there  
556 exists certain limitation and uncertainty in predicting trait maps. Therefore, integrating satellite  
557 remote sensing monitoring methods with in-situ trait data ~~collection~~ can also provide an effective  
558 way to estimate and assess the species diversity at large scales (Cavender-Bares et al., 2022).

#### 559 **4.5 Potential applications**

560 Maps of these key functional traits ~~in terrestrial ecosystem of seed plants~~ highlighted large-scale  
561 variability in space, which will significantly advance ecological analyses and future  
562 interdisciplinary research. First, using the spatially continuous trait maps, one can optimize and  
563 develop trait-flexible vegetation models to reduce ~~uncertainties-uncertainty~~ of conventional  
564 vegetation models based on PFTs, which allows for ~~the~~ exploration of the community assembly  
565 rules based on how plants with different trait combinations perform under a given set of  
566 environmental conditions (Berzaghi et al., 2020). When trait-flexible vegetation models are  
567 available, incorporating trait maps into models will bridge the gap for vegetation classifications  
568 and predictions of vegetation distribution under global change (~~Van-van~~ Bodegom et al., 2012;  
569 Yang et al., 2019). Second, most studies focused on the effects of plant functional traits on  
570 ecosystem carbon processes at individual, species and community scales, while how such effects



571 scale up to regional or larger scales remains challenging. In addition, the assessments of China's  
572 terrestrial ecosystem carbon sink have ~~had~~ large uncertainties ~~so far~~ (Piao et al., 2022). The spatial  
573 continuous trait maps will provide an effective way to link ecosystem characteristics to ecosystem  
574 carbon sink estimates in China (Madani et al., 2018; Šímová et al., 2019). These analyses will help  
575 shed light on the mechanisms underlying plant functional traits and terrestrial ecosystem carbon  
576 storage at a large scale.

## 577 **5 Data availability**

578 The original plant functional trait data collected in this study that ~~were~~ was used for machine  
579 learning models (named by Data file used for machine learning models.csv) and final maps of  
580 plant functional traits ~~in a GeoTIFF format in terrestrial ecosystems in a GeoTIFF format across~~  
581 ~~China~~ (named by plant functional trait category) are now available for the private link  
582 <https://figshare.com/s/c527c12d310cb8156ed2> (An et al., 2023). Once the article is accepted, we  
583 will publicly publish ~~these maps~~ data at the figshare website.

## 584 **6 Conclusions**

585 We generated a set of spatial continuous trait maps at a 1-km spatial resolution using machine  
586 learning methods in combination with field measurements, environmental variables and vegetation  
587 indices. Models for leaf traits (except for LDMC) and WD showed good accuracy and robustness,  
588 whereas models of LDMC had relatively poor precision and robustness. Temperature variables  
589 were the most important predictors for leaf traits (except for LA) and WD, and precipitation  
590 variables were the most important predictors for leaf nutrient traits and LA. We caution that plant  
591 functional trait predictions should be interpreted carefully for the northeastern China and the  
592 Qinghai-Tibet Plateau. The spatial continuous trait maps generated in our study are  
593 complementary to current terrestrial in-situ observations and offer new avenues for predicting  
594 large-scale changes in vegetation and ecosystem functions s under climate scenarios in China.

595

## 596 **Appendix A Data collection from literature**

- 597 An H. and Shangguan Z. P. Photosynthetic characteristics of dominant plant species at different succession stages  
598 of vegetation on Loess Plateau. Chinese Journal of Applied Ecology, 2007, 18, 1175-1180.
- 599 Bai K. D., Jiang D. B., Wan C. X. Photosynthesis-nitrogen relationship in evergreen and deciduous tree species at  
600 different altitudes on Mao'er Mountain, Guangxi. Acta Ecologica Sinica, 2013, 33, 4930-4938.
- 601 Bai W. J., Zheng F. L., Dong L. L., et al. Leaf traits of species in different habits in the water-wind erosion region  
602 of the Loess Plateau. Acta Ecologica Sinica, 2010, 30, 2529-2540.
- 603 Chai Y F., Shang H. L., Zhang X. F., et al. Ecological variations of woody species along an altitudinal gradient in  
604 the Qinling Mountains of Central China: area-based versus mass-based expression of leaf traits. Journal of  
605 Forestry Research, 2021, 32, 599-608.
- 606 Chang Y. N., Zhong Q. L., Cheng D. L., et al. Stoichiometric characteristics of C, N, P and their distribution

607 pattern in plants of *Castanopsis carlesii* natural forest in Youxi. *Journal of Plant Resources and Environment*,  
608 2013, 22, 1-10.

609 Chen F. Y., Luo T. X., Zhang L., et al. Comparison of leaf construction cost in dominant tree species of the  
610 evergreen broadleaved forest in Jiulian Mountain, Jiangxi Province. *Acta Ecologica Sinica*, 2006, 26, 2485-  
611 2493.

612 Chen H. Y., Huang Y. M., He K. J., et al. Temporal intraspecific trait variability drives responses of functional  
613 diversity to interannual aridity variation in grasslands. *Ecology and Evolution*, 2018, 9, 5731-5742.

614 Chen L. X., Xiang W. H., Wu H. L., et al. Tree growth traits and social status affect the wood density of pioneer  
615 species in secondary subtropical forest. *Ecology and Evolution*, 2017, 7, 5366-5377.

616 Chen L., Yang X. G., Song N. P., et al. Leaf water uptake strategy of plants in the arid-semiarid region of Ningxia.  
617 *Journal of Zhejiang University*, 2013, 39, 565-574.

618 Chen Y. H., Han W. X., Tang L. Y., et al. Leaf nitrogen and phosphorus concentrations of woody plants differ in  
619 responses to climate, soil and plant growth form. *Ecography*, 2011, 36, 178-184.

620 Cheng J. H., Chu P. F., Chen D. M., et al. Functional correlations between specific leaf area and specific root length  
621 along a regional environmental gradient in Inner Mongolia grasslands. *Functional Ecology*, 2016, 30, 985-997.

622 Cheng W., Yu C. H., Xiong K. N., et al. Leaf functional traits of dominant species in karst plateau-canyon areas.  
623 *Guihaia*, 2019, 39, 1039-1049.

624 Dong H. and Shekhar R. B. Negative relationship between interspecies spatial association and trait dissimilarity.  
625 *Oikos*, 2019, 128, 659-667.

626 Dong T. F., Feng Y. L., Lei Y. B., et al. Comparison on leaf functional traits of main dominant woody species in  
627 wet and dry habitats. *Chinese Journal of Ecology*, 2012, 31, 1043-1049.

628 Du H. D. Ecological responses of foliar anatomical structural & physiological characteristics of dominant plants at  
629 different site conditions in north Shaanxi Loss Plateau. 2010, Graduation Thesis.

630 Fan Z. X., Zhang S. B., Hao G. Y., et al. Hydraulic conductivity traits predict growth rates and adult stature of 40  
631 Asian tropical tree species better than wood density. *Journal of Ecology*, 2012, 100, 732-741.

632 Feng J. B., Fan S. X., Hou Y. F., et al. Interspecific and intraspecific variation of leaf function traits of herbaceous  
633 plants in a forest-steppe zone, Hebei Province, China. *Journal of Northeast Forestry University*, 2021, 49, 23-  
634 28.

635 Feng Q. H. The study on the response of foliar  $\delta^{13}C$  of different life form plants to altitude in subalpine area of  
636 Western Sichuan, China. 2011, Graduation Thesis.

637 Fu P. L., Zhu S. D., Zhang J. L., et al. The contrasting leaf functional traits between a karst forest and a nearby  
638 non-karst forest in south-west China. *Functional Plant Biology*, 2019, 46, 907-915.

639 Gao S. P., Li J. X., Xu M. C., et al. Leaf N and P stoichiometry of common species in successional stages of the  
640 evergreen broad-leaved forest in Tiantong National Forest Park, Zhejiang Province, China. *Acta Ecologica  
641 Sinica*, 2007, 27, 947-952.

642 Geekiyana N., Goodale, U. M., Cao, K. F., et al. Leaf trait variations associated with habitat affinity of tropical  
643 karst tree species. *Ecology and Evolution*, 2017, 8, 286-295.

644 Geng Y., Ma W. H., Wang L., et al. Linking above- and belowground traits to soil and climate variables: an  
645 integrated database on China's grassland species. *Ecology*, 2017, 98, 1471.

646 Guo F. C. The photosynthetic characteristics of precious broad-leaved tree species in south subtropics and their  
647 relationship with leaf functional traits. 2015, Graduation Thesis.

648 Guo W. J. Exploring the relationship between arbuscular mycorrhizal fungi and plant based on phylogeny and  
649 plant traits. 2015, Graduation Thesis.

650 Hau C. H. Tree seed predation on degraded hillsides in Hong Kong. *Forest Ecology & Management*. 1997, 99,

651 215-221.

652 He J. S., Wang Z. H., Wang X. P., et al. A test of the generality of leaf trait relationships on the Tibetan Plateau.  
653 New Phytologist, 2006, 170, 835-848.

654 He P. C., Wright I. J., Zhu S. D., et al. Leaf mechanical strength and photosynthetic capacity vary independently  
655 across 57 subtropical forest species with contrasting light requirements. New Phytologist, 2019, 223, 607-618.

656 He Y. T. Studies on physioecological traits of 30 plant species in the Subalpine Meadow of the Qinling Mountains.  
657 2007, Graduation Thesis.

658 Hou M. M. Adaptive evolution of some species from sedges (*Carex* *Cyperaceae*) based on phylogeny and leaf  
659 functional traits to habitat in the Poyang Lake Area. 2017, Graduation Thesis.

660 Hou Y., Liu M. X., Sun H. R., et al. Response of plant leaf traits to microhabitat change in a subalpine meadow on  
661 the eastern edge of Qinghai-Tibetan Plateau, China. Chinese Journal of Applied Ecology, 2017, 28, 71-79.

662 Hu Z. Z., Michaletz S. T., Johnson D. J., et al. Traits drive global wood decomposition rates more than climate.  
663 Global Change Biology, 2018, 24, 5259-5269.

664 Hua L., He P., Goldstein G., et al. Linking vein properties to leaf biomechanics across 58 woody species from a  
665 subtropical forest. Plant Biology, 2019, 22, 212-220.

666 Huang J. J. and Wang X. H. Leaf nutrient and structural characteristics of 32 evergreen broad-leaved species.  
667 Journal of East China Normal University (Natural Science), 2003, 1, 92-97.

668 Huang Y. L. The research about the turnover patterns and moisture adaptation mechanism of major species on the  
669 South-North-facing slope. 2012, Graduation Thesis.

670 Iida Y., Kohyama T. S., Swenson N. G., et al. Linking functional traits and demographic rates in a subtropical tree  
671 community: the importance of size dependency. Journal of Ecology, 2014, 102, 641-650.

672 Jia Q. Q. Functional traits of fine roots and their relationship with leaf traits of 50 major species in a subtropical  
673 forest in Gutianshan. 2011, Graduation Thesis.

674 Jiang Y., Chen X., Ma J., et al., Interspecific and intraspecific variation in functional traits of subtropical evergreen  
675 and deciduous broadleaved mixed forests in karst topography, Guilin, Southwest China. Tropical  
676 Conservation Science, 2016, 9.

677 Jin Y., Wang C. K., Zhou Z. H., et al. Co-ordinated performance of leaf hydraulics and economics in 10 Chinese  
678 temperate tree species. Functional Plant Biology, 2016, 43, 1082-1090.

679 Jing G. H. Responses of grassland community structure and functions to management practices on the semi-arid  
680 area of Loess Plateau. 2017, Graduation Thesis.

681 Kang M. Spatial distribution pattern and its causes of woody plant functional traits in Tiantong region, Zhejiang  
682 Province. 2012, Graduation Thesis.

683 Krober W., Li Y., Hardtle W., et al. Early subtropical forest growth is driven by community mean trait values and  
684 functional diversity rather than the abiotic environment. Ecology and Evolution, 2015, 5, 3541-3556.

685 Krober W., Bohnke M., Welk E., et al. Leaf trait-environment relationships in a subtropical broadleaved forest in  
686 south-east China. PloS One, 2012, 7, e35742.

687 Krober W., Zhang, S. R. Ehmgig, M., et al. Linking xylem hydraulic conductivity and vulnerability to the leaf  
688 economics spectrum-a cross-species study. PloS One, 2014, e109211.

689 Li F. Comparison of functional traits in semi-humid evergreen broad-leaved in Western Hill of Kunming. 2011,  
690 Graduation Thesis.

691 Li K. and Xiang W. H. Comparison of specific leaf area, SPAD value and seed mass among subtropical tree  
692 species in hilly area of Central Hunan, China. Journal of Central South University of Forestry & Technology,  
693 2011, 31, 213-218.

694 Li L., McCormack M. L., Ma C.G., et al. Leaf economics and hydraulic traits are decoupled in five species-rich

695 tropical-subtropical forests. *Ecology Letters*, 2015, 18, 899-906.

696 Li Q. Leaf functional traits and their relationships with environmental factors in Beishan Mountain of Jinhua,  
697 Zhejiang Province. 2020, Graduation Thesis.

698 Li S. J., Su P. X., Zhang H. N., et al. Characteristics and relationships of foliar water and leaf functional traits of  
699 desert plants. *Plant Physiology Journal*, 2013, 49, 153-160.

700 Li W. H., Xu F. W., Zheng S. X., et al. Patterns and thresholds of grazing-induced changes in community structure  
701 and ecosystem functioning: species-level responses and the critical role of species traits. *Journal of Applied*  
702 *Ecology*, 2017, 54, 963-975.

703 Li W. Q., Xu Q., Li J., et al. Quantification of ecotone width of returned forest land from farmland based on  
704 specific leaf area. *Journal of West China Forestry Science*, 2017, 46, 117-121.

705 Li X. F., Pei K. Q., Kery M., et al. Decomposing functional trait associations in a Chinese subtropical forest. *PloS*  
706 *One*, 2017, 12, e0175727.

707 Li X. F., Schmid B., Wang F., et al. Net assimilation rate determines the growth rates of 14 species of subtropical  
708 forest trees. *PloS One*, 2016, 11, e0150644.

709 Li X. L., Li X. H., Jiang D. M., et al. Leaf morphological characters of 22 compositae herbaceous species in  
710 Horqin sandy land. *Chinese Journal of Ecology*, 2005, 24, 1397-1401.

711 Li Y. H., Luo T. X., Lu Q., et al. Comparisons of leaf traits among 17 major plant species in Shazhuyu Sand  
712 Control Experimental Station of Qinghai Province. *Acta Ecologica Sinica*, 2005, 25, 994-999.

713 Li Y. L., Meng Q. T., Zhao X. Y., et al. Relationships of fresh leaf traits and leaf litter decomposition in Kerqin  
714 Sandy Land. *Acta Ecologica Sinica*, 2008, 28, 2486-2494.

715 Li Y., Yao J., Yang S., et al. Trait differences research on leaf function of Liaodong oak forest main species in  
716 Dongling mountain. *Guangdong Agricultural Sciences*, 2012, 23, 159-162, 171.

717 Liang X. Y., Ye Q., Liu H., et al. Wood density predicts mortality threshold for diverse trees. *New Phytologist*,  
718 2021, 229, 3053-3057.

719 Li, R., Zhu, S., Chen, H. Y. H., et al. Are functional traits a good predictor of global change impacts on tree species  
720 abundance dynamics in a subtropical forest? *Ecology Letters*, 2015, 18, 1181-1189.

721 Li Y. Y., Shi H., Shao M. A. Cavitation resistance of dominant trees and shrubs in Loess hilly region and their  
722 relationship with xylem structure. *Journal of Beijing Forestry University*, 2010, 32, 8-13.

723 Lin G. G., Guo, D. L., Li, L., et al. Contrasting effects of ectomycorrhizal and arbuscular mycorrhizal tropical tree  
724 species on soil nitrogen cycling: the potential mechanisms and corresponding adaptive strategies. *Oikos*, 2018,  
725 127, 518-530.

726 Liu C. H. and Li Y. Y. Relationship between leaf traits and PV curve parameters in the typical deciduous woody  
727 plants occurring in Southern Huanglong Mountain. *Journal of Northwest Forestry University*, 2013, 28, 1-5.

728 Liu G. F., Freschet G. T., Pan X., et al. Coordinated variation in leaf and root traits across multiple spatial scales in  
729 Chinese semi-arid and arid ecosystems. *New Phytologist*, 2010, 188, 543-553.

730 Liu G. F., Wang L., Jiang L., et al. Specific leaf area predicts dryland litter decomposition via two mechanisms.  
731 *Journal of Ecology*, 2017, 106, 218-229.

732 Liu J. H., Zeng D. H. and Don K. L. Leaf traits and their interrelationships of main plant species in southeast  
733 Horqin sandy land. *Chinese Journal of Ecology*, 2006, 25, 921-925.

734 Liu J. X., Chen J., Jiang M. X., et al. Leaf traits and persistence of relict and endangered tree species in a rare plant  
735 community. *Functional Plant Biology*, 2012, 39, 512-518.

736 Liu L. H. The traits and adaptive strategies of main herbaceous plants and lianas on micro-topographical units in  
737 Huangcangyu reserves of Anhui Province. 2012, Graduation Thesis.

738 Liu M. C., Kong D. L., Lu X. R., et al. Higher photosynthesis, nutrient- and energy-use efficiencies contribute to

739           invasiveness of exotic plants in a nutrient poor habitat in northeast China. *Physiologia Plantarum*, 2017, 160,  
740           373-382.

741   Liu R. H., Bai J. L., Bao H., et al. Variation and correlation in functional traits of main woody plants in the  
742           *Cyclobalanopsis glauca* community in the karst hills of Guilin, southwest China. *Chinese Journal of Plant*  
743           *Ecology*, 2020, 44, 828-841.

744   Liu W. D., Su J. R., Li S. F., et al. Stoichiometry study of C, N and P in plant and soil at different successional  
745           stages of monsoon evergreen broad-leaved forest in Pu'er, Yunnan Province. *Acta Ecologica Sinica*, 2010, 30,  
746           6581-6590.

747   Liu X. C., Jia H. B., Wang Q. Y. Genetic variation and correlation in wood properties of *Betula platyphlla* in  
748           natural Stands. *Journal of Northeast Forestry University*, 2018, 36, 8-10.

749   Liu Y. Y. Spatial distribution and habitat associations of trees in a typical mixed broad-leaved Korean pine (*Pinus*  
750           *koraiensis*) forest. 2014, Graduation Thesis.

751   Luo Y. H., Cadotte M. W., Burgess K. S., et al. Greater than the sum of the parts: how the species composition in  
752           different forest strata influence ecosystem function. *Ecology Letters*, 2019, 22, 1449-1461.

753   Lv J. Z., Miao Y. M., Zhang H. F., et al. Comparisons of leaf traits among different functional types of plant from  
754           Huoshan Mountain in the Shanxi Province. *Plant Science Journal*, 2010, 28, 460-465.

755   Ma J., Wu L. F., Wei X., et al. Habitat adaptation of two dominant tree species in a subtropical monsoon forest:  
756           leaf functional traits and hydraulic properties. *Guihaia*, 2015, 35, 261-268.

757   Mo J. M., Zhang D. Q., Huang Z. L., et al. Distribution pattern of nutrient elements in plants of Dinghushan Lower  
758           Subtropical Evergreen Broad-Leaved Forest. *Journal of Tropical and Subtropical Botany*, 2000, 8, 198-206.

759   Niu C. Y., Meinzer F. C. and Hao G. Y. Divergence in strategies for coping with winter embolism among co-  
760           occurring temperate tree species: the role of positive xylem pressure, wood type and tree stature. *Functional*  
761           *Ecology*, 2017, 31, 1550-1560.

762   Niu D. C., Li Q., Jiang S. G., et al. Seasonal variations of leaf C:N:P stoichiometry of six shrubs in desert of  
763           China's Alxa Plateau. *Chinese Journal of Plant Ecology*, 2013, 37, 317-325.

764   Niu K. C., He J. S. and Lechowicz M. J. Grazing-induced shifts in community functional composition and soil  
765           nutrient availability in Tibetan alpine meadows. *Journal of Applied Ecology*, 2016, 53, 1554-1564.

766   Niu K. C., Zhang S. and Lechowicz M. Harsh environmental regimes increase the functional significance of  
767           intraspecific variation in plant communities. *Functional Ecology*, 2020, 34, 1666-1677.

768   Niu S. L. Photosynthesis research on the predominant legume species in Hunshandak Sandland. 2004, Graduation  
769           Thesis.

770   Qi L. X. Response of leaf traits of *Pinus mongoliensis* and *Pinus massoniana* to elevation gradient in Daiyun  
771           Mountain. 2015, Graduation Thesis.

772   Ren Q. J., Li Q. J., Bu H. Y., et al. Comparison of physiological and leaf morphological traits for photosynthesis of  
773           the 51 plant species in the Maqu alpine swamp meadow. *Chinese Journal of Plant Ecology*, 2015, 39, 593-603.

774   Ren Y. T. The study of leaf functional traits of typical plants across the Alashan Desert. 2017, Graduation Thesis.

775   Ren Y., Wei C. G. and Guo X. Y. Comparison on leaf function traits of six kinds of plant in Ordos. *Journal of Inner*  
776           *Mongolia Forestry Science & Technology*, 2019, 45, 43-46, 55.

777   Rios R. S., Salgado-Luarte C. and Gianoli E. Species divergence and phylogenetic variation of ecophysiological  
778           traits in lianas and trees. *PloS One*, 2007, 9, e99871.

779   Shang K. K. Differentiation and maintenance of relict deciduous broad-leaved forest patterns along micro-  
780           topographic gradient in subtropical area, East China. 2011, Graduation Thesis.

781   Song Y T. Study on functional plant ecology in Songnen Grassland Northeast China. 2012, Graduation Thesis.

782   Song Y T., Zhou D. W., Li Q., et al. Leaf nitrogen and phosphorus stoichiometry in 80 herbaceous plant species of

783 Songnen grassland in Northeast China. *Chinese Journal of Plant Ecology*, 2012, 36, 222-230.

784 Tan X. Y. Research on leaf functional diversity of forest communities in rainy area of south-west China. 2014,  
785 Graduation Thesis.

786 Tang Q. Q. Variation in functional traits of plants in the Subtropical Evergreen and Deciduous Broad-leaved Mixed  
787 Forest. 2016, Graduation Thesis.

788 Tang Y. Inter-specific variations and relationship in leaf traits of major temperate species in northern China. 2011,  
789 Graduation Thesis.

790 Tao J. P., Zuo J., He Z., et al. Traits including leaf dry matter content and leaf pH dominate over forest soil pH as  
791 drivers of litter decomposition among 60 species. *Functional Ecology*, 2019, 33, 1798-1810.

792 Tian M., Yu G. R., He N. P., et al. Leaf morphological and anatomical traits from tropical to temperate coniferous  
793 forests: Mechanisms and influencing factors. *Scientific Reports*, 2016, 6, 19703.

794 Wang B. Analysis of leaf functional traits of 13 species trees in northwestern Fujian Province. 2019, Graduation  
795 Thesis.

796 Wang B. B. A study on ecological stoichiometry of six kinds of dominant shrubs in Huangcangyu Nature Reserve.  
797 2015, Graduation Thesis.

798 Wang G. H. Leaf trait co-variation, response and effect in a chronosequence. *Journal of Vegetation Science*, 2007,  
799 18, 563-570.

800 Wang G. H., Liu J. L. and Meng T. T. Leaf trait variation captures climate differences but differs with species  
801 irrespective of functional group. *Journal of Plant Ecology*, 2015, 8, 61-69.

802 Wang J. Y., Wang S. Q., Li R. L., et al. C:N:P stoichiometric characteristics of four forest types' dominant tree  
803 species in China. *Chinese Journal of Plant Ecology*, 2011, 35, 587-595.

804 Wang K. B. Vegetation ecological features and net primary productivity simulation in Yanggou watershed in the  
805 Loess hill-gully areas of China. 2011, Graduation Thesis.

806 Wang S. S. The traits and adaptive strategies of main herbaceous plants and lianas on micro-topographical units in  
807 Longjishan reserves of Anhui Province. 2016, Graduation Thesis.

808 Wei L. P. Variations in functional traits of main tree species along tree-crown in broadleaved Korean Pine Forest in  
809 Jiaohe, Jilin Province. 2014, Graduation Thesis.

810 Wei L. P., Hou J. H. and Jiang S. S. Changes of leaf functional traits of two main species along tree height in  
811 broad-leaved Korean pine forest. *Guangdong Agricultural Sciences*, 2014, 12, 55-58, 71.

812 Wei L. Y. and Shangguan Z. P. Relation between specific leaf areas and leaf nutrient contents of plants growing on  
813 slopelands with different farming-abandoned periods in the Loess Plateau. *Acta Ecologica Sinica*, 2008, 28,  
814 2526-2535.

815 Wei L. Y., Zhou J. W., Xiao H. G., et al. Variations in leaf functional traits among plant species grouped by growth  
816 and leaf types in Zhenjiang, China. *Journal of Forestry Research*, 2011, 28, 241-248.

817 Wu D. H., Pietsch K. A., Staab M., et al. Wood species identity alters dominant factors driving fine wood  
818 decomposition along a subtropical plantation forests tree diversity gradient in subtropical plantation forests.  
819 *Biotropica*, 2021, 53, 643-657.

820 Wu T. G., Chen B. F., Xiao Y. H., et al. Leaf stoichiometry of trees in three forest types in Pearl River Delta, South  
821 China. *Chinese Journal of Plant Ecology*, 2009, 34, 58-63.

822 Xie Y. J. The characteristics of 20 dominant plant functional traits in evergreen broad-leaf forest in Daming  
823 Mountain Nature Reserve, Guangxi. 2013, Graduation Thesis.

824 Xu M. F., Ke X. H., Zhang Y., et al. Wood densities of six hardwood tree species in Eastern Guangdong and  
825 influencing factors. *Journal of South China Agricultural University*, 2016, 37, 100-106.

826 Xu M. S., Zhao Y. T., Yang X. D., et al. Geostatistical analysis of spatial variations in leaf traits of woody plants in

827 Tiantong, Zhejiang Province. Chinese Journal of Plant Ecology, 2016, 40, 48-59.

828 Xu Y. Z. Biomass estimate and storage mechanisms in northern subtropical forest ecosystems, central China. 2016,  
829 Graduation Thesis.

830 Xun Y. H., Di X. Y. and Jin G. Z. Vertical variation and economic strategy of leaf trait of major tree species in a  
831 typical mixed broadleaved-Korean pine forest. Chinese Journal of Plant Ecology, 2020, 44, 730-741.

832 Yan E. R., Wang X. H., Guo M., et al. C:N:P stoichiometry across evergreen broad-leaved forests, evergreen  
833 coniferous forests and deciduous broad-leaved forests in the Tiantong region, Zhejiang Province, eastern  
834 China. Chinese Journal of Plant Ecology, 2010, 34, 48-57.

835 Yang S. The adaptive strategies of main herbaceous plants traits to different micro-topographical units in  
836 Dashushan Mountain, Hefei. 2017, Graduation Thesis.

837 Yang Y., Xu X., Xu M., et al. Adaptation strategies of three dominant plants in the trough-valley karst region of  
838 northern Guizhou Province, Southwestern China, evidence from associated plant functional traits and  
839 ecostochiometry. Earth and Environment, 2020, 48, 413-423.

840 Yang Z., Fan S. X., Zhou B. C., et al. Leaf function and soil nutrient differences of dominant tree species on  
841 different slope aspects at the south foothills of Taihang Mountains. Journal of Henan Agricultural University,  
842 2020, 54, 408-414.

843 Yin Q. L., Wang L., Lei, M. L., et al. The relationships between leaf economics and hydraulic traits of woody  
844 plants depend on water availability. Science of the Total Environment, 2018, 621, 245-252.

845 Yu Y. H., Zhong X. P. and Chen W. Analysis of relationship among leaf functional traits and economics spectrum  
846 of dominant species in northwestern Guizhou Province. Journal of Forest and Environment, 2018, 38, 196-  
847 201.

848 Yuan S. Preliminary research on plant functional traits and the capability of carbon sequestration of major tree  
849 species in Changbai Mountain Area. 2011, Graduation Thesis.

850 Zhang H., Chen H. Y. H., Lian J. Y., et al. Using functional trait diversity patterns to disentangle the scale-  
851 dependent ecological processes in a subtropical forest. Functional Ecology, 2018, 32, 1379-1389.

852 Zhang J. G., Fu S. L., Wen Z. D., et al. Relationship of key leaf traits of 16 woody plant species in Low  
853 Subtropical China. Journal of Tropical and Subtropical Botany, 2009, 17, 395-400.

854 Zhang J. L., Poorter L., Cao K. F. Productive leaf functional traits of Chinese savanna species. Plant Ecology, 2012,  
855 213, 1449-1460.

856 Zhang J. Y. Comparative study on the different plant functional groups leaf traits at the Maoershan Region. 2008,  
857 Graduation Thesis.

858 Zhang Q. W., Zhu S. D., Jansen S., et al. Topography strongly affects drought stress and xylem embolism  
859 resistance in woody plants from a karst forest in Southwest China. Functional Ecology, 2020, 35, 566-577.

860 Zhang S. B. and Cao K. F. Stem hydraulics mediates leaf water status, carbon gain, nutrient use efficiencies and  
861 plant growth rates across dipterocarp species. Functional Ecology, 2009, 23, 658-667.

862 Zhang S. B., Cao K. F., Fan Z. X., et al. Potential hydraulic efficiency in angiosperm trees increases with growth-  
863 site temperature but has no trade-off with mechanical strength. Global Ecology and Biogeography, 2013, 22,  
864 971-981.

865 Zhang Y., Ren Y. X., Yao J., et al. Leaf nitrogen and phosphorous stoichiometry of trees in *Pinus tabulaeformis*  
866 Carr stands, North China. Journal of Anhui Agricultural University, 2012, 39, 247-251.

867 Zhao Y. T., Ali, A. and Yan, E. R. The plant economics spectrum is structured by leaf habits and growth forms  
868 across subtropical species. Tree Physiology, 2016, 37, 173-185.

869 Zheng X. J., Li S. and Li Y. Leaf water uptake strategy of desert plants in the Junggar Basin, China. Chinese  
870 Journal of Plant Ecology, 2011, 35, 893-905.

- 871 Zheng Y. M. Carbon, nitrogen and phosphorus stoichiometry of plant and soil in the sandy hills of Poyang Lake.  
872 2014, Graduation Thesis.
- 873 Zheng Z. X. Comparison of plant leaf, height and seed functional traits in dry-hot valleys. 2010, Graduation Thesis.
- 874 Zhou J. Y., He J. J., Guo Z. Y., et al. A study on specific leaf area and leaf dry matter content of five dominant  
875 species in Xiangshan Mountain, Huaibei City, Anhui Province. *Journal of Huaibei Normal University*  
876 (Natural Sciences), 2013, 34, 51-54.
- 877 Zhou X., Zuo X. A., Zhao X. Y., et al. Plant functional traits and interrelationship of 34 plant species in south  
878 central Horqin Sandy Land, China. *Journal of Desert Research*, 2015, 35, 1489-1495.
- 879 Zhu B. R., Xu B. and Zhang D. Y. Extent and sources of variation in plant functional traits in grassland. *Journal of*  
880 *Beijing Normal University (Natural Science)*, 2011, 47, 485-489.
- 881 Zhu S. D., Song J. J., Li R. H., et al. Plant hydraulics and photosynthesis of 34 woody species from different  
882 successional stages of subtropical forests. *Plant Cell and Environment*, 2013, 36, 879-891.
- 883 Zhu X. B., Liu Y. M. and Sun S. C. Leaf expansion of the dominant woody species of three deciduous oak forests  
884 in Nanjing, East China. *Chinese Journal of Plant Ecology*, 2005, 29, 125-136.



885 **Appendix B**

886 **Table B1** Summary of statistics in plant functional traits, environmental variables and  
 887 geographical distribution in China.

Trait	Unit	Range	Mean	CV (%)	No. of species	Entries	Sites
SLA	m <sup>2</sup> kg <sup>-1</sup>	0.06–81.68	17.88	54.96	2463	9195	1032
LDMC	g g <sup>-1</sup>	0.06–0.95	0.34	100.00	1582	3957	193
LNC	mg g <sup>-1</sup>	3.41–66.02	21.52	37.44	2335	7407	567
LPC	mg g <sup>-1</sup>	0.09–9.70	1.83	62.19	2074	6266	515
LA	cm <sup>2</sup>	0.0033–2553.33	36.16	259.64	1838	5976	691
WD	g cm <sup>-3</sup>	0.25–1.37	0.68	33.16	768	1788	639
Altitude	m	-144–5454					1430
MAT	°C	-12.07–24.32					1430
MAP	mm	15–2982					1430
Soil total N	g kg <sup>-1</sup>	0.11–10.25					1430
Bulk density	g cm <sup>-3</sup>	0.83–1.45					1430

888 SLA, specific leaf area; LDMC, leaf dry matter content; LNC, leaf N concentration; LPC, leaf P concentration; LA,  
 889 leaf area; WD, wood density; MAT, mean annual temperature; MAP, mean annual precipitation.

Type of variables	Variable name	Abbreviations	Units	Time periods	Spatial resolution	Source
Climate	Mean annual temperature	MAT	°C	1970-2000	1 km	WorldClim version 2.1
	Mean diurnal range	MDR	°C	1970-2000	1 km	WorldClim version 2.1
	Temperature seasonality	TS	°C	1970-2000	1 km	WorldClim version 2.1
	Max temperature of <del>the</del> warmest month	Tmin	°C	1970-2000	1 km	WorldClim version 2.1
	Min temperature of <del>the</del> coldest month	Tmax	°C	1970-2000	1 km	WorldClim version 2.1
	Temperature annual range	TAR	°C	1970-2000	1 km	WorldClim version 2.1
	Isothermality	IS	%	1970-2000	1 km	WorldClim version 2.1
	Mean temperature of <del>the</del> wettest quarter	MTEQ	°C	1970-2000	1 km	WorldClim version 2.1
	Mean temperature of <del>the</del> driest quarter	MTDQ	°C	1970-2000	1 km	WorldClim version 2.1
	Mean temperature of <del>the</del> warmest quarter	MTWQ	°C	1970-2000	1 km	WorldClim version 2.1
	Mean temperature of <del>the</del> coldest quarter	MTCQ	°C	1970-2000	1 km	WorldClim version 2.1
	Mean annual precipitation	MAP	mm	1970-2000	1 km	WorldClim version 2.1
	Precipitation of <del>the</del> wettest month	PEM	mm	1970-2000	1 km	WorldClim version 2.1
	Precipitation of <del>the</del> driest month	PDM	mm	1970-2000	1 km	WorldClim version 2.1
	Precipitation seasonality	PS	%	1970-2000	1 km	WorldClim version 2.1
	Precipitation of <del>the</del> wettest quarter	PEQ	mm	1970-2000	1 km	WorldClim version 2.1
	Precipitation of <del>the</del> driest quarter	PDQ	mm	1970-2000	1 km	WorldClim version 2.1
	Precipitation of <del>the</del> warmest quarter	PWQ	mm	1970-2000	1 km	WorldClim version 2.1
	Precipitation of <del>the</del> coldest quarter	PCQ	mm	1970-2000	1 km	WorldClim version 2.1
	Aridity index	AI	/	1970-2000	1 km	Global CGIAR-CSI
	Solar radiation	RAD	kJ m <sup>-2</sup> day <sup>-1</sup>	1970-2000	1 km	WorldClim version 2.1
Topography	Elevation	/	m		1 km	SRTM 90m V4.1
Soil	Soil sand content	SAND	%	/	1 km	Shangguan et al. (2013)
	Soil silt content	SILT	%	/	1 km	Shangguan et al. (2013)
	Soil clay content	CLAY	%	/	1 km	Shangguan et al. (2013)
	Bulk density	BD	g cm <sup>-3</sup>	/	1 km	Shangguan et al. (2013)
	Soil pH	pH	/	/	1 km	Shangguan et al. (2013)
	Soil organic matter	SOC	g kg <sup>-1</sup>	/	1 km	Shangguan et al. (2013)
	Soil total N	STN	g kg <sup>-1</sup>	/	1 km	Shangguan et al. (2013)
	Soil total P	STP	g kg <sup>-1</sup>	/	1 km	Shangguan et al. (2013)
	Soil alkali-hydrolysable N	SAN	mg kg <sup>-1</sup>	/	1 km	Shangguan et al. (2013)
	Soil available P	SAP	mg kg <sup>-1</sup>	/	1 km	Shangguan et al. (2013)
	Soil available K	SAK	mg kg <sup>-1</sup>	/	1 km	Shangguan et al. (2013)
Cation exchange capacity	CEC	me kg <sup>-1</sup>	/	1 km	Shangguan et al. (2013)	

Continued

Type of variables	Variable name	Abbreviations	Units	Time periods	Spatial resolution	Source
EVI	MODIS EVI long-term monthly averages		/	2001-2018	1 km	MOD13A3 V006
NIR	MODIS NIR long-term monthly averages		/	2001-2018	1 km	MOD13A3 V006
MIR	MODIS MIR long-term monthly averages		/	2001-2018	1 km	MOD13A3 V006
Red	MODIS red long-term monthly averages		/	2001-2018	1 km	MOD13A3 V006
Blue	MODIS blue long-term monthly averages		/	2001-2018	1 km	MOD13A3 V006
MTCI	MTCI long-term monthly averages		/	2003-2011	4.63 km	MTCI level 3 product
Land cover	Land cover map		/	2015	100 m	Copernicus Global Land Service Collection 3

892 The ~~vegetation indices~~~~remote sensing variables~~ are calculated as long-term monthly averages from 2001 to 2018-.

893 Thus ~~thus~~ 12 variables of each ~~remote sensing~~~~vegetation index~~ category are obtained.

894

895

896

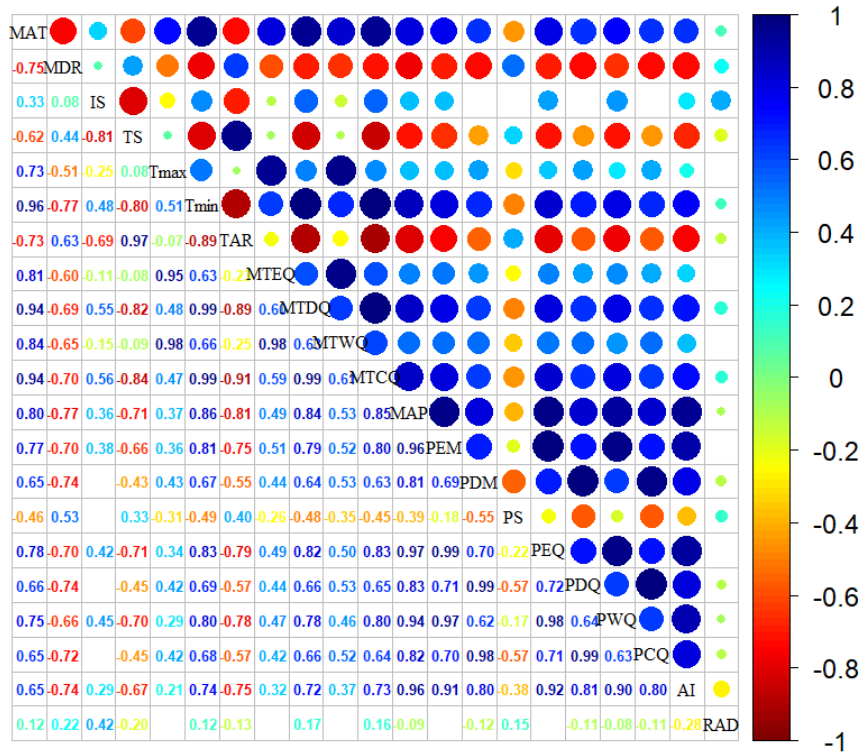
897

898 **Table B3** The number of samples of ~~eight-six~~ plant functional traits used for model training  
899 (80%) and validation (20%).

Traits	No. of samples	No. of samples used for model training	No. of samples used for model validation
SLA	9195	7356	1839
LDMC	3957	3166	791
LNC	7407	5926	1481
LPC	6266	5013	1253
LA	5976	4781	1195
WD	1787	1430	357

900 SLA, specific leaf area ( $\text{m}^2 \text{kg}^{-1}$ ); LDMC, leaf dry matter content ( $\text{g g}^{-1}$ ); LNC, leaf N concentration ( $\text{mg g}^{-1}$ ); LPC,

901 leaf P concentration ( $\text{mg g}^{-1}$ ); LA, leaf area ( $\text{cm}^2$ ); WD, wood density ( $\text{g cm}^{-3}$ ).

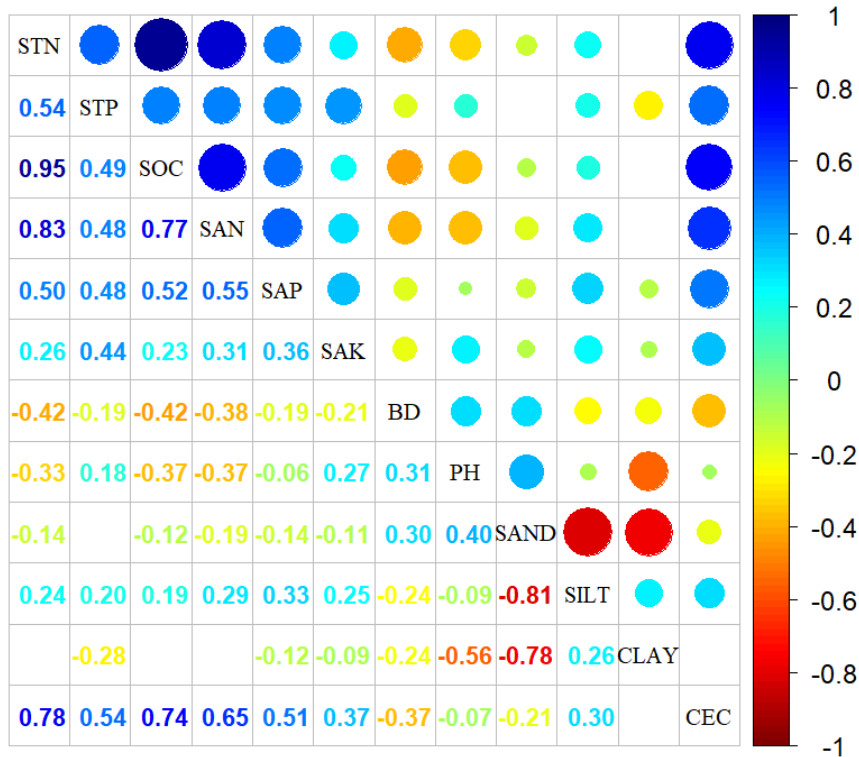


902

903

**Figure B1.** Correlations among climate variables. The blank indicates that the correlations are not significant ( $P > 0.05$ ). The size of the circles is proportional to the correlation coefficient. The abbreviations of climate variables ~~is~~ are seen in Table B2.

905



906

907

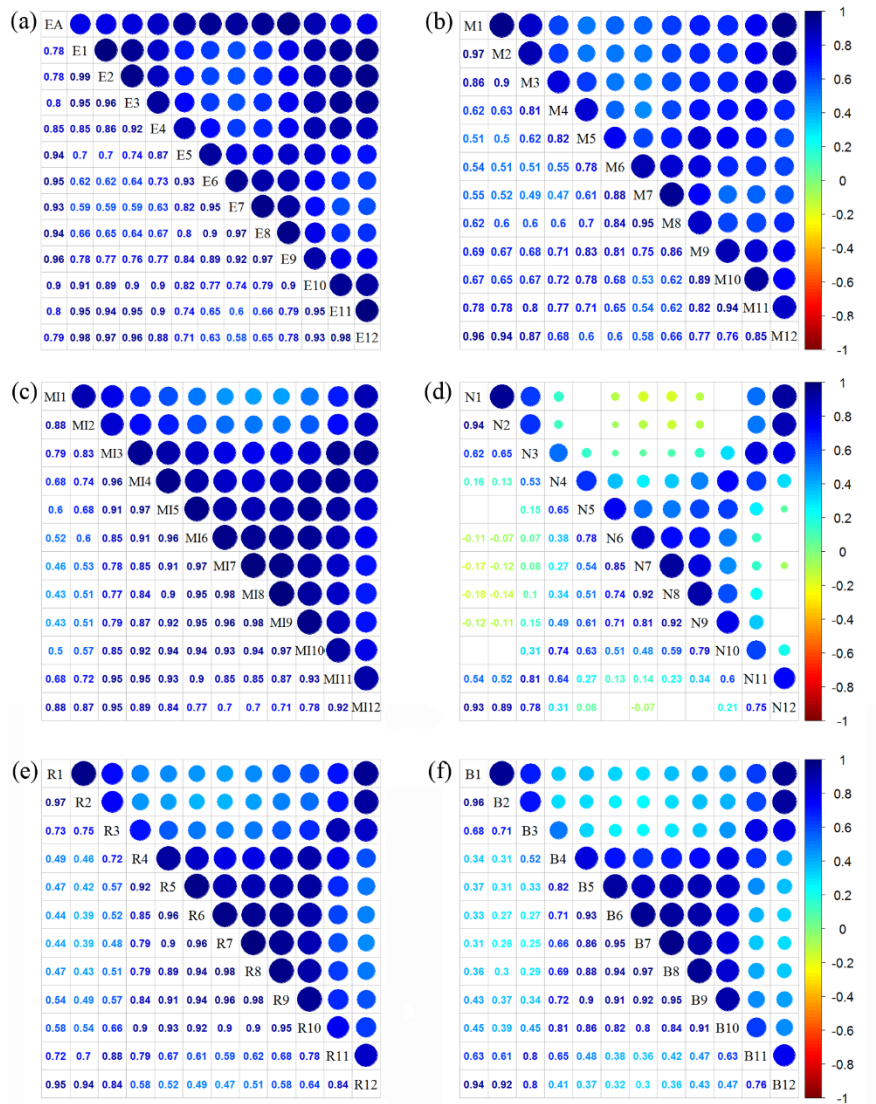
**Figure B2.** Correlations among soil variables. The blank indicates that the correlations are not

908

significant ( $P > 0.05$ ). The size of the circles is proportional to the correlation coefficient. The

909

abbreviations of soil variables ~~is~~ are seen in Table B2.



910

911 **Figure B3.** Correlations among monthly vegetation index~~remote sensing~~ variables. The blank  
 912 indicates that the correlations are not significant ( $P > 0.05$ ). The size of the circles is proportional  
 913 to the correlation coefficient. (a) enhanced vegetation index (EVI); (b) MERIS terrestrial  
 914 chlorophyll index (MTCI); (c) MIR reflectance; (d) NIR reflectance; (e) red reflectance; (f) blue  
 915 reflectance.

916 **Appendix C**

917 **Table C1** Optimal parameter combination and model performance of random forest for plant  
 918 functional traits.

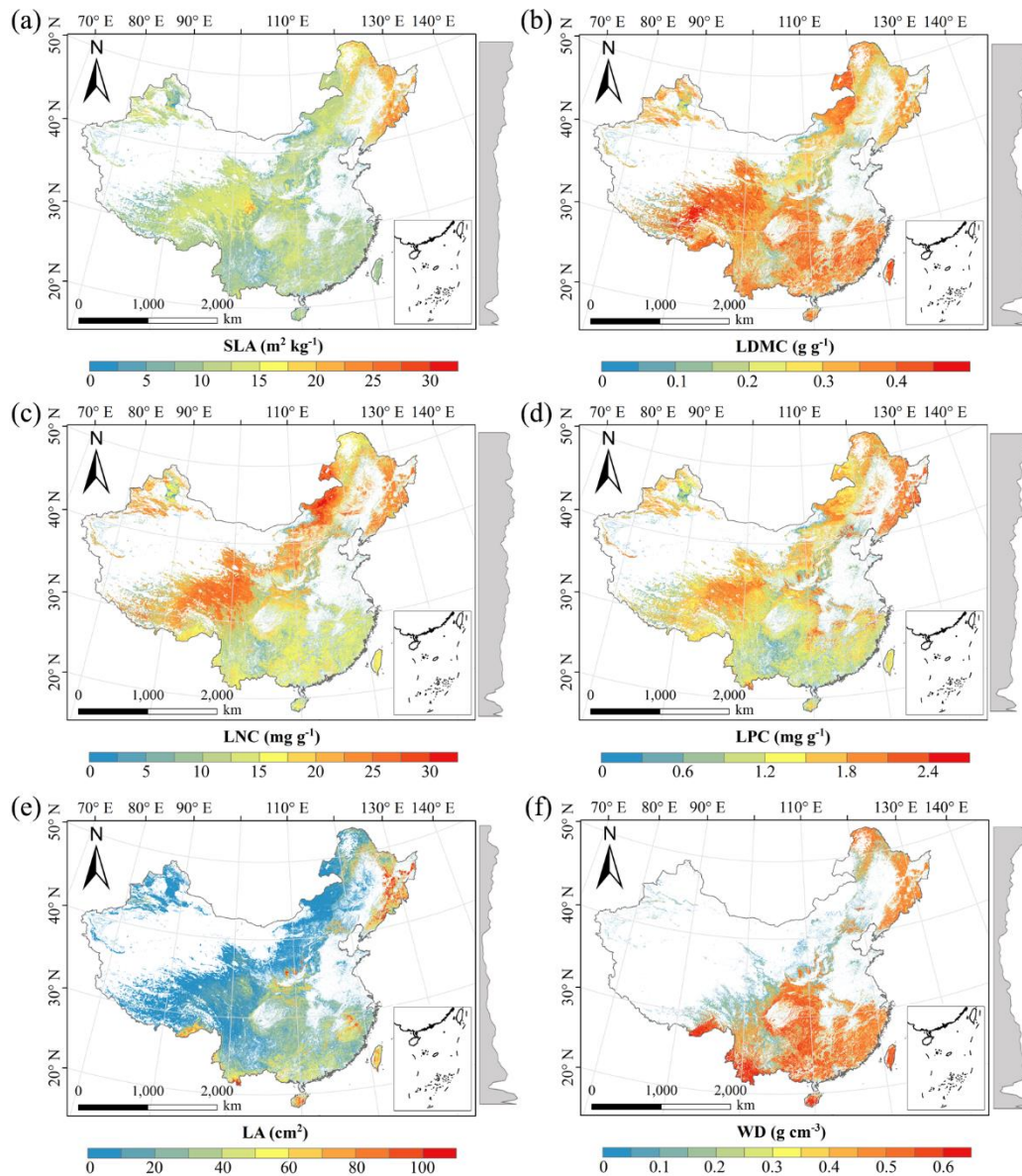
Traits	ntree	mtry	R <sup>2</sup>	NRMSE	MAE
SLA	1000	24	0.47648	0.22	5.134
LDMC	1000	11	0.234	0.20	0.072
LNC	1000	57	0.392	0.00	0.09810
LPC	1000	20	0.58759	0.05	0.12913
LA	1000	18	0.278	0.48	26.622
WD	1000	9	0.534	0.02	0.072

919 SLA, specific leaf area; LDMC, leaf dry matter content; LNC, leaf N concentration; LPC, leaf P concentration; LA,  
 920 leaf area; WD, wood density; R<sup>2</sup>, determinate coefficient; NRMSE, normalized root-mean-square error; MAE,  
 921 mean absolute error.

922  
 923 **Table C2** Optimal parameter combination and model performance of boosted regression trees  
 924 for plant functional traits.

Traits	n.tree	interaction- depth	shrinkage	learning rate	bag fractions	R <sup>2</sup>	NRMSE	MAE
SLA	3000	6	0.01	10	0.75	0.4864 9	0.20	5.082
LDMC	3000	2	0.01	10	0.75	0.2472 8	0.19	0.074
LNC	3000	6	0.01	10	0.70	0.414	0.00	0.09610
LPC	3000	7	0.01	10	0.75	0.594	0.05	0.12913
LA	3000	3	0.001	10	0.75	0.282	0.55	27.556
WD	3000	4	0.01	10	0.70	0.6276 3	0.01	0.06607

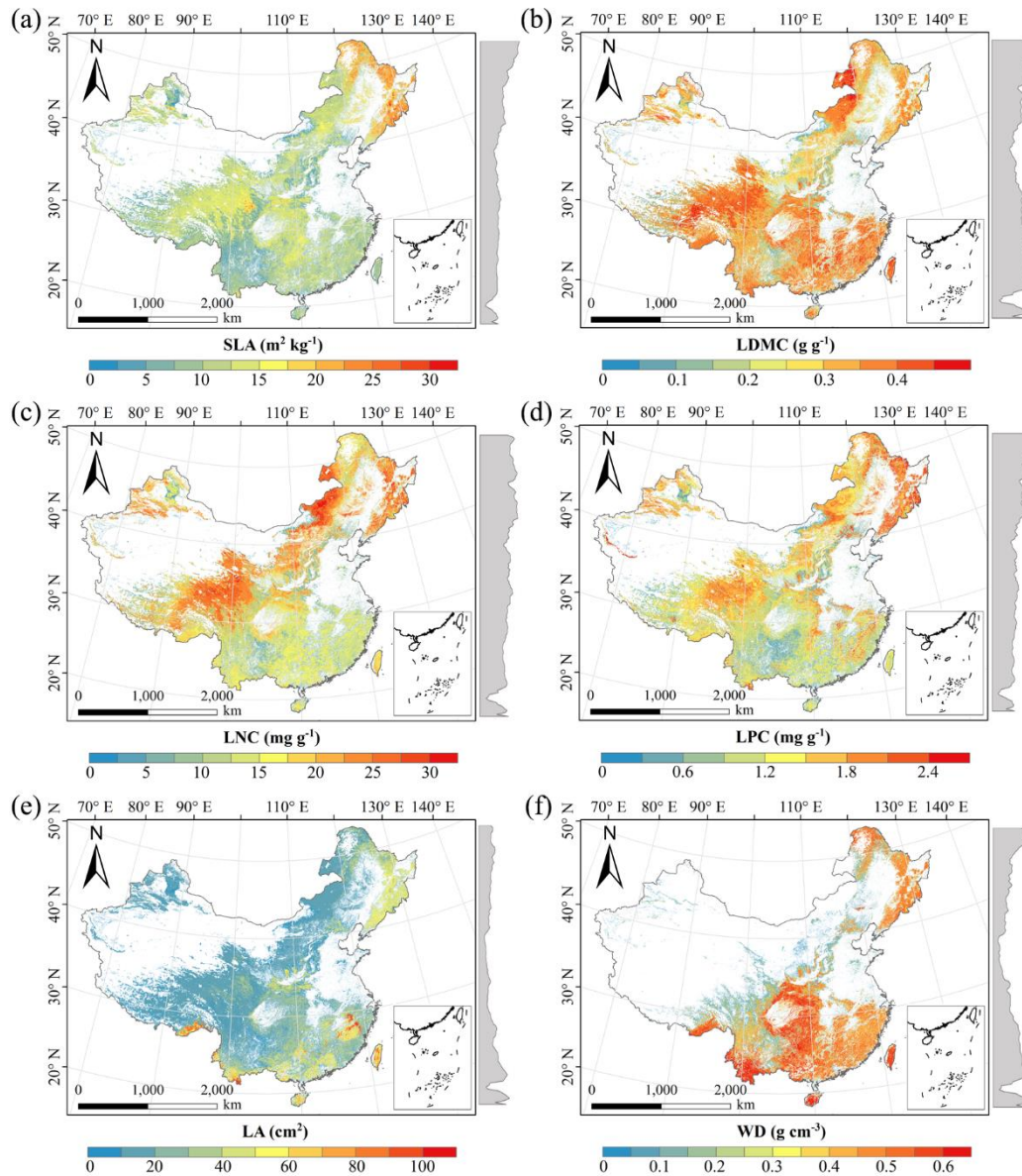
925 SLA, specific leaf area; LDMC, leaf dry matter content; LNC, leaf N concentration; LPC, leaf P concentration; LA,  
 926 leaf area; WD, wood density; R<sup>2</sup>, determinate coefficient; NRMSE, normalized root-mean-square error; MAE,  
 927 mean absolute error.



929

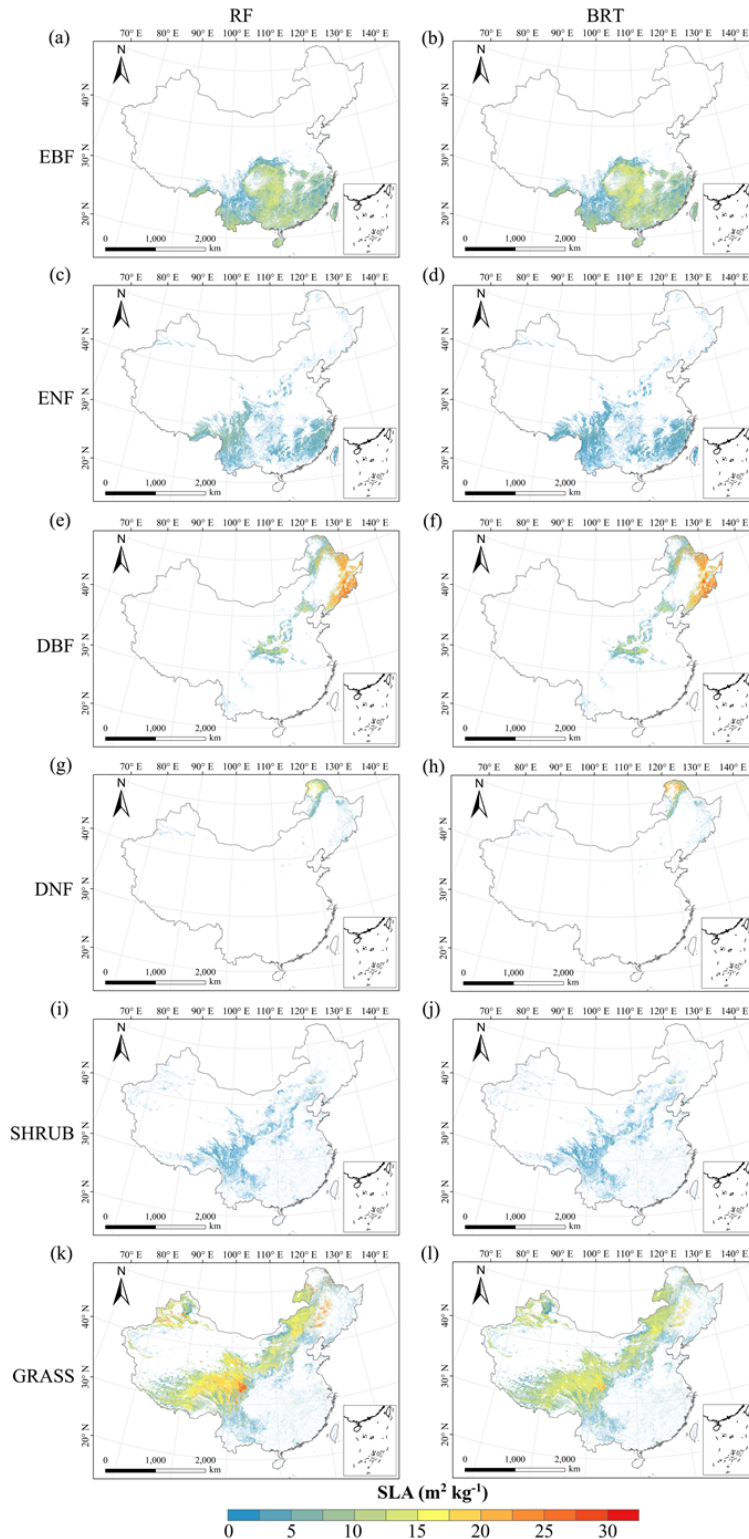
930 **Figure D1.** Spatial distributions of plant functional traits based on random forest. The grey curves  
 931 on the right of maps ~~were~~ are trait distribution along with latitude. The white areas represent  
 932 artificial land cover types and bare vegetation. SLA, specific leaf area; LDMC, leaf dry matter  
 933 content; LNC, leaf N concentration; LPC, leaf P concentration; LA, leaf area; WD, wood density.





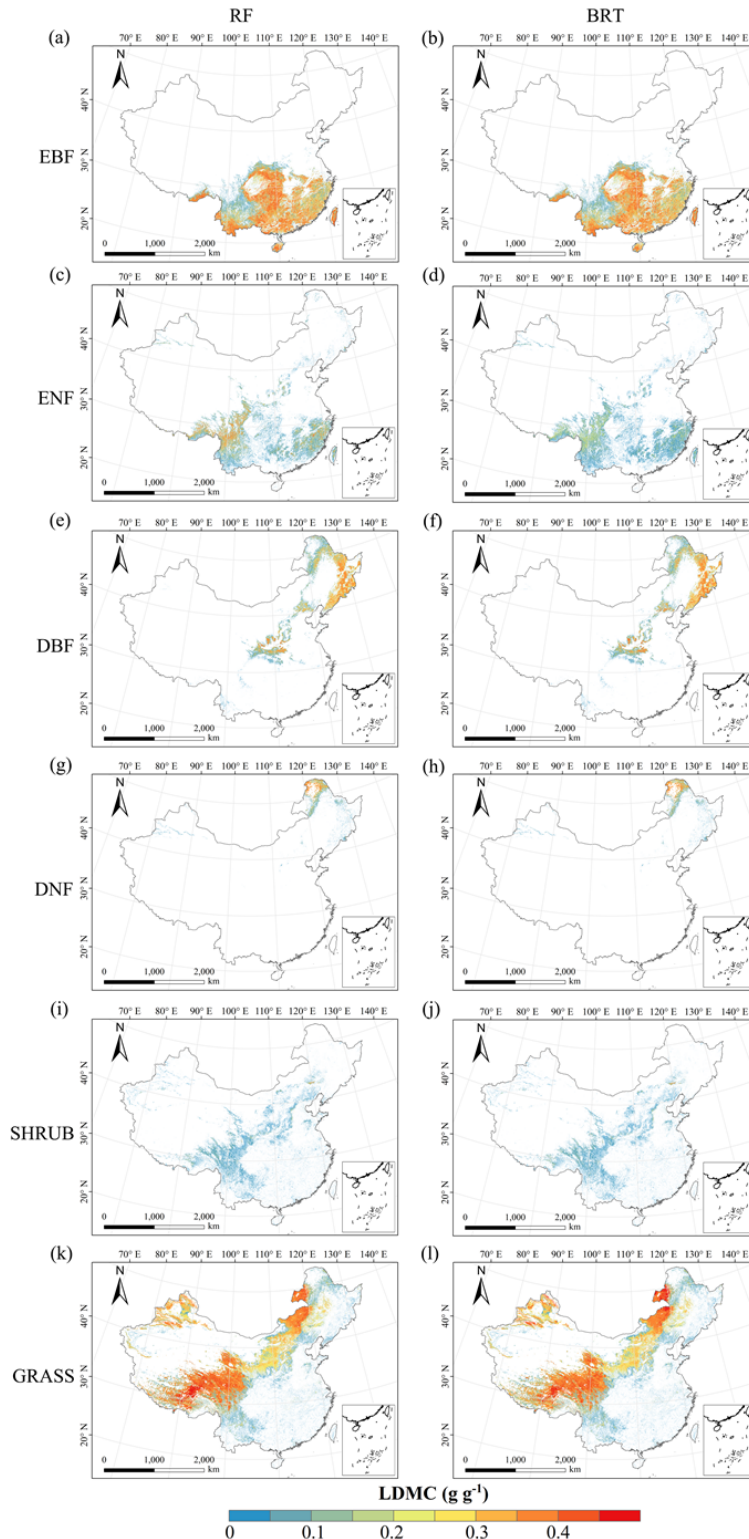
934

935 **Figure D2.** Spatial distributions of plant functional traits based on boosted regression trees. The  
 936 grey curves on the right of maps ~~were~~ are trait distribution along with latitude. The white areas  
 937 represent artificial land cover types and bare vegetation. SLA, specific leaf area; LDMC, leaf dry  
 938 matter content; LNC, leaf N concentration; LPC, leaf P concentration; LA, leaf area; WD, wood  
 939 density.



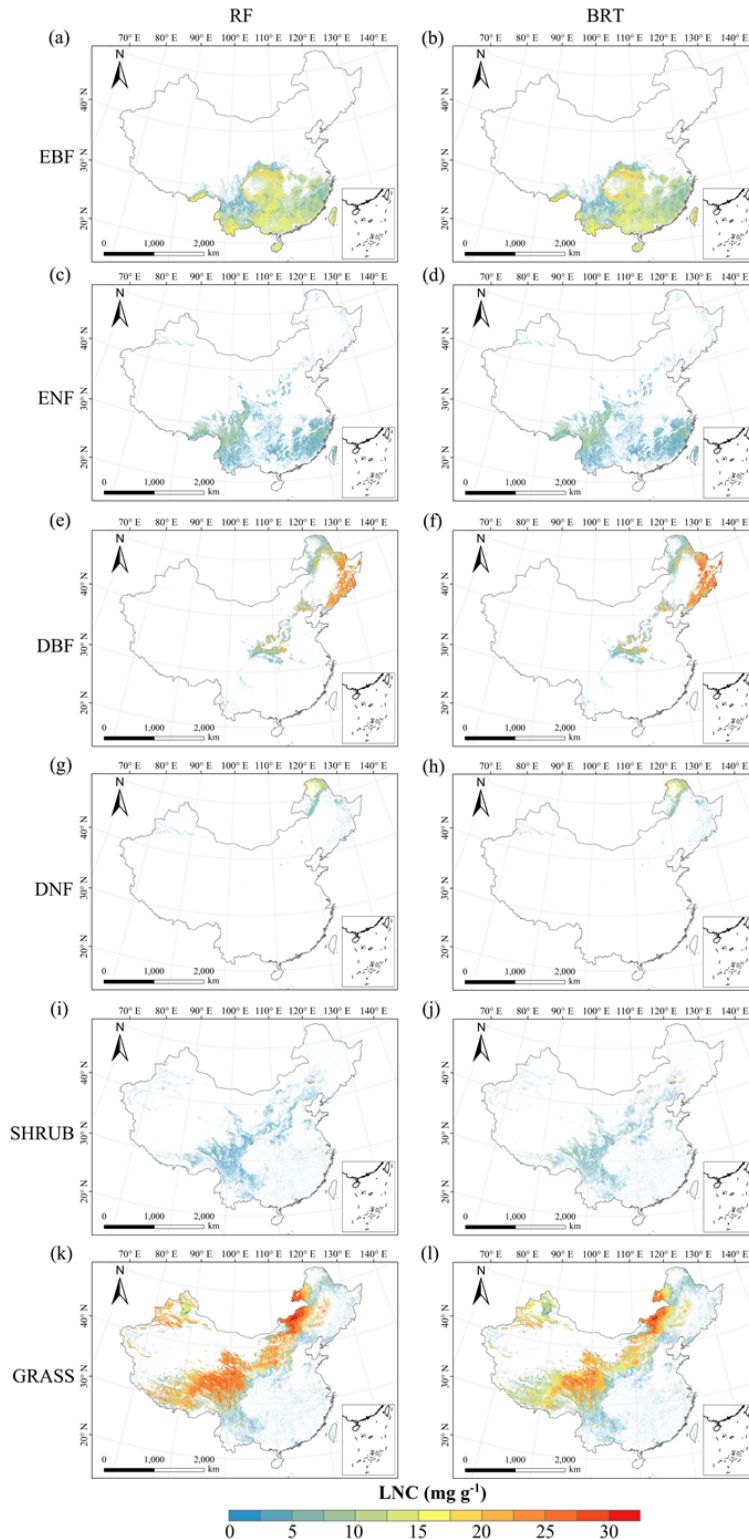
940

941 **Figure D3.** Spatial distribution of specific leaf area (SLA) for each plant functional type. The left  
 942 panel was is obtained from RF method (random forest) method, the right panel was is obtained  
 943 from BRT method (boosted regression trees) method. The white areas represent other natural  
 944 vegetation types and artificial land cover types. EBF, evergreen broadleaf forest; ENF, evergreen  
 945 needleleaf forest; DBF, deciduous broadleaf forest; DNF, deciduous needleleaf forest; SHRUB,  
 946 shrubland; GRASS, grassland.



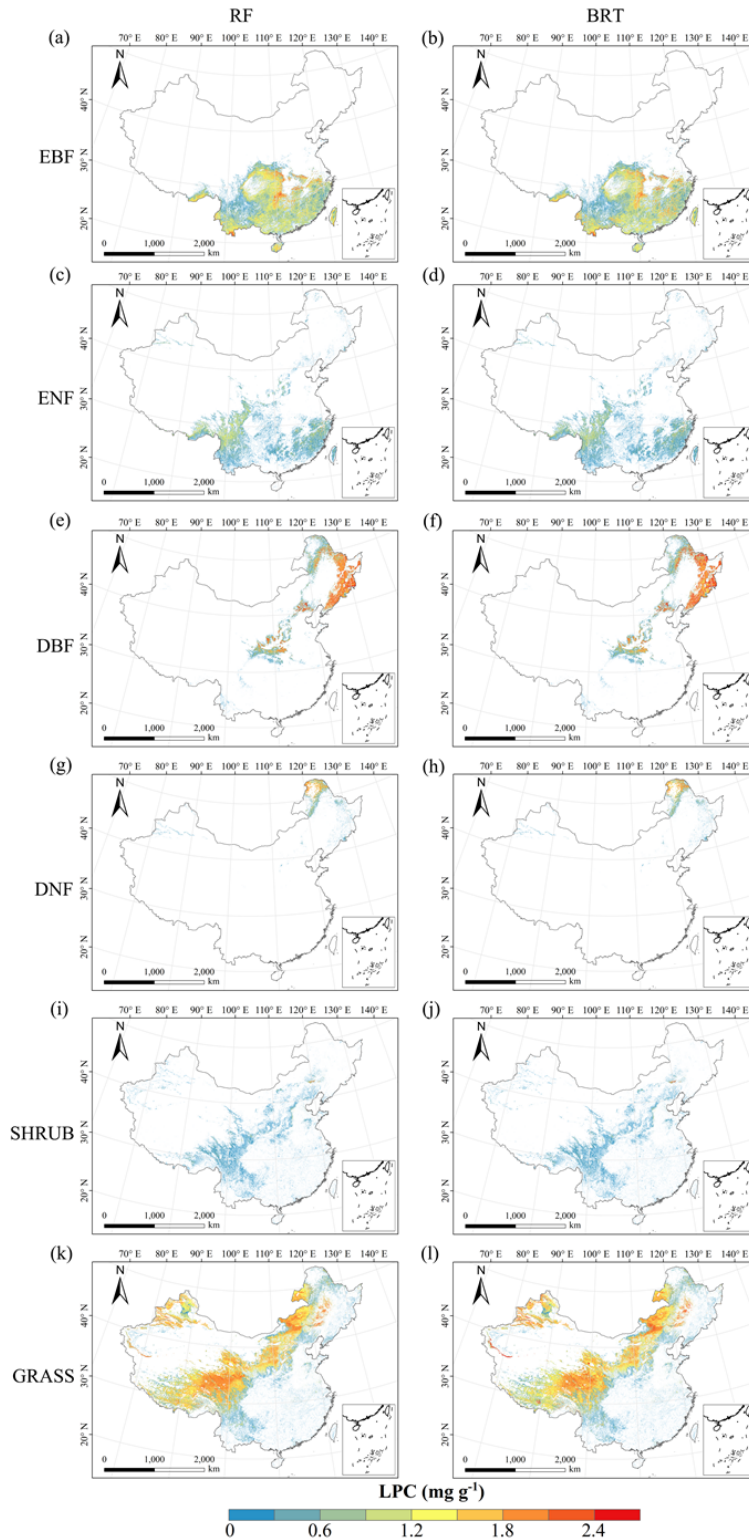
947

948 **Figure D4.** Spatial distribution of leaf dry matter content (LDMC) for each plant functional type.  
 949 The left panel ~~was is~~ obtained from RF ~~method~~-(random forest) method, the right panel ~~was is~~  
 950 obtained from BRT ~~method~~-(boosted regression trees) method. The white areas represent other  
 951 natural vegetation types and artificial land cover types. EBF, evergreen broadleaf forest; ENF,  
 952 evergreen needleleaf forest; DBF, deciduous broadleaf forest; DNF, deciduous needleleaf forest;  
 953 SHRUB, shrubland; GRASS, grassland.



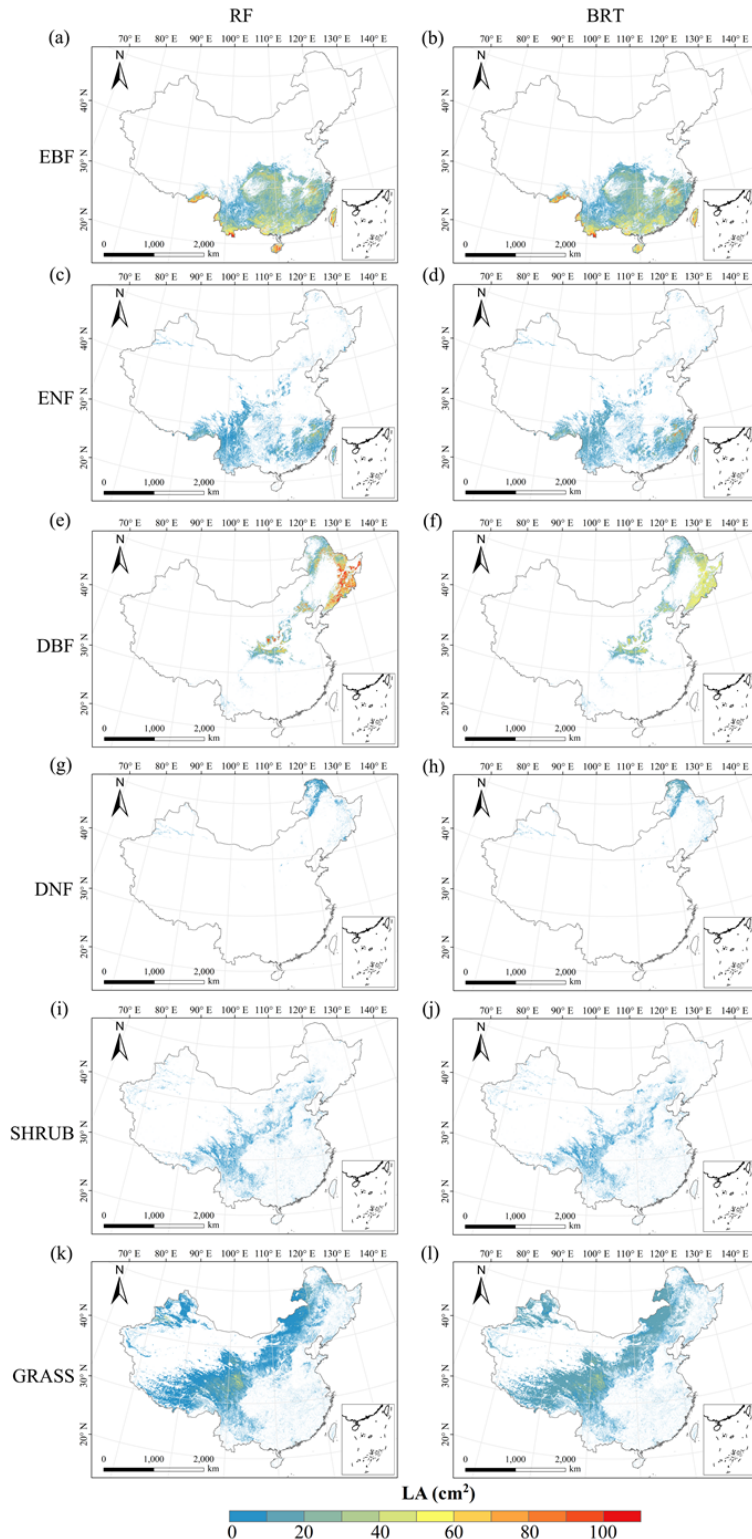
954

955 **Figure D5.** Spatial distribution of leaf N concentration (LNC) for each plant functional type. The  
 956 left panel was is obtained from RF ~~method~~-(random forest) method, the right panel was is obtained  
 957 from BRT ~~method~~-(boosted regression trees) method. The white areas represent other natural  
 958 vegetation types and artificial land cover types. EBF, evergreen broadleaf forest; ENF, evergreen  
 959 needleleaf forest; DBF, deciduous broadleaf forest; DNF, deciduous needleleaf forest; SHRUB,  
 960 shrubland; GRASS, grassland.



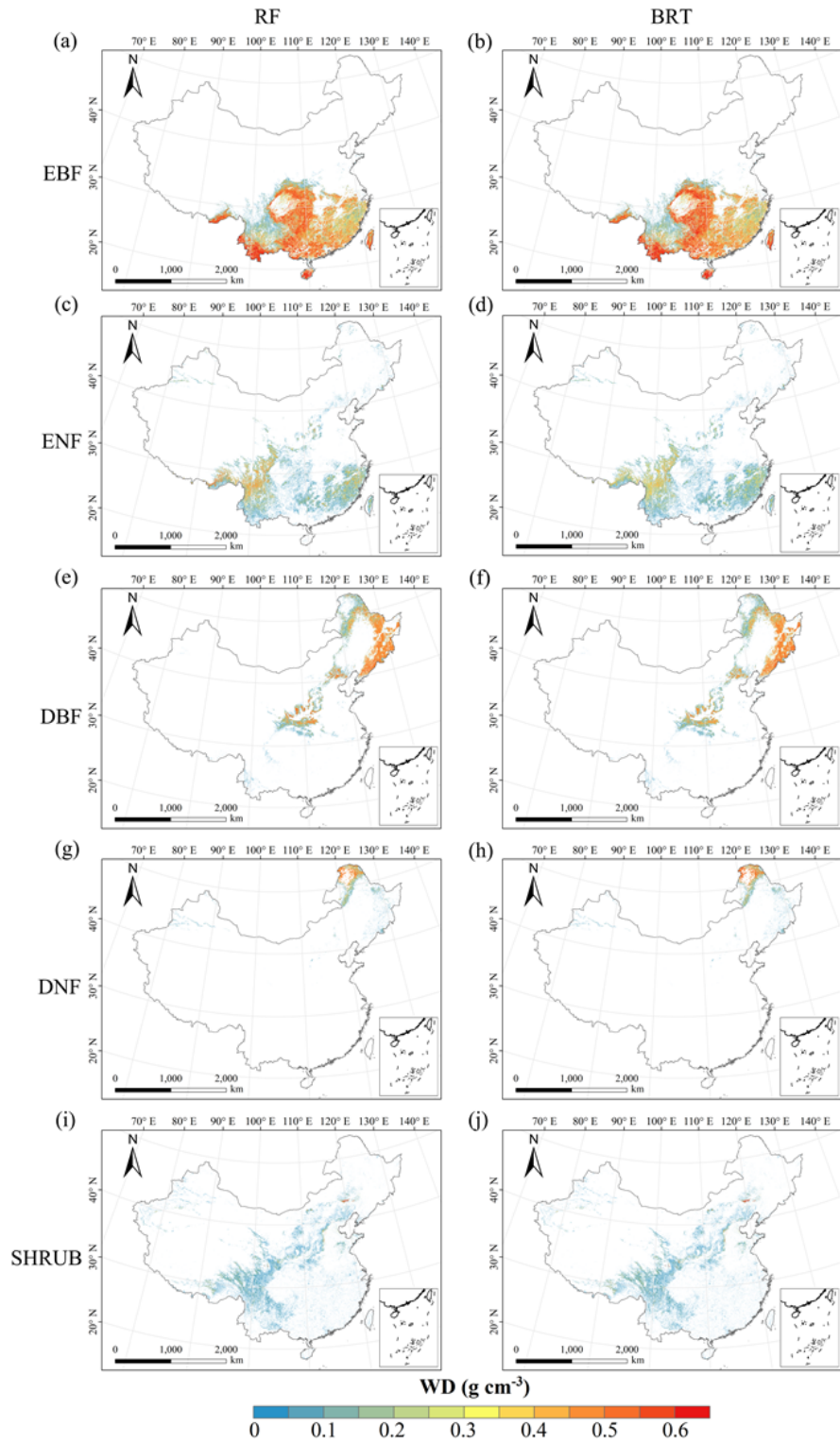
961

962 **Figure D6.** Spatial distribution of leaf P concentration (LPC) for each plant functional type. The  
 963 left panel was-is obtained from RF ~~method~~-method, the right panel was-is obtained  
 964 from BRT ~~method~~-method. The white areas represent other natural  
 965 vegetation types and artificial land cover types. EBF, evergreen broadleaf forest; ENF, evergreen  
 966 needleleaf forest; DBF, deciduous broadleaf forest; DNF, deciduous needleleaf forest; SHRUB,  
 967 shrubland; GRASS, grassland.



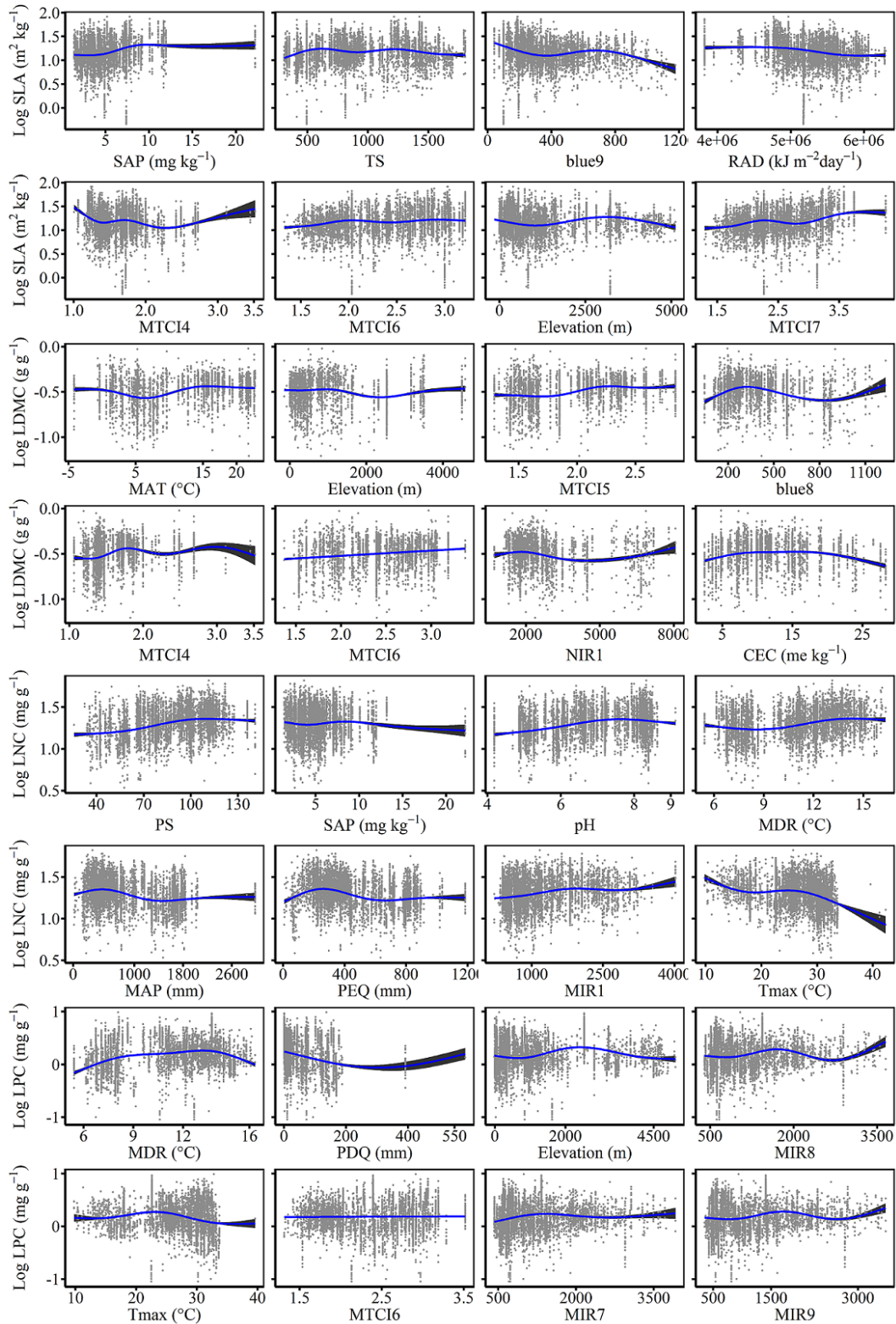
968

969 **Figure D7.** Spatial distribution of leaf area (LA) for each plant functional type. The left panel ~~was~~  
 970 ~~is~~ obtained from RF ~~method~~–(random forest) method, the right panel ~~was-is~~ obtained from BRT  
 971 ~~method~~–(boosted regression trees) method. The white areas represent other natural vegetation  
 972 types and artificial land cover types. EBF, evergreen broadleaf forest; ENF, evergreen needleleaf  
 973 forest; DBF, deciduous broadleaf forest; DNF, deciduous needleleaf forest; SHRUB, shrubland;  
 974 GRASS, grassland.



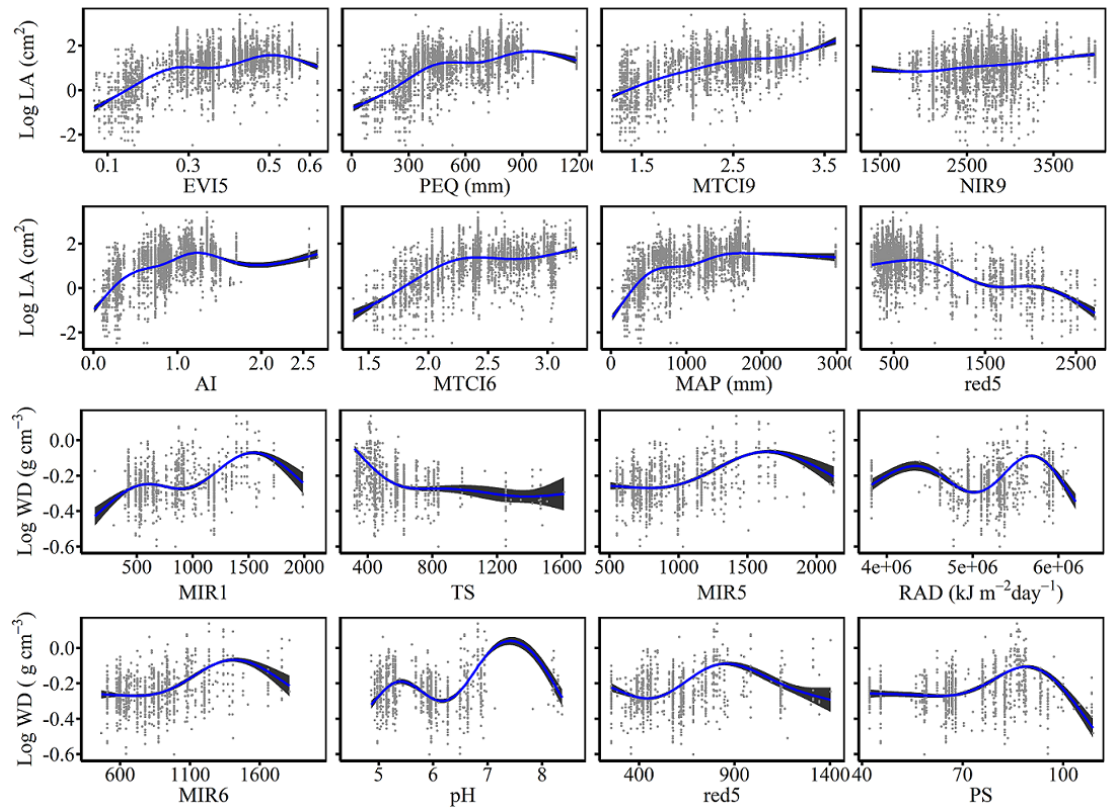
975

976 **Figure D8.** Spatial distribution of wood density (WD) for each plant functional type. The left  
 977 penal was-is obtained from RF method-(random forest) method, the right penal was-is obtained  
 978 from BRT method-(boosted regression trees) method. The white areas represent other natural  
 979 vegetation types and artificial land cover types. EBF, evergreen broadleaf forest; ENF, evergreen  
 980 needleleaf forest; DBF, deciduous broadleaf forest; DNF, deciduous needleleaf forest; SHRUB,  
 981 shrubland.



983  
 984 **Figure E1.** The relationships between SLA (specific leaf area), LDMC (leaf dry matter content),  
 985 LNC (leaf N concentration), LPC (leaf P concentration) and their eight most important predictors.





986

987

988

**Figure E2.** The relationships between LA (leaf area), WD (wood density) and their eight most important predictors.

989 **Appendix F Comparisons between our study with trait maps from previous**  
 990 **studies**

991 Given that the trait maps predicted for China were not available from the literature and [their](#)  
 992 authors, we compared our study with those studies performed at the global scale (~~see~~ Table F1).  
 993 Thus, we extracted the data in China from global trait maps. Before the quantitative comparisons  
 994 with previous studies, we performed two steps to make the data products as comparable as  
 995 possible and improve the consistency between different studies. First, due to different spatial  
 996 resolution of global trait maps (mainly 0.5 °) and our study, we resampled the data products of  
 997 previous studies and our maps to 0.5 ° spatial resolution. In addition, Vallicrosa et al. (2022)  
 998 generated the global maps of LNC and LPC with a 1 km spatial resolution, we also compared the  
 999 frequency distribution of Vallicrosa et al. (2022) with that of our study at a 1 km spatial resolution.  
 1000 Second, our study focused on natural vegetation, so the global trait maps were used to filter out  
 1001 non-natural vegetation (e.g., croplands). For example, Madani et al. (2018) predicted the spatial  
 1002 distributions of SLA that included croplands. We quantitatively compared our maps with previous  
 1003 studies from two perspectives. The comparisons among trait maps were made using frequency  
 1004 plots and spatial correlations (~~Figure Fig. 7, -and~~ Table 54 and [Fig. F1 in Appendix F](#)). And the  
 1005 maps of spatial differences between our study and previous studies were displayed as [Figs. F1-F2-](#)  
 1006 [F5-F6](#) in Appendix F.

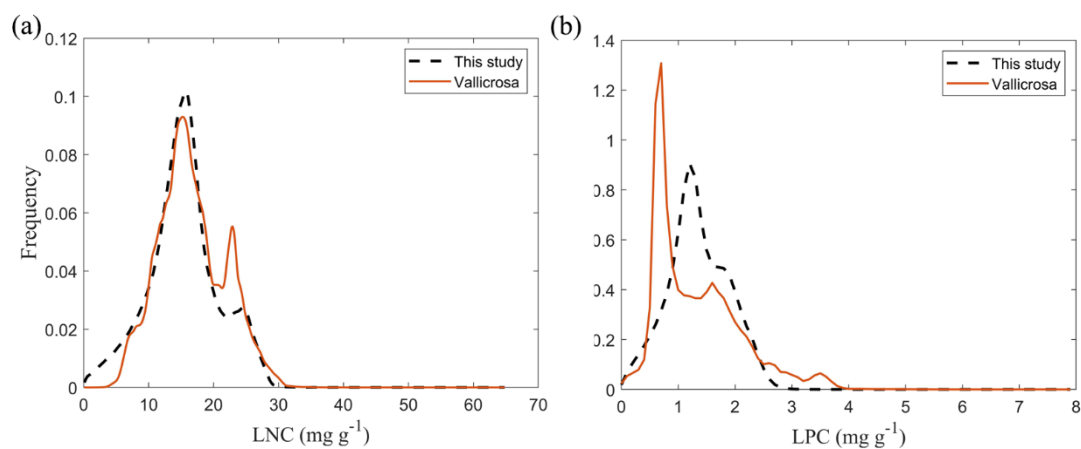
1007  
 1008

**Table F1** Summary ~~table~~ of related trait maps of previous studies used in this study.

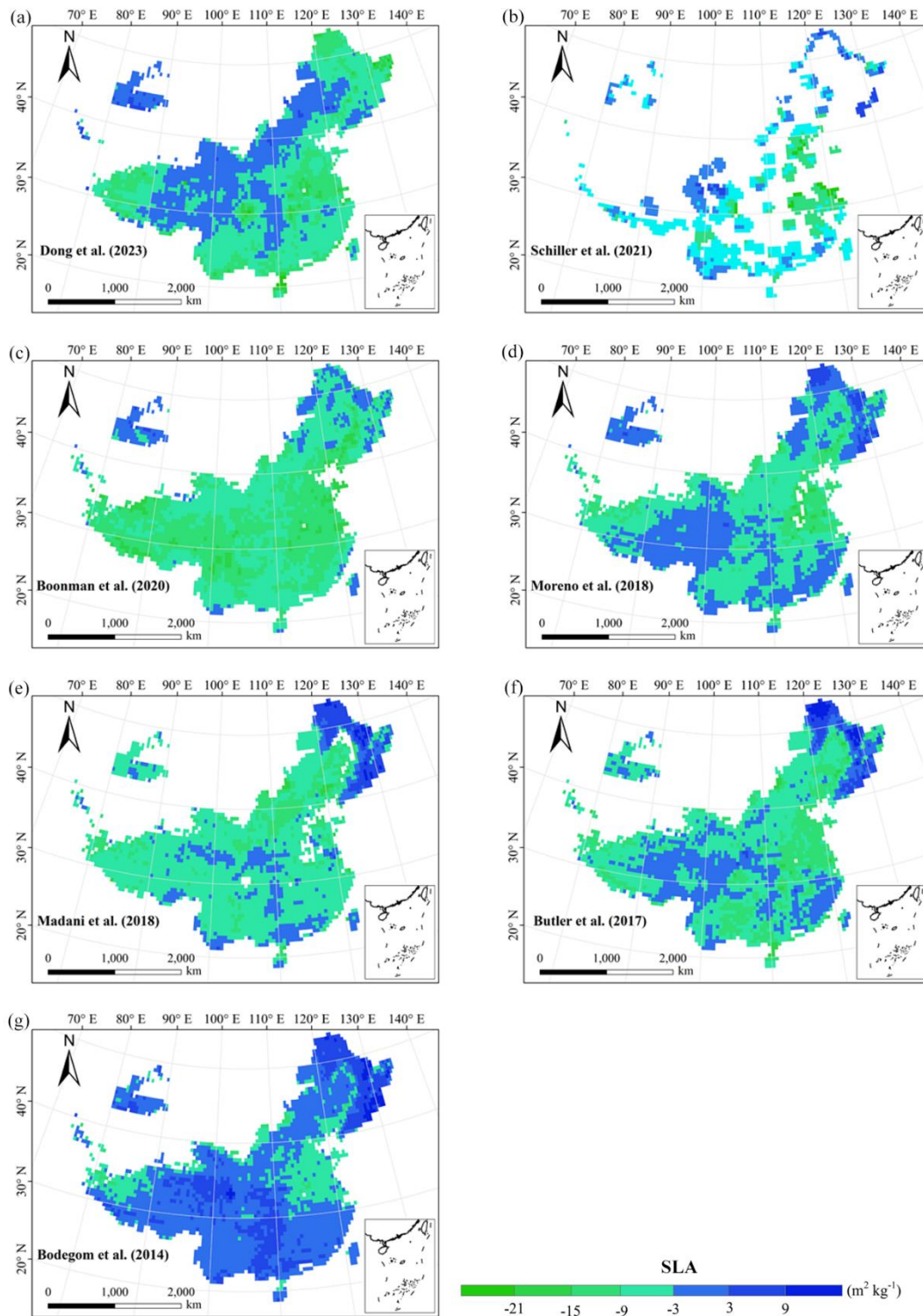
References	Related traits	Methods	Predictors	Consideration of PFT	<del>Spatial Resolution</del> resolution
Dong et al. (2023)	SLA LNC	Optimality models	Climate	Yes	0.5 °
Vallicrosa et al. (2022)	LNC LPC	Neural networks	Climate Soil N and P deposition	Yes	0.0083 °
Schiller et al. (2021)	SLA LNC LA WD	Convolutional Neural Networks	Climate In-situ RGB images	No	0.5 °
Boonman et al. (2020)	SLA LNC WD	Generalized linear model, Generalized additive model, Random forest, Boosted regression trees, Ensemble model	Climate Soil	No	0.5 °
Moreno et al. (2018)	SLA LNC	Regularized linear regression, Random	Climate Elevation	Yes	0.0045 °

	LPC	forest,	Neural	Reflectance		
	LDMC	networks,	Kernel			
		networks				
Madani et al. (2018)	SLA	Generalized additive model		Climate	No	0.5 °
Butler et al. (2017)	SLA	Bayesian model		Climate	Yes	0.5 °
	LNC			Soil		
	LPC					
Bodegom et al. (2014)	SLA	Multiple regression analysis		Climate	No	0.5 °
	WD			Soil		

1009 The resolutions 0.5 °, 0.0083 ° and 0.0045 ° correspond to square grid cell sizes of about 50 km, 1 km and 500 m at  
 1010 the equator. PFT, plant functional type; SLA, specific leaf area; LDMC, leaf dry matter content; LNC, leaf N  
 1011 concentration; LPC, leaf P concentration; LA, leaf area; WD, wood density.

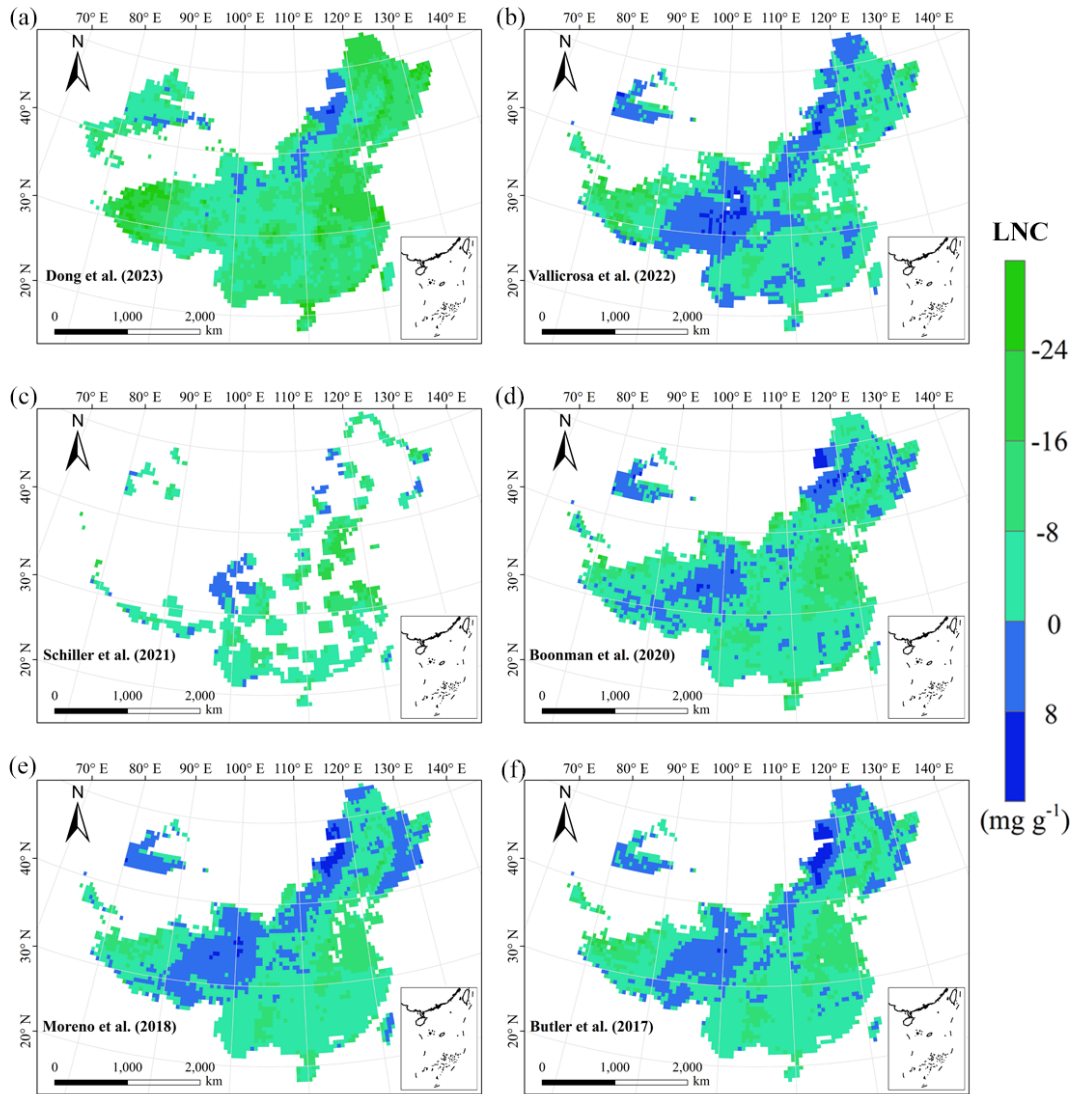


1012  
 1013 **Figure F1.** Frequency distributions of plant functional traits in our study (“This study”, dashed  
 1014 black lines) and Vallicrosa et al. (2022) at 1 km spatial resolution. (a) LNC, leaf N concentration  
 1015 (mg g<sup>-1</sup>); (b) LPC, leaf P concentration (mg g<sup>-1</sup>).



1016  
1017  
1018

**Figure F2.** Spatial differences in SLA (specific leaf area,  $\text{m}^2 \text{kg}^{-1}$ ) between our study and trait maps from previous studies (see Table F1 for citations).

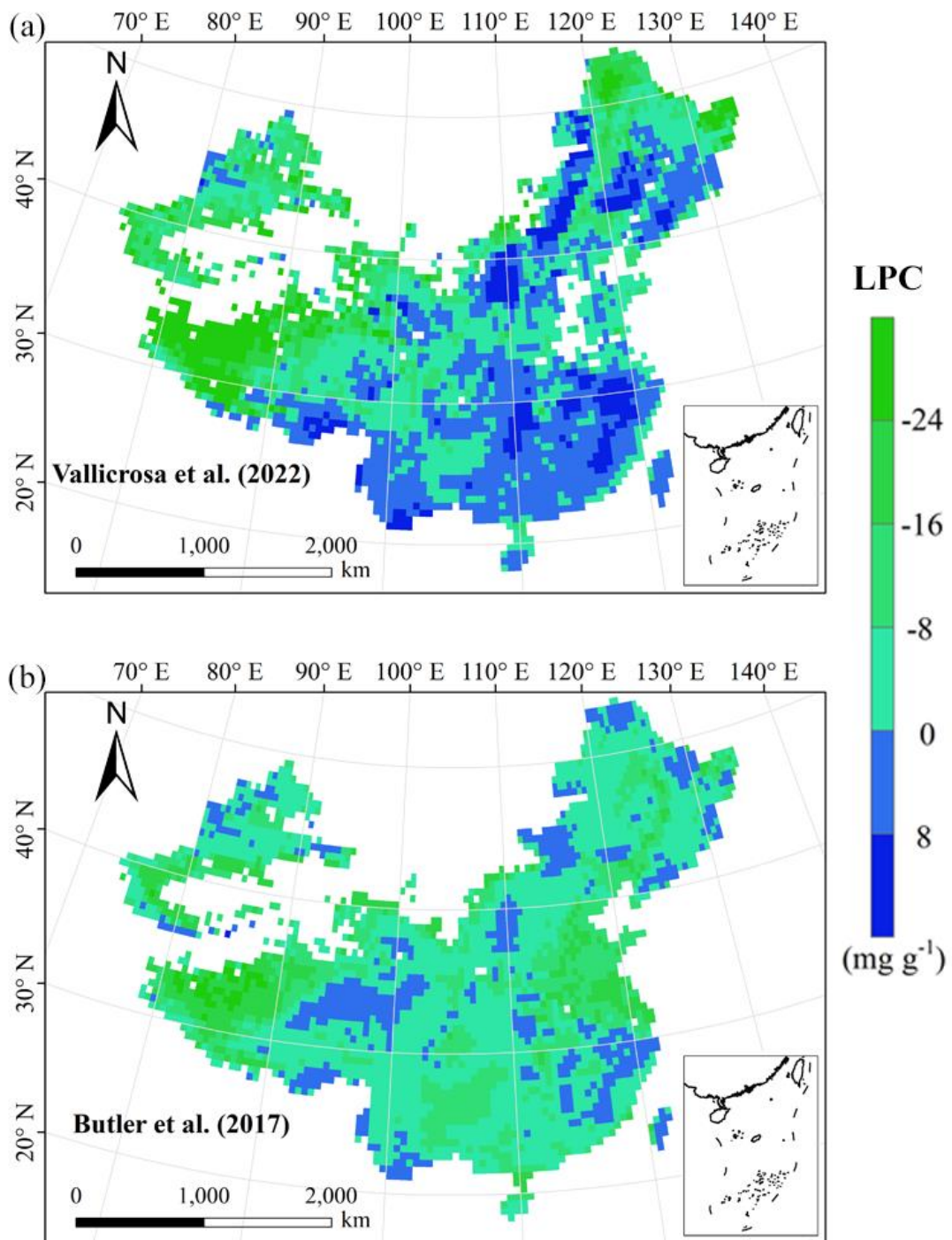


1019

1020 **Figure F3.** Spatial differences in LNC (leaf N concentration,  $\text{mg g}^{-1}$ ) between our study and trait

1021

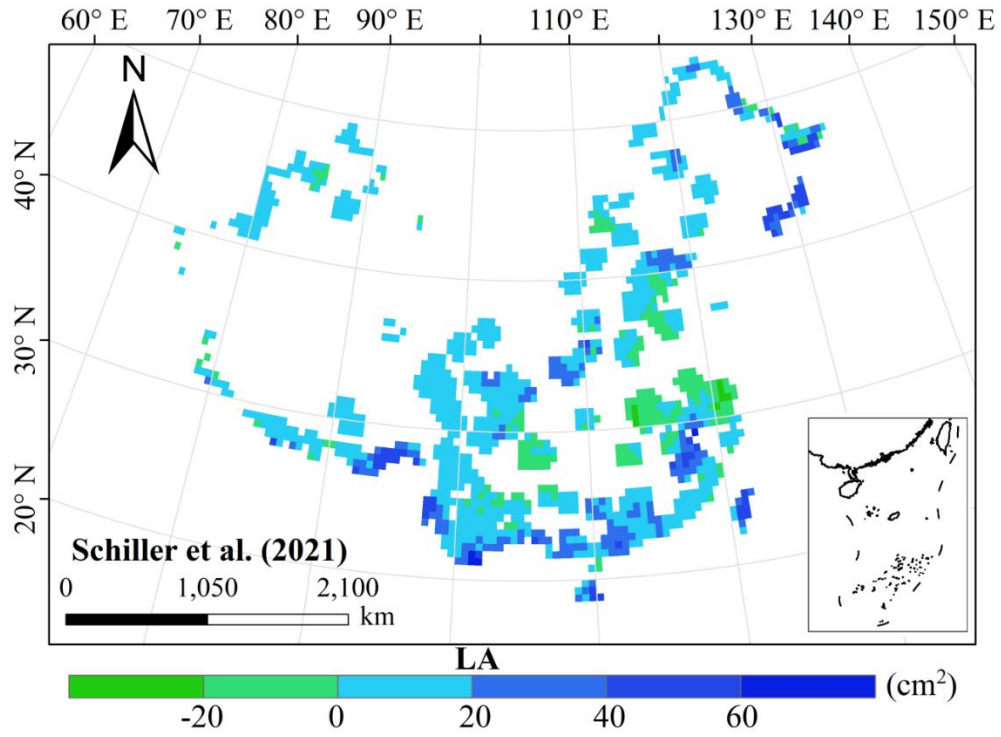
maps from previous studies (see Table F1 for citations).



1022

1023 **Figure F4.** Spatial differences in LPC (leaf P concentration, mg g<sup>-1</sup>) between our study and trait

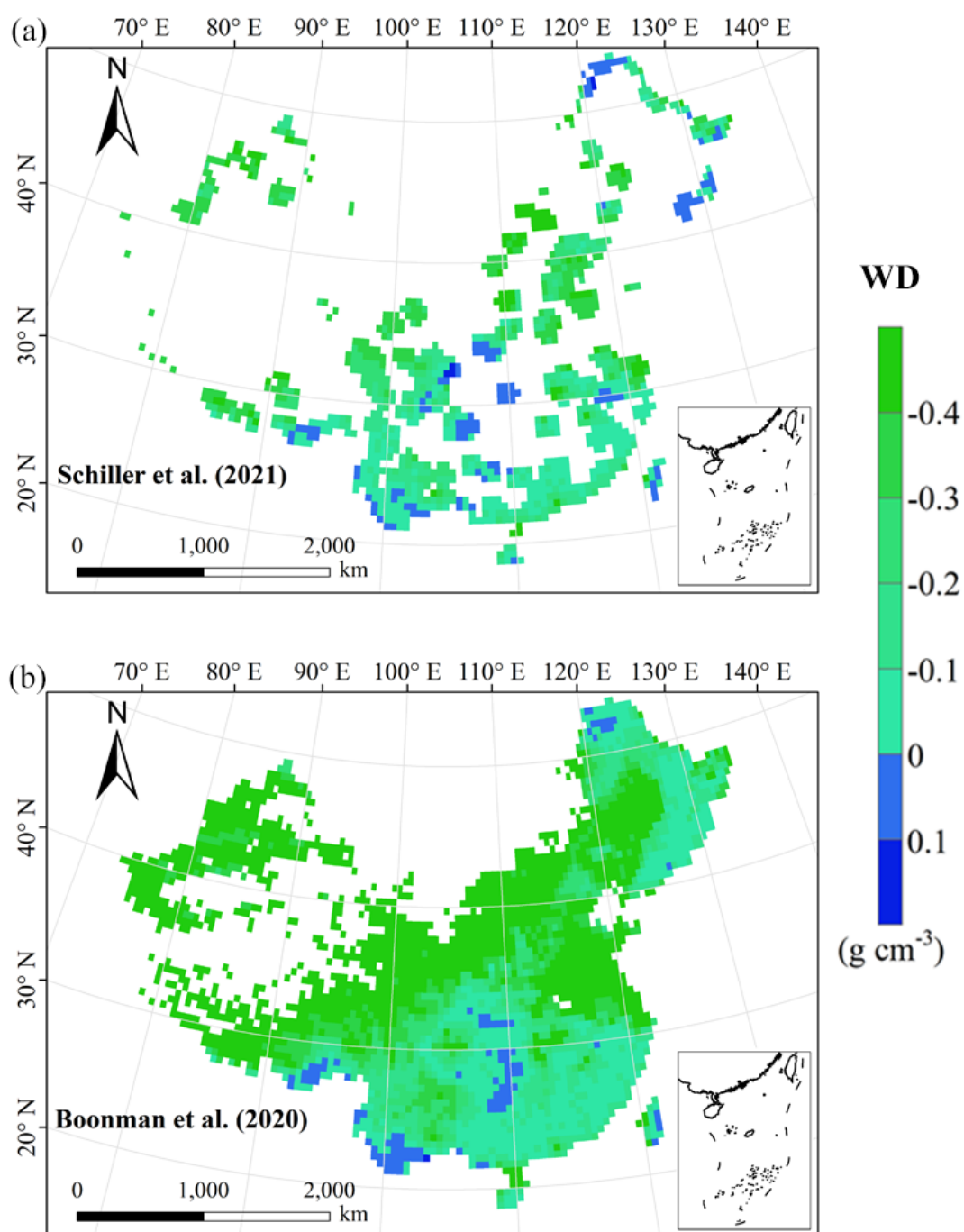
1024 maps from previous studies (see Table F1 for citations).



1025

1026 **Figure F5.** Spatial differences in LA (leaf area, cm<sup>2</sup>) between our study and trait maps from

1027 previous studies (see Table F1 for citations).



1028

1029 **Figure F6.** Spatial differences in WD (wood density,  $\text{g cm}^{-3}$ ) between our study and trait maps

1030 from previous studies (see Table F1 for citations).



1031 **Author contributions.** NA and NL designed the research. NA did the analysis, processed the data  
1032 and wrote the draft of the paper. All co-authors commented on the manuscript and agreed upon the  
1033 final version of the paper.

1034  
1035 **Competing interests.** The contact author has declared that none of the authors has any competing  
1036 interests.

1037  
1038 **Disclaimer.** Publisher's note: Copernicus Publications remains neutral with regard to  
1039 jurisdictional claims in published maps and institutional affiliations.

1040  
1041 **Acknowledgement.** We acknowledge financial supports from the National Natural Science  
1042 Foundation of China (41991234) and the Joint CAS-MPG Research Project (HZXM20225001MI).

1043  
1044 **Financial support.** This work has been supported by the National Natural Science Foundation of  
1045 China (grant no. 41991234) and the Joint CAS-MPG Research Project (grant no.  
1046 HZXM20225001MI).

1047

## 1048 **References**

1049 Ali, A. M., Darvishzadeh, R., Skidmore, A. K., van Duren, I., Heiden, U., and Heurich, M.:  
1050 Estimating leaf functional traits by inversion of PROSPECT: Assessing leaf dry matter  
1051 content and specific leaf area in mixed mountainous forest. *Int. J. Appl. Earth Obs. Geoinf.*,  
1052 45, 66–76, <https://doi.org/10.1016/j.jag.2015.11.004>, 2016.

1053 An, N. N., Lu, N., Fu, B. J., Wang, M. Y., and He, N. P.: Distinct responses of leaf traits to  
1054 environment and phylogeny between herbaceous and woody angiosperm species in China.  
1055 *Front. Plant Sci.*, 12, 799401, <https://doi.org/10.3389/fpls.2021.799401>, 2021.

1056 Bakker, M. A., Carreño-Rocabado, G., and Poorter, L.: Leaf economics traits predict litter  
1057 decomposition of tropical plants and differ among land use types. *Funct. Ecol.*, 25, 473–483,  
1058 <https://doi.org/10.1111/j.1365-2435.2010.01802.x>, 2011.

1059 Berzaghi, F., Wright, I. J., Kramer, K., Oddou-Muratorio, S., Bohn, F. J., Reyer, C. P. O., Sabate,  
1060 S., Sanders, T. G. M., and Hartig, F.: Towards a new generation of trait-flexible vegetation  
1061 models. *Trends Ecol. Evol.*, 35, 191–205, <https://doi.org/10.1016/j.tree.2019.11.006>, 2020.

1062 Blumenthal, D. M., Mueller, K. E., Kray, J. A., Ocheltree, T. W., Augustine, D. J., Wilcox, K. R.,  
1063 and Cornelissen, H.: Traits link drought resistance with herbivore defence and plant  
1064 economics in semi-arid grasslands: The central roles of phenology and leaf dry matter  
1065 content. *J. Ecol.*, 108, 2336–2351, <https://doi.org/10.1111/1365-2745.13454>, 2020.

1066 Bohner, A. Soil chemical properties as indicators of plant species richness in grassland  
1067 communities. Integrating efficient grassland farming and biodiversity, Proceedings of the  
1068 13th International Occasional Symposium of the European Grassland Federation, Tartu,

1069 Estonia, 29–31 August, 48–51, 2005.

1070 Boonman, C. C. F., Benitez-Lopez, A., Schipper, A. M., Thuiller, W., Anand, M., Cerabolini, B. E.  
1071 L., Cornelissen, J. H. C., Gonzalez-Melo, A., Hattingh, W. N., Higuchi, P., Laughlin, D. C.,  
1072 Onipchenko, V. G., Penuelas, J., Poorter, L., Soudzilovskaia, N. A., Huijbregts, M. A. J., and  
1073 Santini, L.: Assessing the reliability of predicted plant trait distributions at the global scale.  
1074 *Global Ecol. Biogeogr.*, 29, 1034–1051, <https://doi.org/10.1111/geb.13086>, 2020.

1075 Breiman, L.: Random forests. *Mach. Learn.*, 45, 5–32, <https://doi.org/10.1023/a:1010933404324>,  
1076 2001.

1077 Bruelheide, H., Dengler, J., Purschke, O., Lenoir, J., Jimenez-Alfaro, B., Hennekens, S. M., Botta-  
1078 Dukat, Z., Chytrý, M., Field, R., Jansen, F., Kattge, J., Pillar, V. D., Schrodte, F., Mahecha, M.  
1079 D., Peet, R. K., Sandel, B., van Bodegom, P., Altman, J., Alvarez-Davila, E., Arfin Khan, M.  
1080 A. S., et al.: Global trait-environment relationships of plant communities. *Nat. Ecol. Evol.*, 2,  
1081 1906–1917, <https://doi.org/10.1038/s41559-018-0699-8>, 2018.

1082 Bruelheide, H., Dengler, J., Jiménez-Alfaro, B., Purschke, O., Hennekens, S. M., Chytrý, M.,  
1083 Pillar, V. D., Jansen, F., Kattge, J., Sandel, B., Aubin, I., Biurrun, I., Field, R., Haider, S.,  
1084 Jandt, U., Lenoir, J., Peet, R. K., Peyre, G., Sabatini, F. M., Schmidt, M., et al.: sPlot – A new  
1085 tool for global vegetation analyses. *J. Veg. Sci.*, 30, 161–186,  
1086 <https://doi.org/10.1111/jvs.12710>, 2019.

1087 Buchhorn, M., Bertels, L., Smets, B., De Roo, B., Lesiv, M., Tsendbazar, N. E., Masiliunas, D.,  
1088 and Linlin, L.: Copernicus Global Land Service: Land Cover 100m: Version 3 Globe 2015-  
1089 2019: Algorithm Theoretical Basis Document. <https://doi.org/10.5281/zenodo.3938968>, 2020.

1090 Butler, E. E., Datta, A., Flores-Moreno, H., Chen, M., Wythers, K. R., Fazayeli, F., Banerjee, A.,  
1091 Atkin, O. K., Kattge, J., Amiaud, B., Blonder, B., Boenisch, G., Bond-Lamberty, B., Brown,  
1092 K. A., Byun, C., Campetella, G., Cerabolini, B. E. L., Cornelissen, J. H. C., Craine, J. M.,  
1093 Craven, D., de Vries, F. T., Diaz, S., Domingues, T. F., Forey, E., Gonzalez-Melo, A., Gross,  
1094 N., Han, W., Hattingh, W. N., Hickler, T., Jansen, S., Kramer, K., Kraft, N. J. B., Kurokawa,  
1095 H., Laughlin, D. C., Meir, P., Minden, V., Niinemets, U., Onoda, Y., Penuelas, J., Read, Q.,  
1096 Sack, L., Schamp, B., Soudzilovskaia, N. A., Spasojevic, M. J., Sosinski, E., Thornton, P. E.,  
1097 Valladares, F., van Bodegom, P. M., Williams, M., Wirth, C., and Reich, P. B.: Mapping local  
1098 and global variability in plant trait distributions. *P. Natl. Acad. Sci. USA*, 114, 10937–10946,  
1099 <https://doi.org/10.1073/pnas.1708984114>, 2017.

1100 Cavender-Bares, J., Schneider, F. D., Santos, M. J., Armstrong, A., Carnaval, A., Dahlin, K. M.,  
1101 Fatoyinbo, L., Hurr, G. C., Schimel, D., Townsend, P. A., Ustin, S. L., Wang, Z. H., and  
1102 Wilson, A. M.: Integrating remote sensing with ecology and evolution to advance  
1103 biodiversity conservation. *Nat. Ecol. Evol.*, 6, 506–519, <https://doi.org/10.1038/s41559-022-01702-5>, 2022.

1105 Clevers, J. G. P. W., and Gitelson, A. A.: Remote estimation of crop and grass chlorophyll and  
1106 nitrogen content using red-edge bands on Sentinel-2 and -3. *Int. J. Appl. Earth Obs. Geoinf.*,

1107 23, 344–351, <https://doi.org/10.1016/j.jag.2012.10.008>, 2013.

1108 Dahlin, K. M., Asner, G. P., and Field, C. B.: Environmental and community controls on plant  
1109 canopy chemistry in a Mediterranean-type ecosystem. *P. Natl. Acad. Sci. USA*, 110, 6895–  
1110 6900, <https://doi.org/10.1073/pnas.1215513110>, 2013.

1111 Darvishzadeh, R., Skidmore, A., Schlerf, M., and Atzberger, C.: Inversion of a radiative transfer  
1112 model for estimating vegetation LAI and chlorophyll in a heterogeneous grassland. *Remote*  
1113 *Sens. Environ.*, 112, 2592–2604, <https://doi.org/10.1016/j.rse.2007.12.003>, 2008.

1114 Diaz, S., Kattge, J., Cornelissen, J. H., Wright, I. J., Lavorel, S., Dray, S., Reu, B., Kleyer, M.,  
1115 Wirth, C., Prentice, I. C., Garnier, E., Bonisch, G., Westoby, M., Poorter, H., Reich, P. B.,  
1116 Moles, A. T., Dickie, J., Gillison, A. N., Zanne, A. E., Chave, J., Wright, S. J., Sheremet'ev, S.  
1117 N., Jactel, H., Baraloto, C., Cerabolini, B., Pierce, S., Shipley, B., Kirkup, D., Casanoves, F.,  
1118 Joswig, J. S., Gunther, A., Falczuk, V., Ruger, N., Mahecha, M. D., and Gorne, L. D.: The  
1119 global spectrum of plant form and function. *Nature*, 529, 167–171,  
1120 <https://doi.org/10.1038/nature16489>, 2016.

1121 Diaz, S., Hodgson, J. G., Thompson, K., Cabido, M., Cornelissen, J. H. C., Jalili, A., Montserrat-  
1122 Marti, G., Grime, J. P., Zarrinkamar, F., Asri, Y., Band, S. R., Basconcelo, S., Castro-Diez, P.,  
1123 Funes, G., Hamzehee, B., Khoshnevi, M., Perez-Harguindeguy, N., Perez-Rontome, M. C.,  
1124 Shirvany, F. A., Vendramini, F., Yazdani, S., Abbas-Azimi, R., Bogaard, A., Boustani, S.,  
1125 Charles, M., Dehghan, M., de Torres-Espuny, L., Falczuk, V., Guerrero-Campo, J., Hynd, A.,  
1126 Jones, G., Kowsary, E., Kazemi-Saeed, F., Maestro-Martinez, M., Romo-Diez, A., Shaw, S.,  
1127 Siavash, B., Villar-Salvador, P., and Zak, M. R.: The plant traits that drive ecosystems:  
1128 Evidence from three continents. *J. Veg. Sci.*, 15, 295–304, <https://doi.org/10.1111/j.1654-1103.2004.tb02266.x>, 2004.

1130 Dong, N., Dechant, B., Wang, H., Wright, I. J., and Prentice, IC.: Global leaf-trait mapping based  
1131 on optimality theory. *Global Ecol. Biogeogr.*, 32, 1152–1162,  
1132 <https://doi.org/10.1111/geb.13680>, 2023.

1133 Du, L., Liu, H., Guan, W., Li, J., and Li, J.: Drought affects the coordination of belowground and  
1134 aboveground resource-related traits in *Solidago canadensis* in China. *Ecol. Evol.*, 9, 9948–  
1135 9960, <https://doi.org/10.1002/ece3.5536>, 2019.

1136 Elith, J., Leathwick, J. R., and Hastie, T.: A working guide to boosted regression trees. *J. Anim.*  
1137 *Ecol.*, 77, 802–813, <https://doi.org/10.1111/j.1365-2656.2008.01390.x>, 2008.

1138 Elith, J., Kearney, M., and Phillips, S.: The art of modelling range-shifting species. *Methods Ecol.*  
1139 *Evol.*, 1, 330–342, <https://doi.org/10.1111/j.2041-210X.2010.00036.x>, 2010.

1140 Elith, J., Graham, C. H., Anderson, R. P., Dudik, M., Ferrier, S., Guisan, A., Hijmans, R. J.,  
1141 Huettmann, F., Leathwick, J. R., Lehmann, A., Li, J., Lohmann, L. G., Loiselle, B. A.,  
1142 Manion, G., Moritz, C., Nakamura, M., Nakazawa, Y., Overton, J. M., Peterson, A. T.,  
1143 Phillips, S. J., Richardson, K., Scachetti-Pereira, R., Schapire, R. E., Soberon, J., Williams, S.,  
1144 Wisz, M. S., and Zimmermann, N. E.: Novel methods improve prediction of species' species'

1145 distributions from occurrence data. *Ecography*, 29, 129–151,  
1146 <https://doi.org/10.1111/j.2006.0906-7590.04596.x>, 2006.

1147 Finzi, A. C., Austin, A. T., Cleland, E. E., Frey, S. D., Houlton, B. Z., and Wallenstein, M. D.:  
1148 Responses and feedbacks of coupled biogeochemical cycles to climate change: examples  
1149 from terrestrial ecosystems. *Front. Ecol. Environ.*, 9, 61–67, <https://doi.org/10.1890/100001>,  
1150 2011.

1151 Foley, J. A., Prentice, I. C., Ramankutty, N., Levis, S., Pollard, D., Sitch, S., and Haxeltine, A.: An  
1152 integrated biosphere model of land surface processes, terrestrial carbon balance, and  
1153 vegetation dynamics. *Global Biogeochem. Cy.*, 10, 603–628,  
1154 <https://doi.org/10.1029/96gb02692>, 1996.

1155 Freschet, G. T., Cornelissen, J. H. C., van Logtestijn, R. S. P., and Aerts, R.: Evidence of the ‘plant  
1156 economics spectrum’ in a subarctic flora. *J. Ecol.*, 98, 362–373,  
1157 <https://doi.org/10.1111/j.1365-2745.2009.01615.x>, 2010.

1158 Grime, J. P.: Benefits of plant diversity to ecosystems: immediate, filter and founder effects. *J.*  
1159 *Ecol.*, 86, 902–910, <https://doi.org/10.1046/j.1365-2745.1998.00306.x>, 1998.

1160 He, N. P., Yan, P., Liu, C. C., Xu, L., Li, M. X., Van Meerbeek, K., Zhou, G. S., Zhou, G. Y., Liu,  
1161 S. R., Zhou, X. H., Li, S. G., Niu, S. L., Han, X. G., Buckley, T. N., Sack, L., and Yu, G. R.:  
1162 Predicting ecosystem productivity based on plant community traits. *Trends Plant Sci.*, 28, 43–  
1163 53, <https://doi.org/10.1016/j.tplants.2022.08.015>, 2023.

1164 Hodgson, J. G., Montserrat-Marti, G., Charles, M., Jones, G., Wilson, P., Shipley, B., Sharafi, M.,  
1165 Cerabolini, B. E. L., Cornelissen, J. H. C., Band, S. R., Bogard, A., Castro-Diez, P., Guerrero-  
1166 Campo, J., Palmer, C., Perez-Rontome, M. C., Carter, G., Hynd, A., Romo-Diez, A., Espuny,  
1167 L. D., and Pla, F. R.: Is leaf dry matter content a better predictor of soil fertility than specific  
1168 leaf area? *Ann. Bot.*, 108, 1337–1345, <https://doi.org/10.1093/aob/mcr225>, 2011.

1169 Hoeber, S., Leuschner, C., Köhler, L., Arias-Aguilar, D., and Schuldt, B.: The importance of  
1170 hydraulic conductivity and wood density to growth performance in eight tree species from a  
1171 tropical semi-dry climate. *Forest Ecol. Manag.*, 330, 126–136,  
1172 <https://doi.org/10.1016/j.foreco.2014.06.039>, 2014.

1173 Jónsdóttir, I. S., Halbritter, A. H., Christiansen, C. T., Althuisen, I. H. J., Haugum, S. V., Henn, J. J.,  
1174 Björnsdóttir, K., Maitner, B. S., Malhi, Y., Michaletz, S. T., Roos, R. E., Klanderud, K., Lee,  
1175 H., Enquist, B. J., and Vandvik, V.: Intraspecific trait variability is a key feature underlying  
1176 high Arctic plant community resistance to climate warming. *Ecol. Monogr.*, 93, [e1555](https://doi.org/10.1002/ecm.1555),  
1177 <https://doi.org/10.1002/ecm.1555>, 2022.

1178 Jung, V., Violle, C., Mondy, C., Hoffmann, L., and Muller, S.: Intraspecific variability and trait-  
1179 based community assembly. *J. Ecol.*, 98, 1134–1140, <https://doi.org/10.1111/j.1365-2745.2010.01687.x>, 2010.

1181 Kattge, J., Diaz, S., Lavorel, S., Prentice, C., Leadley, P., Bonisch, G., Garnier, E., Westoby, M.,  
1182 Reich, P. B., Wright, I. J., Cornelissen, J. H. C., Violle, C., Harrison, S. P., van Bodegom, P.

1183 M., Reichstein, M., Enquist, B. J., Soudzilovskaia, N. A., Ackerly, D. D., Anand, M., Atkin,  
1184 O., et al.: TRY - A global database of plant traits. *Global Change Biol.*, 17, 2905–2935,  
1185 <https://doi.org/10.1111/j.1365-2486.2011.02451.x>, 2011.

1186 Kattge, J., Bonisch, G., Diaz, S., Lavorel, S., Prentice, I. C., Leadley, P., Tautenhahn, S., Werner, G.  
1187 D. A., Aakala, T., Abedi, M., Acosta, A. T. R., Adamidis, G. C., Adamson, K., Aiba, M.,  
1188 Albert, C. H., Alcantara, J. M., Alcazar, C. C., Aleixo, I., Ali, H., Amiaud, B., et al.: TRY  
1189 plant trait database - ~~enhanced~~ **Enhanced** coverage and open access. *Global Change Biol.*, 26,  
1190 119–188, <https://doi.org/10.1111/gcb.14904>, 2020.

1191 King, D. A., Davies, S. J., Tan, S., and Noor, N. S. M.: The role of wood density and stem support  
1192 costs in the growth and mortality of tropical trees. *J. Ecol.*, 94, 670–680,  
1193 <https://doi.org/10.1111/j.1365-2745.2006.01112.x>, 2006.

1194 Kirilenko, A. P., Belotelov, N. V., and Bogatyrev, B. G.: Global model of vegetation migration:  
1195 incorporation of climatic variability. *Ecol. Model.*, 132, 125–133,  
1196 [https://doi.org/10.1016/S0304-3800\(00\)00310-0](https://doi.org/10.1016/S0304-3800(00)00310-0), 2000.

1197 LeBauer, D. S., and Treseder, K. K.: Nitrogen limitation of net primary productivity in terrestrial  
1198 ecosystems is globally distributed. *Ecology*, 89, 371–379, <https://doi.org/10.1890/06-2057.1>,  
1199 2008.

1200 Li, C. X., Wulf, H., Schmid, B., He, J. S., and Schaepman, M. E.: Estimating plant traits of alpine  
1201 grasslands on the Qinghai-Tibetan Plateau using remote sensing. *IEEE J. Sel. Top. Appl.*  
1202 *Earth Obs. Remote Sens.*, 11, 2263–2275, <https://doi.org/10.1109/jstars.2018.2824901>, 2018.

1203 Li, D. J., Ives, A. R., and Waller, D. M.: Can functional traits account for phylogenetic signal in  
1204 community composition? *New Phytol.*, 214, 607–618, <https://doi.org/10.1111/nph.14397>,  
1205 2017.

1206 Li, Y. Q., Reich, P. B., Schmid, B., Shrestha, N., Feng, X., Lyu, T., Maitner, B. S., Xu, X., Li, Y. C.,  
1207 Zou, D. T., Tan, Z. H., Su, X. Y., Tang, Z. Y., Guo, Q. H., Feng, X. J., Enquist, B. J., and  
1208 Wang, Z. H.: Leaf size of woody dicots predicts ecosystem primary productivity. *Ecol. Lett.*,  
1209 23, 1003–1013, <https://doi.org/10.1111/ele.13503>, 2020.

1210 Liang, X. Y., Ye, Q., Liu, H., and Brodribb, T. J.: Wood density predicts mortality threshold for  
1211 diverse trees. *New Phytol.*, 229, [3053–3057](https://doi.org/10.1111/nph.17117), <https://doi.org/10.1111/nph.17117>, 2021.

1212 Liaw, A., and Wiener, M.: Classification and Regression by randomForest. *R News*, 2, 18–22,  
1213 2002.

1214 Liu, H. Y., and Yin, Y.: Response of forest distribution to past climate change: an insight into  
1215 future predictions. *Chinese Science—Sci. Bulletin*, 58, 4426–4436,  
1216 <https://doi.org/10.1007/s11434-013-6032-7>, 2013.

1217 Loozen, Y., Rebel, K. T., Karssenber, D., Wassen, M. J., Sardans, J., Peñuelas, J., and De Jong, S.  
1218 M.: Remote sensing of canopy nitrogen at regional scale in Mediterranean forests using the  
1219 spaceborne MERIS Terrestrial Chlorophyll Index. *Biogeosciences*, 15, 2723–2742,  
1220 <https://doi.org/10.5194/bg-15-2723-2018>, 2018.

1221 Loozen, Y., Rebel, K. T., de Jong, S. M., Lu, M., Ollinger, S. V., Wassen, M. J., and Karssenber,  
1222 D.: Mapping canopy nitrogen in European forests using remote sensing and environmental  
1223 variables with the random forests method. *Remote Sens. Environ.*, 247, 111933,  
1224 <https://doi.org/10.1016/j.rse.2020.111933>, 2020.

1225 Madani, N., Kimball, J. S., Ballantyne, A. P., Affleck, D. L. R., van Bodegom, P. M., Reich, P. B.,  
1226 Kattge, J., Sala, A., Nazeri, M., Jones, M. O., Zhao, M., and Running, S. W.: Future global  
1227 productivity will be affected by plant trait response to climate. *Sci. Rep.*, 8, 1–10,  
1228 <https://doi.org/10.1038/s41598-018-21172-9>, 2018.

1229 Martínez-Vilalta, J., Mencuccini, M., Vayreda, J., and Retana, J.: Interspecific variation in  
1230 functional traits, not climatic differences among species ranges, determines demographic  
1231 rates across 44 temperate and Mediterranean tree species. *J. Ecol.*, 98, 1462–1475,  
1232 <https://doi.org/10.1111/j.1365-2745.2010.01718.x>, 2010.

1233 Matheny, A. M., Mirfenderesgi, G., and Bohrer, G.: Trait-based representation of hydrological  
1234 functional properties of plants in weather and ecosystem models. *Plant Divers.*, 39, 1–12,  
1235 <https://doi.org/10.1016/j.pld.2016.10.001>, 2017.

1236 ~~Moles, A. T., Warton, D. I., Warman, L., Swenson, N. G., Laffan, S. W., Zanne, A. E., Pitman, A.,  
1237 Hemmings, F. A., and Leishman, M. R.: Global patterns in plant height. *J. Ecol.*, 97, 923–932,  
1238 <https://doi.org/10.1111/j.1365-2745.2009.01526.x>, 2009.~~

1239 Moreno-Martínez, Á., Camps-Valls, G., Kattge, J., Robinson, N., Reichstein, M., van Bodegom, P.,  
1240 Kramer, K., Cornelissen, J. H. C., Reich, P., Bahn, M., Niinemets, Ü., Peñuelas, J., Craine, J.  
1241 M., Cerabolini, B. E. L., Minden, V., Laughlin, D. C., Sack, L., Allred, B., Baraloto, C., Byun,  
1242 C., Soudzilovskaia, N. A., and Running, S. W.: A methodology to derive global maps of leaf  
1243 traits using remote sensing and climate data. *Remote Sens. Environ.*, 218, 69–88,  
1244 <https://doi.org/10.1016/j.rse.2018.09.006>, 2018.

1245 Myers-Smith, I. H., Thomas, H. J. D., and Björkman, A. D.: Plant traits inform predictions of  
1246 tundra responses to global change. *New Phytol.*, 221, 1742–1748,  
1247 <https://doi.org/10.1111/nph.15592>, 2019.

1248 NEODC, 2015. NEODC - NERC Earth Observation Data Centre. Natural Environment Research  
1249 Council. <http://neodc.nerc.ac.uk/>.

1250 Peng, C. H.: From static biogeographical model to dynamic global vegetation model: a global  
1251 perspective on modelling vegetation dynamics. *Ecol. Model.*, 135, 33–54,  
1252 [https://doi.org/10.1016/S0304-3800\(00\)00348-3](https://doi.org/10.1016/S0304-3800(00)00348-3), 2000.

1253 Perez-Harguindeguy, N., Diaz, S., Garnier, E., Lavorel, S., Poorter, H., Jaureguiberry, P., Bret-  
1254 Harte, M. S., Cornwell, W. K., Craine, J. M., Gurvich, D. E., Urcelay, C., Veneklaas, E. J.,  
1255 Reich, P. B., Poorter, L., Wright, I. J., Ray, P., Enrico, L., Pausas, J. G., de Vos, A. C.,  
1256 Buchmann, N., Funes, G., Quétier, F., Hodgson, J. G., Thompson, K., Morgan, H. D., ter  
1257 Steege, H., van der Heijden, M. G. A., Sack, L., Blonder, B., Poschlod, P., Vaieretti, M. V.,  
1258 Conti, G., Staver, A. C., Aquino, S., and Cornelissen, J. H. C.: New handbook for

1259 standardised measurement of plant functional traits worldwide. *Aust. Bot.*, 61, 167–234,  
1260 <https://doi.org/10.1071/bt12225>, 2013.

1261 Piao, S. L., He, Y., Wang, X. H., and Chen, F. H.: Estimation of China’s terrestrial ecosystem  
1262 carbon sink: Methods, progress and prospects. *Science Sci. China Earth Sciences*, 65,  
1263 641–651, <https://doi.org/10.1007/s11430-021-9892-6>, 2022.

1264 ~~Potapov, P., Li, X. Y., Hernandez-Serna, A., Tyukavina, A., Hansen, M. C., Kommareddy, A.,~~  
1265 ~~Pickens, A., Turubanova, S., Tang, H., Silva, C. E., Armston, J., Dubayah, R., Blair, J. B.,~~  
1266 ~~Hofton, M.: Mapping global forest canopy height through integration of GEDI and Landsat~~  
1267 ~~data. *Remote Sens. Environ.*, 253, 112165, <https://doi.org/10.1016/j.rse.2020.112165>, 2021.~~

1268 Qiao, J. J., Zuo, X. A., Yue, P., Wang, S. K., Hu, Y., Guo, X. X., Li, X. Y., Lv, P., Guo, A. X., and  
1269 Sun, S. S.: High nitrogen addition induces functional trait divergence of plant community in a  
1270 temperate desert steppe. *Plant and Soil*, 487, 133–156, [https://doi.org/10.1007/s11104-023-](https://doi.org/10.1007/s11104-023-05910-1)  
1271 05910-1, 2023.

1272 Reich, P. B., and Oleksyn, J.: Global patterns of plant leaf N and P in relation to temperature and  
1273 latitude. *P. Natl. Acad. Sci. USA Proc. Natl. Acad. Sci. U. S. A.*, 101, 11001–11006,  
1274 <https://doi.org/10.1073/pnas.0403588101>, 2004.

1275 ~~Reich, P. B., and Cornelissen, H.: The world-wide ‘fast-slow’ plant economics spectrum: a traits~~  
1276 ~~manifesto. *Journal of Ecology*, 102, 275–301, <https://doi.org/10.1111/1365-2745.12211>, 2014.~~

1277 Reich, P. B., Uhl, C., Walters, M. B., and Ellsworth, D. S.: Leaf lifespan as a determinant of leaf  
1278 structure and function among 23 Amazonian tree species. *Oecologia*, 86, 16–24,  
1279 <https://doi.org/10.1007/BF00317383>, 1991.

1280 Ridgeway, G.: Gbm: generalized boosted regression models. R package version 1.5-6, Available at:  
1281 <http://cran.r-project.org/web/packages/gbm/index.html>, accessed 11/02/2009, 2006.

1282 Roderick, M. L., and Berry, S. L.: Linking wood density with tree growth and environment: a  
1283 theoretical analysis based on the motion of water. *New Phytol.*, 149, 473–485,  
1284 <https://doi.org/10.1046/j.1469-8137.2001.00054.x>, 2002.

1285 Romero, A., Aguado, I., and Yebra, M.: Estimation of dry matter content in leaves using  
1286 normalized indexes and PROSPECT model inversion. *Int. J. Remote Sens.*, 33, 396–414,  
1287 <https://doi.org/10.1080/01431161.2010.532819>, 2012.

1288 Sakschewski, B., von Bloh, W., Boit, A., Rammig, A., Kattge, J., Poorter, L., Penuelas, J., and  
1289 Thonicke, K.: Leaf and stem economics spectra drive diversity of functional plant traits in a  
1290 dynamic global vegetation model. *Global Change Biol.*, 21, 2711–2725,  
1291 <https://doi.org/10.1111/gcb.12870>, 2015.

1292 Scheiter, S., Langan, L., and Higgins, S. I.: Next-generation dynamic global vegetation models:  
1293 learning from community ecology. *New Phytol.*, 198, 957–969,  
1294 <https://doi.org/10.1111/nph.12210>, 2013.

1295 Schiller, C., Schmidtlein, S., Boonman, C., Moreno-Martinez, A., and Kattenborn, T.: Deep  
1296 learning and citizen science enable automated plant trait predictions from photographs. *Sci.*

1297 Rep., 11, [16395](https://doi.org/10.1038/s41598-021-95616-0), <https://doi.org/10.1038/s41598-021-95616-0>, ~~2022~~2021.

1298 Shangguan, W., Dai, Y. J., Liu, B. Y., Zhu, A. X., Duan, Q. Y., Wu, L. Z., Ji, D. Y., Ye, A. Z., Yuan,  
1299 H., Zhang, Q., Chen, D. D., Chen, M., Chu, J. T., Dou, Y. J., Guo, J. X., Li, H. Q., Li, J. J.,  
1300 Liang, L., Liang, X., Liu, H. P., Liu, S. Y., Miao, C. Y., and Zhang, Y. Z.: A China data set of  
1301 soil properties for land surface modeling. *J. Adv. Model. Earth Syst.*, 5, 212–224,  
1302 <https://doi.org/10.1002/jame.20026>, 2013.

1303 Siefert, A., Violle, C., Chalmandrier, L., Albert, C. H., Taudiere, A., Fajardo, A., Aarssen, L. W.,  
1304 Baraloto, C., Carlucci, M. B., Cianciaruso, M. V., de, L. D. V., de Bello, F., Duarte, L. D.,  
1305 Fonseca, C. R., Freschet, G. T., Gaucherand, S., Gross, N., Hikosaka, K., Jackson, B., Jung,  
1306 V., Kamiyama, C., Katabuchi, M., Kembel, S. W., Kichenin, E., Kraft, N. J., Lagerstrom, A.,  
1307 Bagousse-Pinguet, Y. L., Li, Y., Mason, N., Messier, J., Nakashizuka, T., Overton, J. M.,  
1308 Peltzer, D. A., Perez-Ramos, I. M., Pillar, V. D., Prentice, H. C., Richardson, S., Sasaki, T.,  
1309 Schamp, B. S., Schob, C., Shipley, B., Sundqvist, M., Sykes, M. T., Vandewalle, M., and  
1310 Wardle, D. A.: A global meta-analysis of the relative extent of intraspecific trait variation in  
1311 plant communities. *Ecol. Lett.*, 18, 1406–1419, <https://doi.org/10.1111/ele.12508>, 2015.

1312 Šímová, I., Sandel, B., Enquist, B. J., Michaletz, S. T., Kattge, J., Violle, C., McGill, B. J., Blonder,  
1313 B., Engemann, K., Peet, R. K., Wiser, S. K., Morueta-Holme, N., Boyle, B., Kraft, N. J. B.,  
1314 Svenning, J. C., and Hector, A.: The relationship of woody plant size and leaf nutrient content  
1315 to large-scale productivity for forests across the Americas. *J. Ecol.*, 107, 2278–2290,  
1316 <https://doi.org/10.1111/1365-2745.13163>, 2019.

1317 Sitch, S., Huntingford, C., Gedney, N., Levy, P. E., Lomas, M., Piao, S. L., Betts, R., Ciais, P., Cox,  
1318 P., Friedlingstein, P., Jones, C. D., Prentice, I. C., and Woodward, F. I.: Evaluation of the  
1319 terrestrial carbon cycle, future plant geography and climate-carbon cycle feedbacks using five  
1320 Dynamic Global Vegetation Models (DGVMs). *Global Change Biol.*, 14, 2015–2039,  
1321 <https://doi.org/10.1111/j.1365-2486.2008.01626.x>, 2008.

1322 Smart, S. M., Glanville, H. C., Blanes, M. d. C., Mercado, L. M., Emmett, B. A., Jones, D. L.,  
1323 Cosby, B. J., Marrs, R. H., Butler, A., Marshall, M. R., Reinsch, S., Herrero-Járegui, C.,  
1324 Hodgson, J. G., and Field, K.: Leaf dry matter content is better at predicting above-ground  
1325 net primary production than specific leaf area. *Funct. Ecol.*, 31, 1336–1344,  
1326 <https://doi.org/10.1111/1365-2435.12832>, 2017.

1327 Telenius, A.: Biodiversity information goes public: GBIF at your service. *Nord. J. Bot.*, 29, 378–  
1328 381, <https://doi.org/10.1111/j.1756-1051.2011.01167.x>, 2011.

1329 Thomas, D. S., Montagu, K. D., and Conroy, J. P.: Changes in wood density of *Eucalyptus*  
1330 *camaldulensis* due to temperature—the physiological link between water viscosity and wood  
1331 anatomy. *Forest Ecol. Manag.*, 193, 157–165, <https://doi.org/10.1016/j.foreco.2004.01.028>,  
1332 2004.

1333 Thomas, S. C.: Photosynthetic capacity peaks at intermediate size in temperate deciduous trees.  
1334 *Tree Physiol.*, 30, 555–573, <https://doi.org/10.1093/treephys/tpq005>, 2010.



1335 Thuiller, W., Lafourcade, B., Engler, R., and Araújo, M. B.: BIOMOD – A platform for ensemble  
1336 forecasting of species distributions. *Ecography*, 32, 369–373, <https://doi.org/10.1111/j.1600->  
1337 0587.2008.05742.x, 2009.

1338 Trabucco, A., and Zomer, R. J.: Global Aridity Index and Potential Evapo-Transpiration (ET0)  
1339 Climate Database v2. CGIAR Consortium for Spatial Information (CGIAR-CSI),  
1340 <https://cgiarcsi.community>, 2018.

1341 Vallicrosa, H., Sardans, J., Maspons, J., Zuccarini, P., Fernández-Martínez, M., Bauters, M., Goll,  
1342 D. S., Ciais, P., Obersteiner, M., Janssens, I. A., and Peñuelas, J.: Global maps and factors  
1343 driving forest foliar elemental composition: the importance of evolutionary history. *New*  
1344 *Phytol.*, 233, 169–181, <https://doi.org/10.1111/nph.17771>, 2022.

1345 ~~Van-van~~ Bodegom, P. M., Douma, J. C., Witte, J. P. M., Ordoñez, J. C., Bartholomeus, R. P., and  
1346 Aerts, R.: Going beyond limitations of plant functional types when predicting global  
1347 ecosystem-atmosphere fluxes: exploring the merits of traits-based approaches. *Global Ecol.*  
1348 *Biogeogr.*, 21, 625–636, <https://doi.org/10.1111/j.1466-8238.2011.00717.x>, 2012.

1349 van Bodegom, P. M., Douma, J. C., and Verheijen, L. M. A fully traits-based approach to modeling  
1350 global vegetation distribution. *P. Natl. Acad. Sci. USA*, 111, 13733–13738,  
1351 <https://doi.org/10.1073/pnas.1304551110>, 2014.

1352 Verheijen, L. M., Aerts, R., Bonisch, G., Kattge, J., and ~~Van-van~~ Bodegom, P. M.: Variation in trait  
1353 trade-offs allows differentiation among predefined plant functional types: implications for  
1354 predictive ecology. *New Phytol.*, 209, 563–575, <https://doi.org/10.1111/nph.13623>, 2016.

1355 Wang, H., Harrison, S. P., Prentice, I. C., Yang, Y. Z., Bai, F., Togashi, H. F., Wang, M., Zhou, S.  
1356 X., and Ni, J.: The China Plant Trait Database: toward a comprehensive regional compilation  
1357 of functional traits for land plants. *Ecology*, 99, 500, <https://doi.org/10.1002/ecy.2091>, 2018.

1358 Webb, C. T., Hoeting, J. A., Ames, G. M., Pyne, M. I., and LeRoy Poff, N.: A structured and  
1359 dynamic framework to advance traits-based theory and prediction in ecology. *Ecol. Lett.*, 13,  
1360 267–283, <https://doi.org/10.1111/j.1461-0248.2010.01444.x>, 2010.

1361 Wright, I. J., Dong, N., Maire, V., Prentice, I. C., Westoby, M., Diaz, S., Gallagher, R. V., Jacobs,  
1362 B. F., Kooyman, R., Law, E. A., Leishman, M. R., Niinemets, U., Reich, P. B., Sack, L., Villar,  
1363 R., Wang, H., and Wilf, P.: Global climatic drivers of leaf size. *Science*, 357, 917–921,  
1364 <https://doi.org/10.1126/science.aal4760>, 2017.

1365 Wright, I. J., Reich, P. B., Westoby, M., Ackerly, D. D., Baruch, Z., Bongers, F., Cavender-Bares,  
1366 J., Chapin, T., Cornelissen, J. H. C., Diemer, M., Flexas, J., Garnier, E., Groom, P. K., Gulias,  
1367 J., Hikosaka, K., Lamont, B. B., Lee, T., Lee, W., Lusk, C., Midgley, J. J., Navas, M. L.,  
1368 Niinemets, U., Oleksyn, J., Osada, N., Poorter, H., Poot, P., Prior, L., Pyankov, V. I., Roumet,  
1369 C., Thomas, S. C., Tjoelker, M. G., Veneklaas, E. J., and Villar, R.: The worldwide leaf  
1370 economics spectrum. *Nature*, 428, 821–827, <https://doi.org/10.1038/nature02403>, 2004.

1371 Wullschleger, S. D., Epstein, H. E., Box, E. O., Euskirchen, E. S., Goswami, S., Iversen, C. M.,  
1372 Kattge, J., Norby, R. J., van Bodegom, P. M., and Xu, X.: Plant functional types in earth

1373 system models: past experiences and future directions for application of dynamic vegetation  
1374 models in high-latitude ecosystems. *Ann. Bot.*, 114, 1–16,  
1375 <https://doi.org/10.1093/aob/mcu077>, 2014.

1376 Yan, P., He, N. P., Yu, K. L., Xu, L., and Van Meerbeek, K.: Integrating multiple plant functional  
1377 traits to predict ecosystem productivity. *Commun. Biol.*, 6, 239,  
1378 <https://doi.org/10.1038/s42003-023-04626-3>, 2023.

1379 Yang, Y. Z., Zhu, Q. A., Peng, C. H., Wang, H., Xue, W., Lin, G. H., Wen, Z. M., Chang, J., Wang,  
1380 M., Liu, G. B., and Li, S. Q.: A novel approach for modelling vegetation distributions and  
1381 analysing vegetation sensitivity through trait-climate relationships in China. *Sci. Rep.*, 6,  
1382 24110, <https://doi.org/10.1038/srep24110>, 2016.

1383 Yang, Y. Z., Wang, H., Harrison, S. P., Prentice, I. C., Wright, I. J., Peng, C. H., and Lin, G. H.:  
1384 Quantifying leaf-trait covariation and its controls across climates and biomes. *New Phytol.*,  
1385 221, 155–168, <https://doi.org/10.1111/nph.15422>, 2018.

1386 Yang, Y. Z., Zhao, J., Zhao, P. X., Wang, H., Wang, B. H., Su, S. F., Li, M. X., Wang, L. M., Zhu,  
1387 Q. A., Pang, Z. Y., and Peng, C. H.: Trait-Based Climate Change Predictions of Vegetation  
1388 Sensitivity and Distribution in China. *Front. Plant Sci.*, 10, 908,  
1389 <https://doi.org/10.3389/fpls.2019.00908>, 2019.

1390 Yurova, A. Y., and Volodin, E. M.: Coupled simulation of climate and vegetation dynamics. *Izv.,*  
1391 *Atmos.–Ocean. Phys.*, 47, 531–539, <https://doi.org/10.1134/s0001433811050124>, 2011.

1392 Zaehle, S., and Friend, A. D.: Carbon and nitrogen cycle dynamics in the O-CN land surface  
1393 model: 1. Model description, site-scale evaluation, and sensitivity to parameter estimates.  
1394 *Global Biogeochem. Cy.*, 24, [GB1005n/a-n/a](https://doi.org/10.1029/2009gb003521), <https://doi.org/10.1029/2009gb003521>, 2010.